

Ecosystem Consequences of Sea Level Rise and Salinization in North Carolina's Coastal Wetlands

by

Emily Ury

University Program in Ecology
Duke University

Date: _____

Approved:

Emily S. Bernhardt, Co-Advisor

Justin Wright, Co-Advisor

Jennifer Swenson

Marcelo Luiz Ardón Sayao

Xi Yang

Dissertation submitted in partial fulfillment of
the requirements for the degree of Doctor
of Philosophy the University Program in Ecology
in the Graduate School
of Duke University

2021

ABSTRACT

Ecosystem Consequences of Sea Level Rise and
Salinization in North Carolina's Coastal Wetlands

by

Emily Ury

University Program in Ecology
Duke University

Date: _____

Approved:

Emily S. Bernhardt, Co-Advisor

Justin Wright, Co-Advisor

Jennifer Swenson

Marcelo Luiz Ardón Sayao

Xi Yang

An abstract of a dissertation submitted in partial
fulfillment of the requirements for the degree
of Doctor of Philosophy in the University Program in Ecology
in the Graduate School of
Duke University

2021

Copyright © 2021 by Emily Ury
All rights reserved except the rights granted by the
Creative Commons Attribution-Noncommercial License

Abstract

Climate change is driving vegetation community shifts in coastal regions of the world, where low topographic relief makes ecosystems particularly vulnerable to sea level rise, salinization, storm surge, and other effects of global climate change. Salinization has clear effects on vegetation, as few plant species can survive in brackish water, and these shifts in vegetation lead to declines in biomass carbon stocks, as well as significant changes in habitat structure and biodiversity. The rate and extent of these impacts on other wetland ecosystem properties and function is far less certain. This dissertation investigates the ecosystem consequences of saltwater intrusion in coastal wetlands, from shifting vegetation at the landscape scale, to soil biogeochemistry and wetland carbon cycling.

Coastal plant communities globally are highly vulnerable to future sea-level rise and storm damage, but the extent to which these habitats are affected by the various environmental perturbations associated with chronic salinization remains unclear. In 2016, a series of vegetation plots across the Albemarle-Pamlico Peninsula that had been surveyed 7-13 years earlier were revisited in order to measure changes in tree basal area and community composition over time. I found reduced tree basal area in plots at lower elevations and with higher current soil salt content, while these factors explained only a small fraction of the measured changes in tree community composition. This decadal comparison provides convincing evidence that increases in soil salinity and saturation can explain recent changes in tree biomass, and potential shifts in community composition in low-elevation sites along the North Carolina coast.

In Chapter 3, I quantified land and land cover change in the Alligator River National Wildlife Refuge (ARNWR), North Carolina's largest coastal wildlife preserve, from 1985 to 2019 using classification algorithms applied to a long-term record of satellite imagery. Despite ARNWR's protected status, and in the absence of any active forest management, 32 % (31,600 hectares) of the 99,347 hectare study area has changed land cover classification during the study period. A total of 1151 hectares of land was lost to the sea and ~19,300 hectares of coastal forest habitat were converted to shrubland or marsh habitat. As much as 11 % of all forested cover in the refuge transitioned to ghost forest, a unique land cover class that is characterized by standing dead trees and fallen tree trunks. This is the first attempt to map and quantify coastal ghost forests using remote sensing. These unprecedented rates of deforestation and land cover change due to climate change may become the status quo for coastal regions worldwide, with implications for wetland function, wildlife habitat and global carbon cycling.

Salinization of freshwater wetlands is a symptom of climate change induced sea level rise. The ecosystem consequences of increasing salinity are poorly constrained and highly variable within prior observational and experimental studies. Chapter 4 presents the results of the first attempt to conduct a salinization experiment in a coastal forested wetland. Over four years, marine salts were applied to experimental plots several times annually with the goal of raising soil salinity to brackish levels while soil porewater in control plots remained fresh. Each year I measured aboveground and belowground vegetation biomass along with soil carbon stocks and fluxes. Despite adding more than 1.5 kg of salt per m² to our experimental plots over four years, the ecosystem responses to salt treatments were subtle and varied over the multi-year experiment. In the final year of the experiment, soil respiration was suppressed,

and bulk and aromatic soil carbon became less soluble as a result of salt treatments. The more stable carbon pools—soil organic carbon and vegetation associated carbon—remained unaffected by the salt treatment. This experiment demonstrates substantial ecosystem resistance to low dose salinity manipulations.

The inconsistent soil carbon responses to experimental salinization I observed in the field led me to question how differences in soil pH and base saturation might alter the impacts of salinity of soil microbial activity. To test this, I performed a salt addition experiment on two series of wetland soils with independently manipulated salt concentrations and solution pH to tease apart the effect of these seawater components on soil carbon cycling (Chapter 5). Microbial respiration and dissolved organic carbon solubility were depressed by marine salts in both soils, while pH manipulation alone had no effect. Salinity treatments had a far greater effect on soil pH than did our intentional pH manipulation and there was a strong interaction between salt treatments and soil type that affected the magnitude of soil carbon responses. Site soils varied significantly in pH and base saturation, suggesting that the interaction between salinity and edaphic factors is mediating soil carbon processes. The degree of salinization and the effective pH shift following seawater exposure may vary widely based on initial soil conditions and may explain much of the variation in reports of salt effects on soil carbon dynamics. I suggest that these edaphic factors may help explain the heretofore inconsistent reports of carbon cycle responses to experimental salinization reported in the literature to date.

Dedication

To my high school science fair team coach, aka, Dad. I am on this path because of you. And to my Mom, for the support that has always kept me on my path.

Contents

Abstract	iv
Dedication	vii
Contents	viii
List of Tables	xi
List of Figures	xii
List of Abbreviations	iv
Acknowledgements	v
1 Introduction	1
1.1 Sea level rise and salinization of freshwater wetlands	2
1.2 Coastal landscape change.....	2
1.3 Biogeochemical responses to wetland salinization.....	4
1.4 Introduction to study region	6
1.4.1 Albemarle-Pamlico Peninsula.....	6
1.4.2 Timberlake Observatory for Wetland Restoration	7
1.5 Dissertation outline.....	8
2 Succession, regression and loss: does evidence of saltwater exposure explain recent changes in the tree communities of North Carolina’s Coastal Plain?.....	10
2.1 Introduction.....	11
2.2 Methods.....	13
2.2.1 Study Area.....	13
2.2.2 Data collection and measurement.....	16
2.2.3 Data Analysis.....	17
2.3 Results.....	18

2.4 Discussion	28
3 Rapid deforestation of a coastal landscape driven by sea level rise and extreme events.....	32
3.1 Introduction.....	33
3.2 Methods.....	36
3.2.1 Study location.....	36
3.2.2 Image pre-processing.....	39
3.2.3 Land Cover Classification.....	39
3.2.4 Statistical Analysis.....	41
3.3 Results.....	42
3.4 Discussion.....	50
4 Ecosystem carbon consequences of a four-year salt addition experiment in a coastal forested wetland.....	55
4.1 Introduction.....	55
4.2 Methods.....	57
4.2.1 Site description and experimental design.....	57
4.2.2 Vegetation monitoring.....	58
4.2.3 Soil Collection and analysis.....	59
4.2.4 Statistical Analysis.....	61
4.3 Results.....	61
4.3.1 Direct effects of salt treatment.....	61
4.3.2 Indirect effects of salt treatment.....	63
4.3.3 Salt effects on vegetation.....	65
4.3.4 Salt effects on soil carbon.....	66
4.4 Discussion.....	70

5	Seawater is more than just salt: disentangling the effects of salinization and pH on coastal soil carbon cycling	78
5.1	Introduction.....	78
5.2	Methods.....	81
5.2.1	Site description and sample collection.....	81
5.2.2	Experimental set-up and treatment application	82
5.2.3	Response measurements	85
5.2.4	Statistical Analysis.....	86
5.3	Results.....	87
5.3.1	Site characteristics.....	87
5.3.2	Treatment effects on soil salinity and soil pH.....	88
5.3.3	Salinity effects on soil carbon	90
5.4	Discussion.....	96
6	Conclusion.....	101
	Appendix A – Supplementary materials for chapter 2.....	105
	Appendix B – Supplementary materials for chapter 3.....	115
	Appendix C – Supplementary materials for chapter 4.....	118
	Appendix D – Supplementary materials for chapter 5	133
	Table 16 continued	141
	References	143

List of Tables

Table 1: Ordination statistics.....	22
Table 2: Summary of net area change for each vegetation class.....	44
Table 3: Soil ion content in 2020.....	63
Table 4: Summary of experimental salt addition studies.....	74
Table 5: Experimental treatment solution salinity and pH.....	83
Table 6: Site characteristics and soil chemical properties.....	88
Table 7: Site information and physical characteristics.....	106
Table 8: Soil chemistry data.....	108
Table 9: Vegetation Summary.....	109
Table 10: Accuracy Assessment for classifications.....	115
Table 11: Confusion matrix for the Landsat 8 classifier.....	116
Table 12: Confusion matrix for the Landsat 7 Classifier.....	116
Table 13: Confusion matrix for the Landsat 5 Classifier.....	116
Table 14: Salt addition and sampling schedule.....	122
Table 15: Supplementary data tables for Chapter 4.....	123
Table 16: ANOVA results for all response variables.....	140

List of Figures

Figure 1: Study location on the Albemarle-Pamlico Peninsula.....	15
Figure 2: Ordinations of site characteristics and tree species.....	21
Figure 3: Species abundance ordination plot.	24
Figure 4: Correlation plots for community composition change.....	25
Figure 5: Correlation plots for tree biomass.	27
Figure 6: Study location in Eastern North Carolina	38
Figure 7: Classification schematic and examples of each vegetation class	38
Figure 8: Areas of vegetation change in the Alligator River National Wildlife Refuge.	44
Figure 9: Maps of spatial predictors of vegetation change.....	45
Figure 10: Model coefficient estimates for drivers of vegetation change.....	48
Figure 11: Timeseries of change in Alligator River National Wildlife Refuge.....	49
Figure 12. Soil chloride content (left) and soil moisture (right)	62
Figure 13: Average pH in experimental plots.....	64
Figure 14: Growth (%) of trees in control versus salt treatment plots	65
Figure 15: Substrate induced respiration (SIR) across all sites and sampling dates.	66
Figure 16: CO ₂ flux from carbon mineralization assays	67
Figure 17: Dissolved organic carbon (DOC) across all sampling dates and sites.....	68
Figure 18: Phenolic compounds in soil water extracts	69
Figure 19: Soil organic content measured as loss on ignition (LOI).	70
Figure 20: Schematic of experimental design.	84
Figure 21: Measured salinity and pH.....	89
Figure 22: Initial C mineralization rate.....	91

Figure 23: Accumulation curve (top panels) and cumulative CO ₂ mineralization (bottom panels) from soil incubations over 21 days.....	92
Figure 24: Effect of salinity treatment on DOC, phenolic compounds and SUVA ₂₅₄	94
Figure 25: Effect of salinity on DOC and phenolics in relation to one another.....	95
Figure 26: Total soil organic matter lost on ignition at 500 °C.	96
Figure 27: Full correlation matrix.	110
Figure 28: Normalized correlation plots.	111
Figure 29: Species change plots.....	114
Figure 30: Coefficients of environmental predictors over time.	117
Figure 31: Timberlake property map.....	118
Figure 32: Timeline of salt additions.....	118
Figure 33: Soil extractable ion concentrations	120
Figure 34: Soil extractable nutrient concentrations	120
Figure 35: Tree growth (%) from 2015-2021	121
Figure 36: Treatment effect on DOC in the initial filtrate	133
Figure 37: Initial C mineralization rate from the soil incubation assays	134
Figure 38: Phenolic concentration (above) and UV absorbance at 254 nanometers	135
Figure 39: Effect of salinity on DOC and SUVA ₂₅₄ in relation to one another.....	136
Figure 40: Effective salinity in the initial filtrate (top) and final extract (bottom).	137
Figure 41: Effective pH by salinity treatment	138
Figure 42: Effective pH by pH treatment.....	139

List of Abbreviations

ANOVA	Analysis of Variance
Ca	Calcium
Cl	Chloride
CO ₂	Carbon dioxide
DEM	Digital Elevation Model
DOC	Dissolved Organic Carbon
K	Potassium
LOI	Loss On Ignition
Mg	Magnesium
Na	Sodium
NASA	National Aeronautics and Space Administration
NH ₄	Ammonium
NO ₃	Nitrate
NOAA	National Oceanic and Atmospheric Administration
PO ₄	Phosphate
SIR	Substrate Induced Respiration
SO ₄	Sulfate
SOC	Soil Organic Carbon
TDN	Total Dissolved Nitrogen
TOWeR	Timberlake Observatory for Wetland Restoration
USGS	United State Geological Survey
UV-Vis	Ultraviolet-Visible

Acknowledgements

The completion of this dissertation was only possible with the help of fantastic collaborators and advocates, to whom I owe an enormous debt of gratitude. To my advisors, Emily and Justin, you have filled my time at Duke with so much energy and love for science. I am grateful for your fantastic mentorship, your limitless support of my research, and, more importantly, of me as a person. I could not have asked for a better advising team, and I hope to one day live up to the example of your great leadership.

To Bernhardt and Wright lab group members past, present and pseudo: Alice Carter, Jackie Gerson, Mike Vlah, Amanda DelVecchia, Audrey Thellman, Anna Wade, Jake Nash, Jenny Rocca, Marie Simonin, Phil Savoy, Richard Marinos, Jessica Brandt, Joanna Blaszcak, Matt Ross, Eric Moore, Steve Anderson, Aaron Berdanier, Yongli Wen, Christina Bergemann, Jonny Behrens, Jasmine Parham, Spencer Rhea, Cari Ficken, Aspen Reese, Rachel Mitchell, Greg Ames, Eric Ungberg, Dave DeLaMater, Anita Simha, Richard Wong, and Anna Nordseth, thank you for the feedback, the inspiration and most importantly the laughs.

And to all the members of my academic community through the River Center, the University Program in Ecology, and the Duke Biology Department, you are too many to name, but you have made this place home for the past five years.

To everyone who has ever braved the waters at Timberlake with me – you are my heroes – especially Steve Anderson, who saved my life on more than one occasion and always turned a field day into a great day. To Brooke Hassett, literally none of this would have been possible without you, thank you!

To my dissertation committee members, Marcelo Ardón, Jennifer Swenson and Xi Yang. Each of your expertise has elevated my work and I am grateful for all of the feedback you have given me. I am so fortunate to have such a kind and supportive committee; it has been a pleasure working with you all. And thank you to Xi Yang's lab members who adopted me in Fall 2019 for an inspiring stint as a visiting graduate student at the University of Virginia. I am also extremely grateful for the support from several other academic mentors and Duke faculty members: Sonia Silvestri, Dean Urban, Jean Philippe Gibert, Marie Claire Chelini, Kathleen Donohue, Dan Richter, Bill Schlesinger, Martin Doyle, Jim Heffernan, Kateri Salk, and Ryan Emmanuel.

I owe a huge debt of gratitude to the Biology Department, Ecology Program and Nicholas School administrators who make all research possible and helped me out of a bind on numerous occasions, especially Anne Lacy, Danielle Wiggins, Randy Smith, Jim Tunney, Jo Bernhardt, Jill Danforth, Michael Barnes, and the Biology Department IT staff. Thank you.

This dissertation was funded with support from the NSF Coastal SEES Collaborative Research Award #1426802, a NASA Earth and Space Science Fellowship, the North Carolina Sea Grant/Space Grant Graduate Research Fellowship, the Duke Biology Department, and the Duke Wetlands Center. Chapter 2 was made possible thanks to the participants of the Carolina Vegetation Survey, chiefly T.R. Wentworth, M.S. Schafale, and A. S. Weakley. Chapter 3 was conducted with support from the Duke Data+ program through the Rhodes Information Initiative and with help from our partners at Alligator River National Wildlife Refuge, in particular Scott Lanier. Others without whom this work would not have been possible include Patrick Gray, Ethan Baruch, Matthew Stillwagon, Pete Lazaro, Kelsey Marton, Melinda Martinez, Justine Neville, Wyatt Jerrigan, Laura Nasland, Joy Reed, Tyler Edwards,

Kaitlyn Chang, Haynes Lynch, Adam Kosinski, and the students and TAs of the Duke Field Ecology Class.

Lastly, I would like to thank my lab mates, friends, cohort and family for their unending support. To Alice Carter and Jackie Gerson who started this journey with me in 2016, it's been a pleasure to have you with me every step of the way. To my neighbors on Oakland Ave, Sarah Solie, Emily Levy and Sam Cohen, I am so fortunate to have you and your baking prowess in my life, especially during the pandemic times. To my Williams friends and New Haven ladies, thanks for nerding out with me and being supportive of my never-ending pursuit of school. Thanks to my loving parents, Michael and Joan Ury, who have always been there for me and for giving me the advice I don't want to hear, but need to hear anyways, and to my sister Liz for always being proud of me. And thank you Owen for your support during the final stretch and for constantly reminding me of how fun it is to do science.

1

Introduction

Climate change is causing sea level rise and saltwater intrusion, with significant impacts on coastal wetlands and their ecological functions. Wetlands provide a suite of ecosystem services, including coastal protection, habitat provisioning, water filtration and long-term carbon storage (Zedler 2003; Mitsch and Gosselink 2015). As water levels and salinity increase, coastal freshwater wetlands, whose plants and soils are not adapted to saline conditions, are being dramatically altered in ways that will compromise their continued provision of these services. Eventually, total ecosystem collapse may be an outcome of sea level rise (Mulholland *et al.* 1997; Herbert *et al.* 2015). The North American Coastal Plain was recently identified as a global biodiversity hotspot, but one that is extremely imperiled by sea level rise (Noss *et al.* 2015). Advancing our understanding of how coastal ecosystems respond to sea level rise and salinization are vital for protecting or adaptively managing these valuable ecosystems in the face of global change.

1.1 Sea level rise and salinization of freshwater wetlands

By the end of the current century, sea level rise may inundate up to 76,000 km² of land in the coterminous US (Haer *et al.* 2013). Vulnerability to sea level rise is not equally distributed along the coast -- geologic and anthropogenic factors shape landscape risk to sea level rise. The Atlantic Coastal Plain is experiencing greater than average rates of relative sea level rise due to glacial isostatic adjustment and a pervasive history of land drainage (Douglas and Richard Peltier 2002; Church *et al.* 2013). In low-lying areas, the effects of sea level rise such as shoreline erosion and vegetation die-off are already highly visible on the landscape, making this all the more pressing of an issue to study.

While sea level rise is one driver of the salinization of freshwater ecosystems, the impact of marine salts extends far beyond the coastal fringe. In coastal plain landscapes characterized by their low topographic relief, marine salts can be mixed and diffused well inland through both groundwater intrusion and surface water incursion (Nicholls 2004; Herbert *et al.* 2015; Tully *et al.* 2019). The inland reach of saltwater is exacerbated during extreme events. Droughts concentrate salts in surface and porewater due to evaporation, and storm surges deliver saline water directly overland. These extreme events that further the impact of salinization are becoming more frequent and intense with climate change (Meehl *et al.* 2007; Cloern *et al.* 2016; Vitousek *et al.* 2017). For these reasons, salinization of coastal landscapes has been named the 'leading edge of climate change' (Ardón *et al.* 2013, 2016).

1.2 Coastal landscape change

The loss of shoreline wetlands due to sea level rise is a well-studied ecological progression (Reed 1995; Kirwan and Megonigal 2013; Blankespoor *et al.* 2014; Borchert *et al.* 2018).

Impacts of salinization on inland freshwater ecosystems are more complex and harder to predict. The combined effects of acute salinization events on top of chronically increasing salinity due to sea level rise are difficult to tease apart. Described as an ‘ecological ratchet’, sea level rise driven vegetation changes tend to occur in bursts driven by extreme events hitting areas already weakened by a slowly shifting baseline (Fagherazzi *et al.* 2019). From the Gulf of Mexico (Williams *et al.* 1999) to New Brunswick, Canada (Robichaud and Bégin 1997), the demise of coastal wetlands has not been confined to the saltmarsh fringe (Desantis *et al.* 2007; Doyle *et al.* 2010). ‘Ghost forests,’ a term coined to describe a stand die-off event in coastal forested wetlands, have been spotted with increasing frequency in coastal areas (Kirwan and Gedan 2019). The loss of coastal forests has severe implications for wildlife habitat and carbon storage (Taillie, Moorman, Smart, *et al.* 2019; Smart *et al.* 2020). The widespread loss of aboveground biomass in coastal forests alone would be a significant disruption to the global carbon cycle (Windham-Myers *et al.* 2018). Still, there is much we do not know about the causes and consequences of shifting vegetation in coastal regions due to sea level rise and salinization.

Advances in remote sensing technology and data availability have revolutionized the way we study landscape ecology and understand landscape change (Crowley and Cardille 2020). Advances in vegetation detection, such as the use of Lidar (Light detection and ranging) for measuring aboveground biomass, help assess the rates and spatial patterns of coastal change (Riegel *et al.* 2013; Smart *et al.* 2020). One of the most valuable resources for studying climate change driven landscape change is the Landsat record (Kennedy *et al.* 2014). This 30+ year archive of global satellite imagery is long enough to discern trends driven by extreme events

or sea level rise. This dissertation leverages the Landsat record to map vegetation in service of further understanding of the spatial and temporal drivers of ecological change.

1.3 Biogeochemical responses to wetland salinization

Biogeochemical responses to wetland salinization are extremely complex. Salinity is a multivariate stressor because of its multiple components, not just sodium and chloride, but also sulfate and other base cations. It causes ionic stress for plants and microorganisms, and changes the chemical status of wetland soils and porewater, affecting biochemical interactions and processes within the soil matrix (Herbert *et al.* 2015; Luo *et al.* 2019; Tully *et al.* 2019). Introduction of marine salts can shift the alkalinity of wetland soils and alter redox patterns through the introduction of novel electron acceptors such as sulfate (Tully *et al.* 2019). These shifts in chemical status have numerous implications for carbon sequestration and nutrient retention, important functions with value to socio-ecological systems (Herbert *et al.* 2015; Tully *et al.* 2019). Additionally, there are many indirect effects of salinity on wetland biogeochemistry such as those mediated by vegetation responses and those cascading from alterations to soil carbon chemistry (e.g., solubility and sorption). These feedbacks have not been well studied and there is much we do not yet know about the impacts of salinization on wetland biogeochemical cycling.

Predicting the outcomes of salinization on different biogeochemical pathways is made more difficult by disagreement and inconsistencies between observations and experimental outcomes found in the literature (Herbert *et al.* 2015). Studying the effects of salinization on freshwater wetlands has been primarily through observational gradient studies, lab experiments, and small-scale field experiments. Gradient studies compare wetland properties

and ecological functions across natural salinity changes, typically along an estuary (Neubauer *et al.* 2005; Krauss and Whitbeck 2012; Chambers *et al.* 2013). Experimental salt addition studies are typically conducted in laboratory settings using soil slurries (Chambers *et al.* 2011; Marton *et al.* 2012; Neubauer *et al.* 2013; Liu, Ruecker, *et al.* 2017; Wen *et al.* 2019), intact soil cores, (Weston *et al.* 2006, 2011; Ardón *et al.* 2018; Helton *et al.* 2019; Doroski *et al.* 2019) or in outdoor mesocosms (Chambers *et al.* 2014; Charles *et al.* 2019). Advantages of these approaches include the high degree of control over experimental conditions, but the disadvantage is that contrived conditions may obstruct our understanding of natural ecological phenomenon. In addition, these studies typically only examine the soil component of the ecosystem, excluding the potential for plant-soil feedbacks to alter salinity responses. Salt addition studies in the field are typically small in scale, exclude large vegetation, and offer less control over external environmental variables (Neubauer *et al.* 2013; Herbert *et al.* 2018; Helton *et al.* 2019). Variable outcomes between these studies may be attributed to either site differences, methodological approach, or a combination of the two and this results in a high degree of uncertainty surrounding the effect of salinization on both individual biogeochemical processes and total ecosystem responses. In this dissertation, we use both field and laboratory experiments to push the boundary of our understanding of salinity effects on wetland biogeochemistry and situate our findings in the context of this divided body of literature.

1.4 Introduction to study region

1.4.1 *Albemarle-Pamlico Peninsula*

The Albemarle-Pamlico Peninsula is a low-lying region on the east coast of North Carolina, bounded by the second largest estuary in the United States. The Outer Banks buffer this region from saline ocean waters, coastal winds, and direct impacts from storms. With the help of this protection, this landscape is dominated by unique pocosin wetlands, palustrine forest and shrub communities. These wetlands may be either deciduous (bald cypress, swamp black gum, red maple, many species of oaks and other bottomland hardwoods), evergreen (Atlantic white cedar, loblolly and pond pine) or a mix of both, and are often surrounded by a fringe of fresh or salt marshes (Schafale M and Weakley A 1990). Up to 90% of all wetlands in this region may have been cleared (Richardson 1983). The majority of the region was logged during the 19th and 20th centuries followed by large-scale agriculture (Carter 1975). Extensive ditching and active drainage is required to farm in this landscape and much of the eastern portion of the peninsula has since been returned to wetland owing to the fact that it is too low and wet to drain and manage profitably (Poulter 2005).

This region is precariously poised on the precipice of change due to sea level rise. Average elevation in the region is just 1.5 meters above sea level (Moorhead and Brinson 1995). In this flat landscape, wind-driven tides can move brackish coastal waters through the drainage canals and ditches several miles inland (Manda *et al.* 2014, 2018). Work by Bhattachan and others (2018) demonstrated the role of artificial drainage ditches in increasing the landscape's vulnerability to salinization. This region is expected to experience up to 100 cm of sea level rise by 2100 (Vermeer and Rahmstorf 2009; Haer *et al.* 2013). The factors that make this landscape so vulnerable to sea level rise are also what make it such a valuable study system.

We can investigate ecological transitions here in a setting that may be decades ahead of neighboring states and other regions of the world. The return of farmland back to wetland provides a useful test case in which to study restoration approaches in the context of rapidly shifting environmental change.

1.4.2 Timberlake Observatory for Wetland Restoration

The Timberlake Observatory for Wetland Restoration (TOWeR) is one of the largest restored wetland projects in the country. Located in Tyrrell County, North Carolina (35°54'22" N, 76°09'25" W), this formerly agricultural land was restored to wetland by the Great Dismal Swamp Mitigation Bank, LLC. In 2004, 440 hectares were planted with wetland tree saplings and, after ditch-filling, the property was re-flooded in an attempt to return the hydrology to a pre-agricultural state (Needham 2006; Ardón *et al.* 2010). The project was monitored briefly as is standard for a mitigation bank site, and to date, research activities on the property have expanded to include numerous projects on wetland restoration (Marcelo Ardón *et al.* 2010; M. Ardón *et al.* 2010; Morse *et al.* 2012; Carmichael and Smith 2016), natural saltwater incursion (Ardón *et al.* 2013, 2016), salt addition experiments (Ardón *et al.* 2018; Helton *et al.* 2019) including this dissertation, and other research.

Initial research interests at the site began with the goal of understanding the capacity of this large restoration project to improve water quality impaired by intensive agriculture in the watershed. Following a natural saltwater intrusion event during the centennial drought of 2007-2008 the focus of these research activities shifted. In addition to the efficacy of wetland restoration, TOWeR has been and continues to be used to study the consequences of salinization on wetland abilities to capture and store nutrients. In concert with these efforts, the work in this dissertation focuses on the impact of salinization on another important

wetland function: carbon cycling. In this dissertation, I look at the biogeochemical consequences of salinization on carbon cycling through a large-scale salt addition experiment conducted on the TOWeR property.

1.5 Dissertation outline

In this dissertation I investigate the effect of salinization on coastal wetlands. The work here is presented in 6 chapters. Following this introduction, the 2nd and 3rd chapters focus on coastal wetland vegetation change and its drivers while the 4th and 5th chapters assess the biogeochemical consequences of salinization on carbon cycling in wetlands. Chapter 2 uses data from regional vegetation surveys to assess plant community change over time. The primary objectives were to compare historical vegetation data from the Carolina Vegetation Survey, with a more recent attempt to resurvey the same sites and to assess changes in the context of evidence of saltwater intrusion. This chapter was published in March 2020 as: Ury, EA, Anderson SM, Peet, RK, Bernhardt, ES, and Wright JP. 2020. Succession, Regression and Loss: does evidence of saltwater exposure explain recent changes in the tree communities of North Carolina's Coastal Plain? *Annals of Botany* 125: 255-263. Chapter 3 uses remote sensing to establish 30 years of vegetation change in the Alligator River National Wildlife Refuge. The aim of this chapter is to assess the pace and timing of these changes and their spatial and temporal drivers. This chapter was recently accepted for publication in the journal *Ecological Applications*.

The second half of this dissertation consists of work conducted as part of a four-year-long salt addition experiment conducted at the TOWeR site. Chapter 4 reports the outcome of the salt addition experiment on wetland carbon cycling with a particular focus on how

responses change over time and their context in a largely divided literature on the same subject. Chapter 5 describes a laboratory experiment, designed to investigate variation observed within the previous chapter. Specifically, I investigate how carbon cycling responds to shifts in salinity, pH and the interaction between these two variables on soils with divergent characteristics. Finally, Chapter 6 is a conclusion to the work presented here and its broader impacts.

2

Succession, regression and loss: does evidence of saltwater exposure explain recent changes in the tree communities of North Carolina's Coastal Plain?

Emily A. Ury, Steven M. Anderson, Robert K. Peet, Emily S. Bernhardt, and
Justin P. Wright

This chapter is adapted from its published form in
Annals of Botany (2020), <https://doi.org/10.1093/aob/mcz039>

Author Contributions: RP led the Carolina Vegetation Survey; SA led the second field survey. EU led the data analysis and writing the manuscript. All authors contributed to revising the manuscript and gave final approval for publication.

2.1 Introduction

The southeastern Coastal Plain of the United States is an important biodiversity hotspot (Myers *et al.* 2000; Noss *et al.* 2015) and a region that has undergone significant land-use change over the past century (Herbert *et al.* 2015). By the end of this century this region may experience 100 cm of sea level rise (Vermeer and Rahmstorf 2009) resulting in not only loss of wetlands along the coastal fringe, but also forested ecosystems further inland may experience negative consequences such as loss of biodiversity, invasion by *Phragmites australis*, or conversion to open water. In advance of large-scale flooding due to sea level rise, saltwater intrusion occurs, defined as the landward movement of seawater into areas that have normally experienced freshwater inputs (Nicholls 2004). Low topographic relief, artificial drainage networks and erosion associated with agricultural land use have made this region extremely vulnerable to salt water intrusion (Bhattachan *et al.* 2018). This process is further exacerbated by the maritime winds and storm surges that drive salt inland, processes becoming more intense and frequent due to climate change (Vitousek *et al.* 2017). Thus, saltwater intrusion is seen as the leading edge of climate change (Ardón *et al.* 2013, 2016). On the Coastal Plain of North Carolina, signs of sea level rise and salinization are already apparent on the landscape (Stroh *et al.* 2008; Liu, Conner, *et al.* 2017); in this study we are particularly concerned with determining the effects of salinization of the tree communities within these wetlands.

The effects of sea level rise and salinization are by no means germane to forests of the Coastal Plain of North Carolina; studies across the Southeastern US including South Carolina (Stroh *et al.* 2008; Liu, Conner, *et al.* 2017), Georgia (Pennings *et al.* 2005), Louisiana (Shirley and Battaglia 2006), and Florida (Williams *et al.* 1999; Desantis *et al.* 2007) investigate similar

effects of saltwater intrusion on plant communities. A 2015 review by (Herbert *et al.* 2015) summarizes the literature records of wetland salinization around the world and its primary drivers. While sea level rise is the primary driver of coastal wetland salinization in the South Eastern United States, there are multiple mechanisms by which freshwater ecosystems are becoming more saline. Irrigation leading to saltwater intrusion through groundwater is a prominent issue in parts of Australia (Hart *et al.* 1990), land subsidence from agriculture results in relative sea level rise in Italy (Antonellini *et al.* 2008), water diversion reduces river flow leading to saltwater intrusion in the Mekong and Yellow River deltas of Vietnam and China (Wassmann *et al.* 2004; Cui *et al.* 2009), and road salt accumulation is problematic for wetlands in the North Eastern US (Kaushal *et al.* 2005). Variation in salinization mechanism, as well as salt type (ie. road salts versus marine salts), will affect receiving ecosystems differently, but there is no doubt that salinization of freshwater ecosystems is having effects at broad scales (Kaushal *et al.* 2018).

Little is known about the effects of salinization on the forest communities of North Carolina's Coastal Plain beyond the estuarine fringe. The effects of salinity and sea level have been well studied in saltmarsh vegetation (Reed 1995; Pennings *et al.* 2005; Silvestri *et al.* 2005), but prior work has not considered how salinization is affecting the distribution and diversity of trees within the forests of the Coastal Plain. There is a need to study the impacts of sea level rise on freshwater wetland plant communities, particularly tree diversity and biomass as these are important benchmarks of community structure and carbon storage.

The Carolina Vegetation Survey has undertaken a comprehensive survey of the vegetation composition of the Carolinas with survey plots distributed across the two states (Peet *et al.* 2018). The vegetation of North Carolina's Coastal Plain follows typical patterns of

coastal fringe to upland progression, with extensive palustrine (freshwater, non-tidal) and pocosin (shrub-scrub and evergreen) wetlands (Moorhead and Brinson 1995). Data from the Carolina Vegetation Survey have been used to monitor changes in biodiversity, in particular the response to acute disturbances such as hurricanes and fires (Reilly *et al.* 2006; Xi *et al.* 2008; Palmquist *et al.* 2014). Records from the Carolina Vegetation Survey allow us to track changes in forest community over the past two decades.

The focus of this study is to determine whether the effects of salinization are already perceivable in the tree community composition and structure of this sentinel ecosystem. In this study, we use comprehensive forest survey data of 34 plots to determine whether current tree composition and basal area were correlated with saltwater exposure or saltwater exposure risk. For a subset of these sites, we compared present survey data with the Carolina Vegetation Survey dataset to examine whether tree composition and basal area is changing more rapidly in sites with saltwater exposure or exposure risk. We hypothesized that the magnitude of community composition change, and the percent change of basal area, would be related to environmental indicators of salinization at each site, specifically elevation, soil chloride content and other salt ions found in sea water.

2.2 Methods

2.2.1 *Study Area*

Sites for this study are located on the Albemarle-Pamlico Peninsula in northeastern North Carolina (Figure 1). The Albemarle and Pamlico sounds form the second largest estuary complex in North America and the peninsula spans 5,000 km² just inside the barrier islands

of North Carolina. The mean annual temperature is 16.6°C and mean annual precipitation is 1320 mm/yr, which is evenly distributed across seasons (Plymouth Weather Station, Washington Country, NC) (see Ardón *et al.* (2010) for a detailed description of the region). This region is also prone to severe storms and hurricanes in late summer and early fall. More than half of the land area is less than 1 meter above sea level (Poulter and Halpin 2008). Soils of the study sites are mainly Pungo muck and Hyde loam, which are deep, poorly drained, high in organic content and highly acidic (NRCS 2017). Vegetation communities include brackish marshes, mesic mixed hardwood forests, Atlantic white cedar forests, estuarine pine woodlands, and cypress-gum swamps (Schafale 2012).

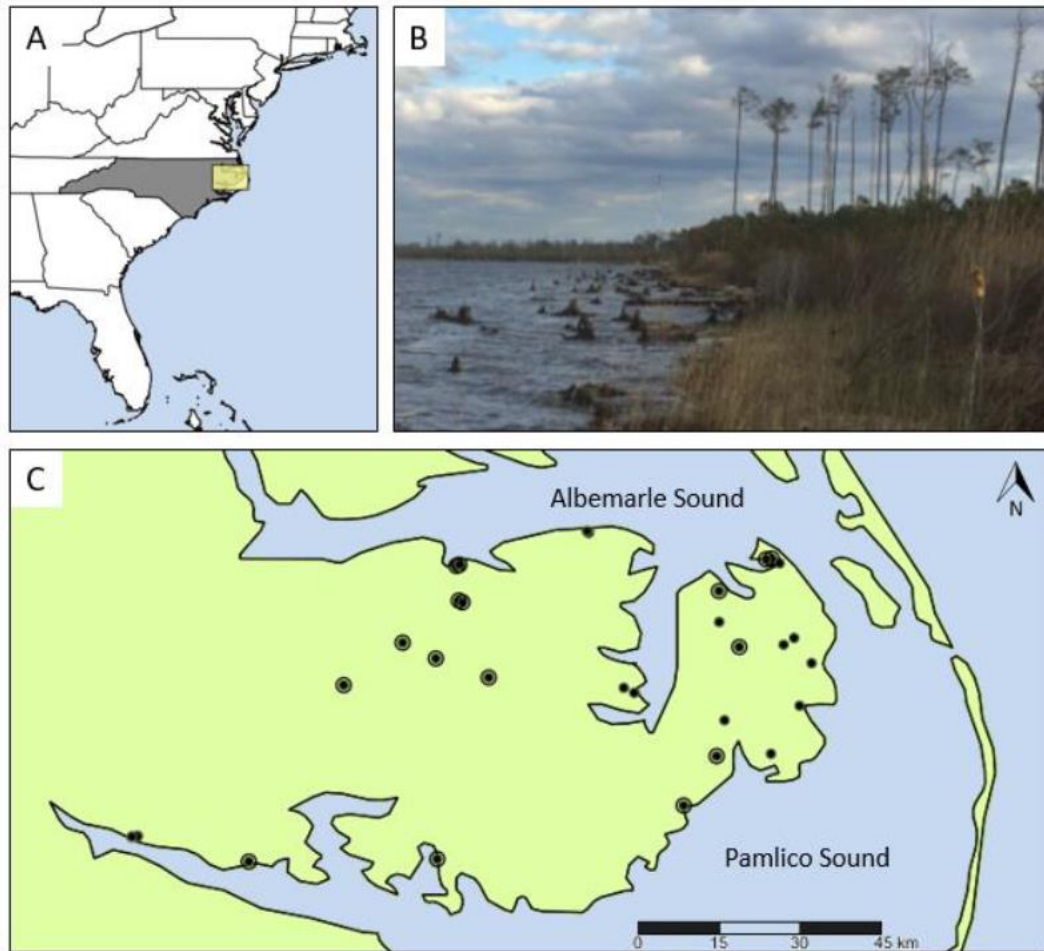


Figure 1: Study location on the Albemarle-Pamlico Peninsula. A) The Atlantic coast of the United States, the state of North Carolina and inset of our study region. B) Photo of a coastal forest retreat (credit: Steve Anderson) on the Albemarle Sound. C) The Albemarle Pamlico Peninsula and study sites (concentric dots are sites that have historic survey data).

2.2.2 Data collection and measurement

Vegetation plots for this study are located in forested stands within public lands. Sixteen sites were established and measured by the Carolina Vegetation Survey between 2003 and 2009 (Peet *et al.* 2012). We located the original plots and resurveyed the vegetation in June and July of 2016. An additional 18 new plots were established for this study (in 2015 or 2016) for a total of 34 plots. New plots were established on public or federally-owned property and using the same protocol as the Carolina Vegetation Survey (Peet *et al.* 1998). Plot sizes vary between 100 and 1000 square meters to capture the diversity of the species present in a given homogeneous community (larger plots being necessary in more heterogeneous areas). The sites span many vegetation community types and include wetlands of varying inundation period. Site elevation was acquired from the USGS National Elevation Dataset (U.S. Geological Survey 2017) and soil type from the National Resources Conservation Service (Soil Survey Staff 2017).

For collection of vegetation data, each site was subdivided into modules of 10x10 meters as described in Peet *et al.* (1998). We measured the diameter at breast height (DBH) of every tree over 5 cm diameter in each module. For each species we calculated the total basal area ($\text{m}^2/\text{hectare}$).

For analysis of soil characteristics, ten soil cores, to ten centimeters depth, were collected at each site along a diagonal transect within one of the modules. Each core was sectioned into two, 5 cm deep sections. For each section, roots and rocks were removed and soils were passed through a 2mm sieve, homogenized and composited for analysis of soil properties and ion concentrations. To characterize the soil properties at each site, for each core section we

measured pH, bulk density, % soil moisture, and loss on ignition (LOI) in a 500 °C oven for four hours. To estimate salt exposure, soils for each plot were analyzed for major ions that occur in seawater (Cl^- , SO_4^{2-} , Ca^{2+} , Mg^{2+} , K^+ , and Na^+). For characterization of soil cation content we measured water extractable base cations (Ca^{2+} , Mg^{2+} , K^+ , and Na^+) using a CS12A column on a Dionex ICS 2000 (Dionex Corporation, Sunnyvale, CA). The Dionex ICS 2000 was also used to analyze water extractable anions (Cl^- , SO_4^{2-}) on an AS-18 analytical column. To understand soil nutrient content, ammonium (NH_4^+) was measured using the phenolate method, and nitrate (NO_3^-) was measured using the hydrazine reduction method using a flow-through analyzer (Lachat QuickChem 8500, Lachat Instruments, Loveland, CO) (APHA 1998).

2.2.3 Data Analysis

Data analyses were performed in R 3.3.3 (R Development Core Team 2017). We calculated total basal area of each species at each site for both the historical Carolina Vegetation Survey sites and the sites measured in this study. To compare tree community composition to environmental characteristics, we created an ordination plot using total basal area data from plots surveyed in 2015 and 2016. The *metaMDS* function in the ‘vegan’ package (Oksanen *et al.* 2016) was used to create a 2-dimensional non-metric multidimensional scaling (NMDS) ordination using species basal area and Bray-Curtis dissimilarity. A total of 28 species were included in the analysis (four species present in the survey plots were eliminated from the analysis because they fell below the rarity cut-off: 0.5% of the total basal area). The function *envfit* was used to fit environmental variables to the ordination. This function is used to assess the significance of each variable in predicting the arrangement of the vegetation communities

using permutation tests. Further analysis of environmental characteristics was conducted using the *corPlot* function from the package ‘psych’ to look for correlation between variables.

To understand how vegetation is changing over time, we created a second ordination that included the data from the historical Carolina Vegetation Survey (also using *metaMDS* and the same parameters specified for the first NMDS). Simple Euclidean distances were calculated between samples of resurveyed sites as a proxy for community composition change over time. These distances were normalized by the number of years between resampling, to yield a rate for community composition change over time. Community composition change over time was then compared to the environmental characteristics measured for each site in the 2016 survey using simple linear regression.

Finally, we used the total basal area of each plot from the Carolina Vegetation Survey and from the resurvey sites measured in this study to calculate a percent change in total basal area. The percent change in basal area over time was also normalized by the number of years between surveys and compared to the environmental characteristics using linear regression.

2.3 Results

The NMDS ordination of all trees and environmental factors demonstrates which drivers are most strongly correlated with tree community composition. The NMDS ordination (Figure 2) of species abundance (total basal area) data for the 34 vegetation plots surveyed in this study during 2015 and 2016 arranges each surveyed plot by community dissimilarity (stress: 0.178, non-metric fit $R^2 = 0.969$). In this ordination we fit all of the measured environmental parameters (for soil characteristics, only data from the top section, 0-5cm depth, were used in these analyses; no significant differences were found between these results and analyses which

included the 5-10cm soil core section); arrows indicate the direction and relative importance of significantly correlated environmental factors. Four of the thirteen characteristics measured at each site are significantly correlated ($p < 0.05$) with the arrangement of tree communities in the ordination space: Cl^- , K^+ , Na^+ , and elevation ($R^2 = 0.23, 0.21, 0.26$ and 0.25 respectively, see

Table 1). Two primary gradients emerge from these fitted variables: all of the marine salt-associated ions in one direction, and with elevation approximately orthogonal to salts. The results from fitting the environmental data to the community composition ordination suggest that these environmental factors are contributing to the distribution of tree species across this region. Neither soil nitrogen (nitrate or ammonium) nor organic carbon appear to be important correlates for community composition. See Appendix A: Table 7, Table 8 and Figure 27 for complete site information, soil characteristics and correlations between environmental characteristics..

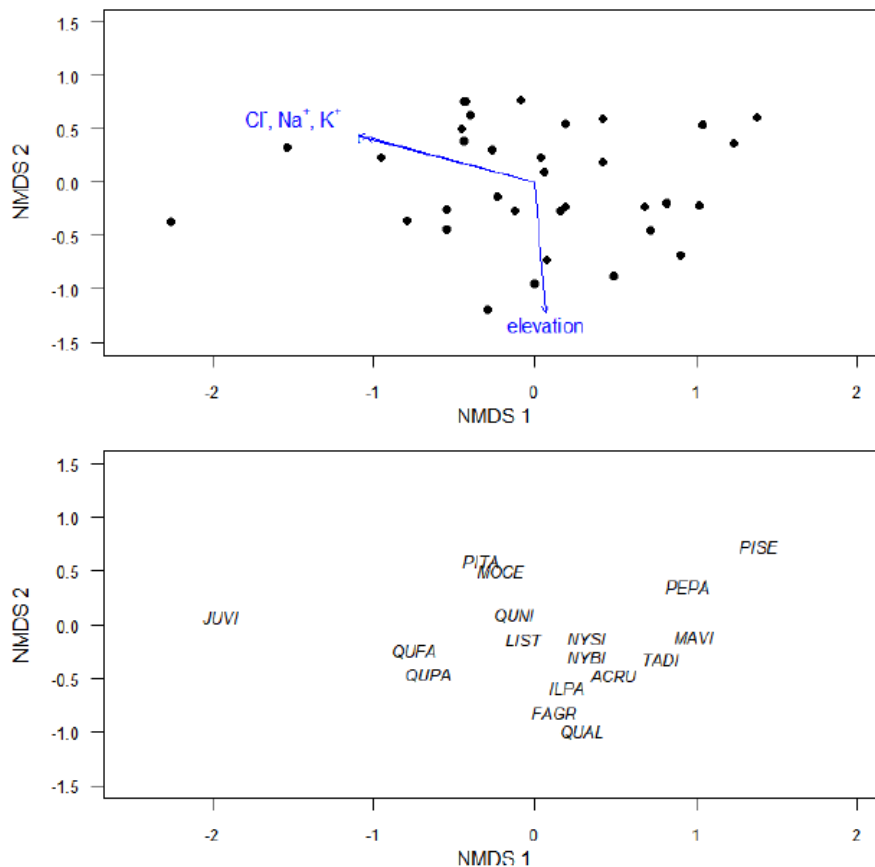


Figure 2: Ordinations of site characteristics and tree species. Ordinations of site characteristics and species. A. NMDS of the species abundance (basal area) in each of 34 plots surveyed in 2015/2016. Vectors represent the environmental factors measured at each plot that are significantly correlated with the tree community distribution. B. Major tree species in ordination space denoted by species code. (ACRU = *Acer rubrum*, FAGR = *Fagus grandifolia*, ILPA = *Ilex opaca*, JUVI = *Juniperus virginiana*, LIST = *Liquidambar styraciflua*, MAVI = *Magnolia virginiana*, MOCE = *Morella cerifera*, NYBI = *Nyssa biflora*, NYSI = *Nyssa sylvatica*, PEPA = *Persea palustris*, PISE = *Pinus serotina*, PITA = *Pinus taeda*, QUAL = *Quercus alba*, QUNI = *Quercus nigra*, QUPA = *Quercus pagoda*, TADI = *Taxodium distichum*. Other species present but not displayed on the NMDS: *Carya tomentosa*, *Chamaecyparis thyoides*, *Cornus florida*, *Gordonia lasianthus*, *Liriodendron tulipifera*, *Oxydendrum arboretum*, *Prunus serotina*, *Quercus* multiple species, *Sassafras albidum*, *Ulmus* multiple species.)

Table 1: Ordination statistics. Coefficients and correlation scores for environmental parameters fitted to the tree community composition ordination for 34 vegetation plots surveyed in 2015-2016 on the Coastal Plain of North Carolina demonstrating the significance of elevation and salt as drivers of current community assemblage.

VECTORS	NMDS1	NMDS2	r2	Pr(>r)	Significance
chloride	-0.92663	0.37598	0.2322	0.021	*
sulfate	-0.93927	0.34318	0.1663	0.058	
elevation	0.05237	-0.99863	0.2478	0.01	**
bulk density	-0.52053	-0.85384	0.1017	0.187	
moisture	0.4896	0.87195	0.0578	0.404	
organic carbon	0.72116	0.69276	0.1402	0.093	
pH	-0.75017	0.66125	0.1022	0.183	
sodium	-0.93051	0.36626	0.2095	0.022	*
potassium	-0.9328	0.36038	0.2618	0.008	**
magnesium	-0.61085	0.79174	0.1462	0.072	
calcium	-0.41313	0.91067	0.0835	0.243	
nitrate	0.23275	-0.97254	0.1402	0.094	
ammonium	-0.54522	-0.8383	0.049	0.462	

Significance codes: 0 > *** > 0.001 > ** > 0.01 > * > 0.5

Data from 16 Carolina Vegetation Survey plots collected in 2003 and 2009 were used to examine how tree communities are changing over time. A second NMDS ordination with data from both sample points (stress: 0.181, non-metric fit $R^2 = 0.967$) visually represents the shift in community composition in ordination space over time (Figure 3). Arrows represent how far and in what direction a plot's tree community has moved since the plot was. The movement of plots over time appears stochastic overall, without clear trends emerging in the direction or magnitude of community shift.

To understand the pattern of overall plot movement we calculated vector length and normalized it by time between resampling events. Most plots experienced a small shift in community composition and a few plots changed more dramatically. When we compared the magnitude of change in community composition over time to environmental factors (Figure 4) we found that elevation, sulfate (SO_4^{2-}) and sodium (Na^+) were significantly, although weakly, correlated with community composition change. In contrast to our hypothesis, chloride (Cl^-) does not appear to be significantly correlated with the magnitude of community composition change.

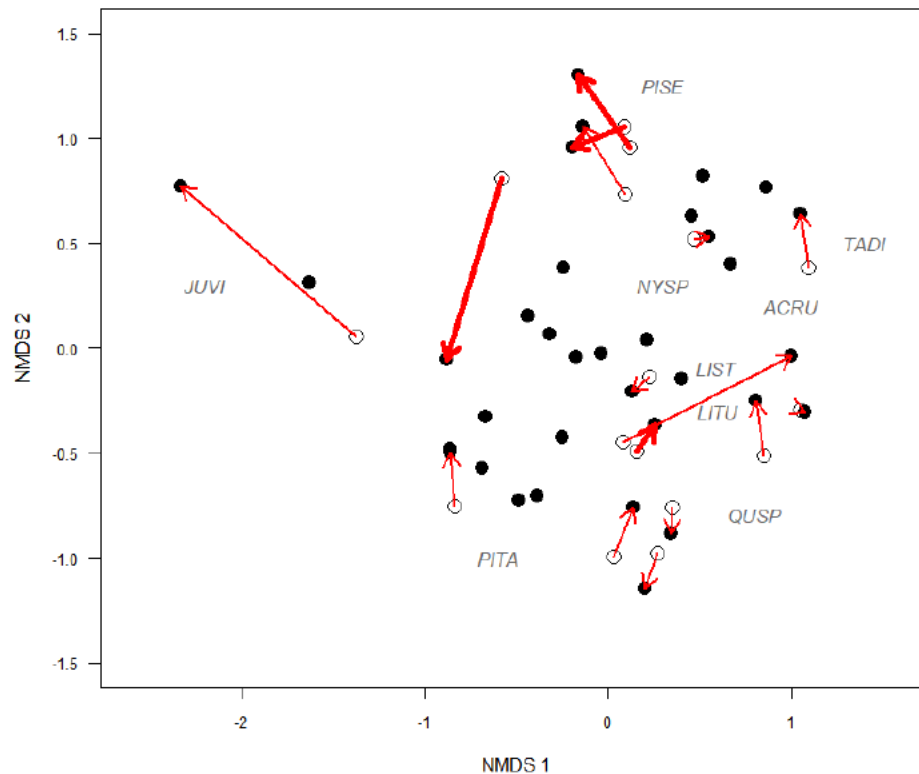


Figure 3: Species abundance ordination plot. NMDS of the species abundance (basal area) of all vegetation plots, from the Coastal Plain of North Carolina, surveyed in this study (solid circles) and 16 sites with historic data (open circles), surveyed in 2003 or 2009 by the Carolina Vegetation Survey. Arrows connect plots which were resurveyed in the same location; bolded arrows denotes original survey was conducted in 2003. Common taxa position in species space are denoted by their species code and grouped to avoid overlapping labels for clarity (ACRU = *Acer rubrum*; JUVI = *Juniperus virginiana*; LIST = *Liquidambar styraciflua*; LITU = *Liriodendron tulipifera*; NYSP = *Nyssa* species [biflora or sylvatica]; PISE = *Pinus serotina*; PITA = *Pinus taeda*; QUSP = *Quercus*, multiple species; TADI = *Taxodium distichum*).

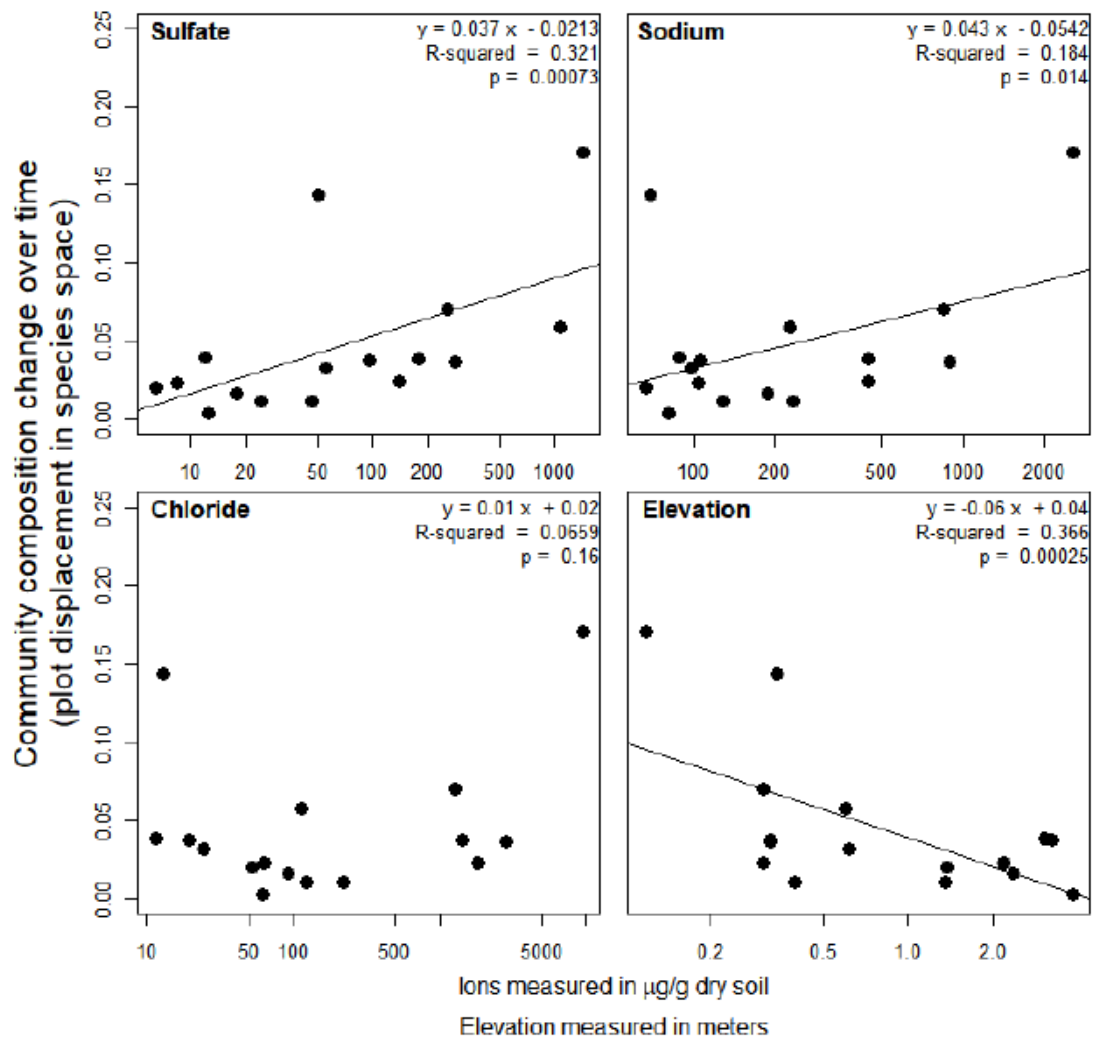


Figure 4: Correlation plots for community composition change. Community composition change for resurveyed vegetation plots on the Coastal Plain of North Carolina (y-axis is the length of the arrows in Figure 3, normalized over time) is correlated with environmental parameters associated with saltwater intrusion.

Finally, we assessed total basal area change over time at each site. As anticipated in early to mid-successional dominated forests in protected lands, we observed that the majority of plots are gaining basal area (12 of 16 sites). The range for percent change of basal area is -9.6% to 118 % and the median is 33.8%. However, several plots have experienced a loss of basal area since the first survey (7 or 13 years previous). Our results show that 37.5% of sites have grown less than 10% over the course of the study. Figure 5 shows the correlations between percent change in basal area and the environmental factors. In contrast to our results for community composition change, the change in basal area is significantly correlated with the environmental factors associated with salinization: sodium, sulfate, chloride and elevation are all correlated with change in total basal area ($R^2 = 0.56; 0.52; 0.35; \text{ and } 0.48$). Other environmental factors measured that were significantly correlated with percent basal area change include soil moisture, Ca^{2+} , Mg^{2+} , K^+ , and NH_4^+ (Appendix A: Figure 28).

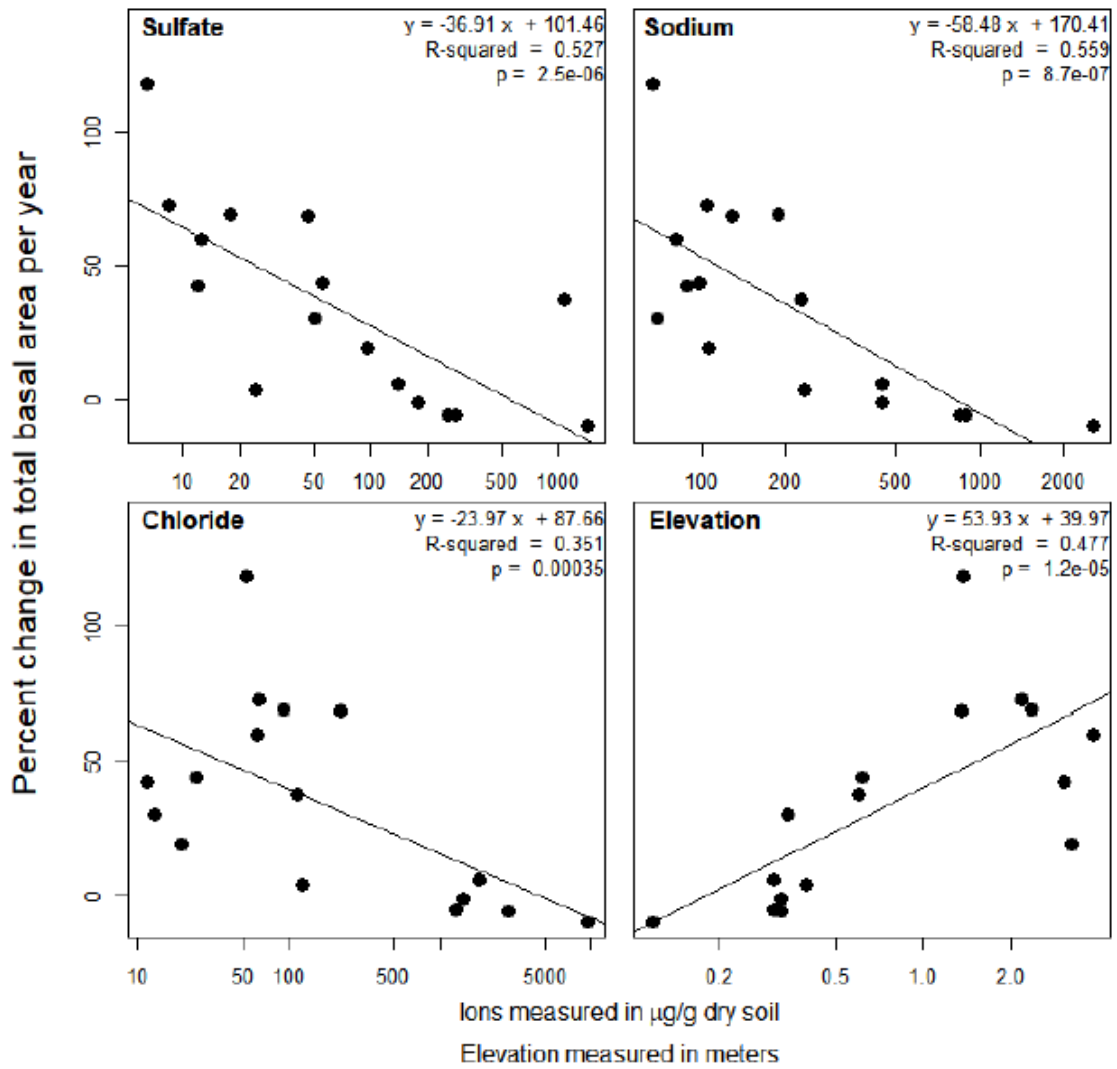


Figure 5: Correlation plots for tree biomass. For each resurveyed vegetation plot from the North Carolina Coastal Plain we show percent change in total basal area per year compared to environmental characteristics.

2.4 Discussion

Our study presents two major conclusions. First, shifts in community composition of coastal wetland forests may be correlated with indicators of salinization. Second, in our study plots that demonstrate the most severe evidence of salinization, we observed a loss of tree basal area. Loss of basal area during the period of this study is a striking finding given the absence of development, deforestation, fire, disease, or other major disturbance in our surveyed plots. Furthermore, loss of basal area is an important indicator of loss of biomass, which raises concerns about the ability of these forests to maintain their functions as carbon sinks (Slik *et al.* 2010).

The literature on the effects of saltwater intrusion on vegetation generally addresses either very fine scale responses at the level of individual plants or plants species, or at the landscape scale. Fine scale investigations include germination or greenhouse experiments of particular species at different salinity and inundation levels (propagule bank study by Battaglia and Collins (2006), greenhouse studies by White *et al.* (2014), and Hanley *et al.* (2016)) and offer insight as to how certain species will respond, but may not reflect the context of natural ecosystems. Conversely, studies which treat large scale processes such as land use change (Shirley and Battaglia 2006) do not always detail the pathways of community composition change. Few studies have been conducted to look specifically at the effects of saltwater intrusion on plants at the community level. Our work focuses on change over intermediate time and spatial scales and addresses how forests stands are changing over decadal time periods. This work is important for understanding patterns of change within a landscape and identifying areas for further research.

Our study region, the Albemarle-Pamlico Peninsula, much of the area is protected wild land where one expects to find trends of forest growth and succession. This is the case for the majority of the sites measured in this study, but the occurrence of areas that are experiencing basal area loss runs counter to such expectations. The sites that are growing poorly or losing basal area could potentially be the canary in the coal mine for the rest of the region. Evidence presented here demonstrates that indicators of saltwater intrusion such as soil ion content and elevation are correlated with the current tree community composition of the Albemarle-Pamlico peninsula. Furthermore, indicators of salinization are correlated with the decline in basal area experienced at sites across the region. These findings are important because loss of tree biomass has implication for global carbon budgets and biodiversity, and moreover the region may be a model against which to compare other coastal ecosystems.

The current community assemblage of trees within our study region reflects the natural environmental gradients present across the landscape and that species partition according to their individual environmental niche requirements and environmental tolerance. For example, *Juniperus virginiana* L. is one of the most salt tolerant species and is the dominant species present in the plot with the highest soil chloride content (Appendix A: Table 9). We also find that *J. virginiana* is in decline at this site which indicates the potential that despite being relative more salt tolerant than most species, environmental change may be pushing conditions past habitability for some species (Desantis *et al.* 2007). Overall, we find that sites experiencing the most loss are ones with lower overall tree basal area to begin with. From this, we infer that these sites were already considerably more vulnerable resulting in reduced productivity. It was in these areas we observed anecdotally the apparent transition from coastal forest to shrub-

grass (i.e., *Myrica*, *Iva*, *Spartina*, *Phragmites*) dominated systems. This loss of tree-dominated wetlands could have significant implications on carbon budgets (Kasischke *et al.* 2013).

Previous work demonstrates that the growth of many tree species, including *Pinus taeda*, *Juniperus virginiana*, *Taxodium distichum*, *Nyssa biflora* and *Liquidambar styraciflua*, are impeded by salinity or flooding (Hosner and Others 1960; Conner and Askew 1992; Tolliver *et al.* 1997; McCarron *et al.* 1998), but the majority of this evidence is obtained from greenhouse studies or field germination studies. Several field studies have been conducted to examine tree survival following natural saltwater intrusion events (Conner 1995), but few studies have tracked forested plots over time (Williams *et al.* 1999, 2003), and this is the first study of its kind to look at tree response to indicators of saltwater intrusion on the Coastal Plain of North Carolina. We assert, that more work of this kind is necessary to understand community-level response to environmental change.

The challenge of data collection in large, biologically diverse forests is one of the reasons there has been very little research on these communities compared to coastal salt marshes. Given the short time frame of this study, 7-13 years between repeat surveys, it is particularly surprising to see that some sites showed such large changes in both composition and in total basal area. Interestingly, even though many of the sites were mature forests, sites that were losing basal area were generally those that had less starting basal area, which helps to rule out the hypothesis that sites with low growth were simple at a growth plateau (Appendix A: Figure 29).

The environmental characteristics investigated in this study, namely elevation and soil ion content, are indicative of past saltwater exposure but not exposure mechanism (Ardón *et al.* 2016). In this region, drought plays a significant role in concentrating solutes in surface

water and soil moisture. Storm surges from hurricanes and other storms also play a large role in delivering salt inland in this region and other parts of the world (Conner 1995; Doyle *et al.* 2007; Hoepfner *et al.* 2008). Human induced climate change may increase the prevalence of storm events across the globe and the Southeastern US is expected to experience more hurricanes (Doyle *et al.* 2007). Short-duration flooding events associated with storms bring a combined threat of stress from inundation and salinity: oxygen deprivation from waterlogged soils and osmotic stress from salts (Jackson and Colmer 2005; Munns and Tester 2008). While plants may often recover from acute short term salinity stress, recurring short term exposure may eventually lead to plant community shift. Low elevation coastal forests are particularly vulnerable to this threat and may not be able to cope with a shifting baseline for flood exposure.

Future work should consider the influence of local weather patterns that drive or exacerbate the chronic effects of sea level rise including floods and droughts, as well as the multiple anthropogenic stressors that impact ecosystems such as pollutants, fire and land-use change. Results from this study, which indicate a potential shift in the carbon storage capacity of coastal forests, should prompt further investigation of how carbon stocks, particularly in trees, are changing in response to global change. Finally, in order to overcome the methodological limitations of studying vegetation change, future research should consider the efficiency of scale and move to remote sensing tools for detection and monitoring of plant community change.

3

Rapid deforestation of a coastal landscape driven by sea level rise and extreme events

Emily A. Ury, Xi Yang, Emily S. Bernhardt, and Justin P. Wright

This chapter is adapted from its published form in

Ecological Applications (2021)

Author Contributions: EU, JW, and EB conceived of the ideas and project design, EU and XY performed the remote sensing analysis, EU and EB led the writing of the manuscript and all authors contributed substantially to revising the writing and gave final approval for publication.

3.1 Introduction

Climate change is transforming landscapes around the world and in the case of many coastal regions, change is occurring faster than ecosystems are able to adapt. Sea level rise may inundate up to 76,000 km² of land in the coterminous US alone (Haer *et al.* 2013). Around the world, coastal landscapes are experiencing inundation, saltwater intrusion, coastal storms and other extreme events associated with anthropogenically driven climate change (Meehl *et al.* 2007; Church *et al.* 2013; Cloern *et al.* 2016). Shoreline loss and marsh migration are well documented ecosystem responses to sea level rise (Wasson *et al.* 2013; Fagherazzi *et al.* 2019), however, in low-lying coastal plain landscapes, the impacts of sea level rise and saltwater intrusion are not confined to the coastal margins (Manda *et al.* 2014; White and Kaplan 2017; Bhattachan *et al.* 2018). Low-lying coastal landscapes often support forested wetland vegetation; these tree-dominated communities are not well adapted to permanently saline conditions and their response to sea level rise is not well understood (Munns and Tester 2008). The Atlantic Coastal Plain of North America is characterized by bottomland forested wetlands and fringing marshes (Brinson 1991). These wetlands are important wildlife habitat, provide valuable ecosystem services, and are globally important carbon sinks (Brinson 1991; Duarte *et al.* 2013; Spivak *et al.* 2019).

Historic land use of coastal plain regions has resulted in a landscape that is particularly vulnerable to sea level rise. The construction of drainage ditches for agriculture and channelization for navigation has increased the connectivity of the landscape interior to saline coastal waters (Bhattachan *et al.* 2018). Salt moves up-gradient due to diffusion and its effects on vegetation often precede other visible evidence of sea level rise (Tully *et al.* 2019). Land drainage for agriculture and forestry has further accelerated the effects of sea level rise by

inducing subsidence of the ground's surface through oxidation of previously anoxic soils (Holden *et al.* 2004). As a result, modification of coastal plain landscapes has altered the pathways and spatial patterns of ecological change.

Extreme events further complicate our attempts to measure and predict salinization in coastal landscapes and increases in the number of extreme events (storms, drought, fire and flooding) are an additional impact of climate change (Meehl *et al.* 2007). Without accounting for disturbance events, elevation is the primary determinant of the forest-marsh boundary and the rate of lateral wetland retreat (Schieder and Kirwan 2019). However, disturbance events, which are prevalent in coastal environments, exert control on the timing and pace of lateral retreat. Both coastal storms and droughts can increase the inputs of saltwater into coastal interiors (Tully *et al.* 2019). Major coastal hurricanes can reverse the flow of water in coastal creeks and canals and deliver sea spray far inland. Droughts in these low elevation landscapes can allow wind tides to mix saltwater miles upstream through stagnant creeks and canals. These disturbance driven inputs of marine salts exacerbate the gradual processes associated with sea level rise, leading to an “ecological ratchet” effect, whereby each salt loading disturbance enhances the potential for an ecosystem state change to occur in response to chronic sea level rise (Fagherazzi *et al.* 2019; Hillebrand and Kunze 2020). The location and timing of extreme events may thus determine much of the spatiotemporal patterns of coastal landscape change.

One of the most striking transitions observed in coastal landscapes in recent decades is the rapid mortality of entire stands of trees, or “ghost forests,” characterized by a high density of standing dead trees and indicating recent, rapid, and synchronous tree mortality (Kirwan and Gedan 2019). Recent work in coastal forests around the Chesapeake Bay describes a fringe of ghost forest at the transition between healthy trees and migrating salt

marshes (Schieder and Kirwan 2019). Indeed, we might expect this ghost forest fringe to be the natural outcome of marsh migration in response to sea level rise marking the inland extent of saline conditions. Coastal trees can withstand periodic salinity exposure, but the osmotic stress of chronically saline conditions will impede germination and eventually lead to tree mortality (Munns and Tester 2008; Kirwan and Gedan 2019). In this study, we seek to understand the rates and spatial patterns of ghost forest formation and other pathways of coastal vegetation change in service of understanding the drivers and extent of change in coastal plain landscapes.

Remote sensing is valuable for understanding landscape-scale response to changing environmental conditions. Numerous remote sensing platforms, sensors and techniques have been used to study vegetation and vegetation change—among them the Landsat satellite record holds one of the longest running datasets which can be applied to look at change over time (Adam *et al.* 2010; Kennedy *et al.* 2014). Here, we demonstrate the utility of remote sensing time series for understanding ecosystem responses to global climate change. We measured the magnitude, the trajectory and the spatial distribution of land and forested wetland loss throughout this vulnerable coastal landscape over the last 35 years. We asked three questions. First, what proportion of the land area and of forested wetlands were lost? Second, to what extent do losses of land and forest occur beyond the coastal fringe? Third, are the temporal trends in land and forest loss driven by gradual sea level rise or by extreme events?

3.2 Methods

3.2.1 Study location

The Atlantic Coastal Plain of the United States is experiencing rapid rates of relative sea level rise – estimated 3-4 mm/year compared with global mean sea level rise of 1-2 mm/year (Douglas and Richard Peltier 2002; Church *et al.* 2013). Protected by a string of barrier islands, the Coastal Plain of North Carolina is characterized by large areas of intact coastal forest at low elevation and with little topographic relief. The Alligator River National Wildlife Refuge (NWR) is the second largest protected area in the state of North Carolina and an ideal place to study the pace and drivers of vegetation change because of the distinct lack of development, forestry, and other anthropogenic activities. The median elevation of our study area is less than 0.5 meters above sea level. Soils are largely peat based and poorly drained with water table depth ranging from -20 cm to +10 cm above the ground (Poulter 2005). The region was also extensively drained for agriculture and forestry during the mid-20th century resulting in a dense network of ditches and canals across the landscape (approximately 4 km of drainage length per square-kilometer area) (Poulter and Halpin 2008).

Vegetation includes high and low pocosins (poorly drained peatlands of the South Eastern United States characterized by dense shrubby vegetation), freshwater and brackish marshes (mainly *Caladium jamaicense* and *Spartina sp.*), hardwood swamps (various *Quercus* species, *Acer rubrum* and *Liquidambar styraciflua*) and bald cypress (*Nyssa sylvatica*) (Brinson 1991). The Refuge was established in 1984 to protect the unique pocosin wetland habitat and associated wildlife including several endangered species: the red wolf, the red-cockaded woodpecker and the American alligator as well as the globally threatened Atlantic white cedar (*Chamaecyparis thyoides*) ecosystem. The specific region of interest includes most of Alligator

River NWR and surrounding natural lands but excludes major roads, waterbodies, agricultural land and the Dare County Bombing Range (Figure 6). The study area was affected by the Pains Bay Fire during the summer of 2011 and Hurricane Irene which made landfall in August of the same year. The fire affected approximately 97 km² within the 615 km² refuge (US Fish and Wildlife Services Southeast Region Fire Management Organization 2011) and the hurricane brought a 2-meter storm surge to the nearest gauge station in the Pamlico Sound (NOAA 2016). The storm surge was said to have inundated the Refuge with water cresting over Highway 264, more than 2 km inland from the coast (conversations with refuge manager Scott Lanier).



Figure 6: Study location in Eastern North Carolina (green shaded area).

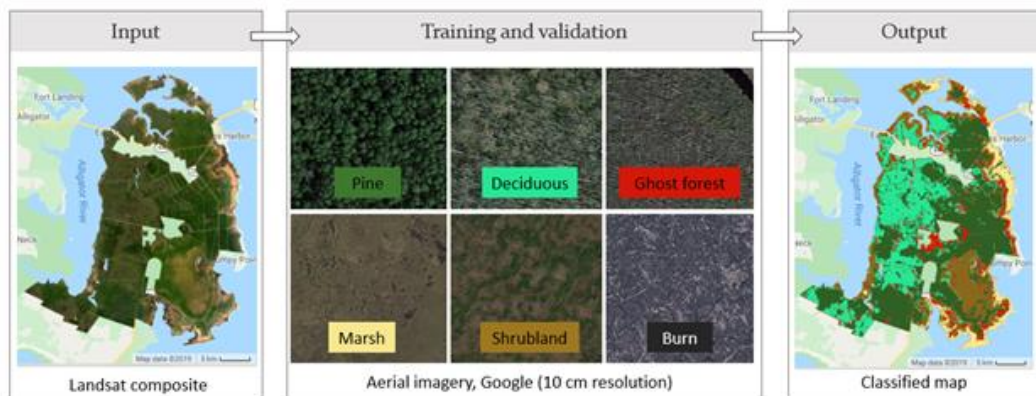


Figure 7: Classification schematic and examples of each vegetation class as seen in Google Earth imagery.

3.2.2 Image pre-processing

Google Earth Engine (GEE) was used to generate annual composite images using scenes from the Landsat Satellite record from the United States Geological Survey (USGS). We used images from three of Landsat's instruments, Landsat 5 Thematic Mapper (TM), Landsat 7 Enhanced Thematic Mapper Plus (ETM+) and Landsat 8 Operational Land Imager (OLI) to span the period from 1985-2019. For each imager, only the atmospherically corrected Tier 1 Surface Reflectance product was used. All available scenes of the study region were clipped to apply a water mask generated from the same year's annual water occurrence values from the JCR Yearly Water Classification History (Pekel *et al.* 2016). For each year we used both a winter (November – March) and summer (May – September) composite to generate the input to our classifier. The composite for each season is generated from the stack of images within the seasonal window, clouds and cloud shadow pixels were masked out, and pixels were reduced to the median reflectance of each band. Each composite was inspected for clouds and other artifacts or distortions, and if present, the contributing images were removed individually. For some years, a suitable composite was not achieved and thus left out of the analysis. The two seasonal composites were combined such that the input for the classifier contains twelve bands in total, six (blue, green, red, NIR, SWIR1 and SWIR2) from each season.

3.2.3 Land Cover Classification

Training data for vegetation classes was collected from Google Earth imagery (collected March 24, 2017, 10 cm RGB) and from North Carolina orthophotos available from the USGS (collected Feb 28, 2012 and April 11, 2010, 15 cm RGB). Randomly generated validation points ($n = 500$) were classified by hand with additional points added to improve spatial coverage of all classes. Vegetation was classified into the following categories: pine, deciduous, shrub,

marsh, and ghost forest. Ghost forest pixels were characterized by the density of visibly dead trees present in the high-resolution imagery. Ghost forest stands are easily distinguished due to the lack of branches on snags and the presence of fallen tree trunks. Because the orthophotos were collected in the winter, it was easy to distinguish between the pine and deciduous classes (see Figure 7). For some analyses, pine and deciduous classes are combined into one class: 'forested wetland'. There is no need to distinguish between forested wetland and upland forest in this study because the entire region is considered wetland (either woody or emergent herbaceous) according to the USGS National Land Cover Database (Yang *et al.* 2018). The shrubland class consists of mixed scrub-shrub type vegetation, with some herbaceous vegetation visible and large trees mostly absent. The marsh class consists of either freshwater or saltwater herbaceous species. Due to the Pains Bay Fire of 2011 that affected a large portion (16%) of the study area, a burn category was also included in the 2012 imagery demarcating areas which burned beyond reasonable recognition of the vegetation. In 2012, large areas of pine trees exhibited browning needles, most likely due to drought or fire. These trees largely recovered in subsequent years, but the unusual coloring reduced the accuracy of the classifier, so an addition class was added in 2012 (called "dry pine") which was then later merged back into the pine class for analysis.

We used a random forest decision tree algorithm (Breiman 2001) to classify the composited inputs for each year of training datasets (2010, 2012 and 2017). Our use of spectral signatures for detecting and classifying vegetation follows standard approaches of remote sensing land cover land use classification (Asner 1998; Ustin *et al.* 2009; Ustin 2013). The reflectance of bare tree trunks is distinct from both live trees and understory vegetation allowing us to detect ghost forests as a unique class. Accuracy assessment was performed on

these years using k-fold cross-validation with 5 groups. The classifier that was trained on 2017 data was then applied to the other annual composites from Landsat 8 OLM (2015-2019). The classifier that was trained on 2010 data was used to classify the composites from Landsat 5 TM (1985-2011).

3.2.4 Statistical Analysis

Statistical analyses were run in the R statistical computing environment (R Development Core Team 2017). Classification was done using the R package “randomForest” (Liaw and Wiener 2002) with Ntree and mtry default values. Other R packages used for data transformation and visualization included “raster” (Hijmans 2020), “rgdal” (Bivand *et al.* 2016), “alluvial” (Bojanowski and Edwards 2016) and the *Tidyverse* (Wickham *et al.* 2019). We used bivariate logistic regression (`glm()` function, family = binomial) to determine the influence of topographic characteristics on forest loss and ghost forest formation. In these models, forest loss is a binary response variable indicating if a pixel was classified as forest at the start of the study period but not at the end. Environmental predictors for channels and coastline were generated by calculating a simple linear distance raster in R using tools from the “raster” package and derived from the National Hydrography Dataset (NHD) flowlines for the State of North Carolina and 30m resolution Digital Elevation Model (DEM) from the USGS. A bootstrapping approach with random draws of 1000 pixels using a 500 m exclusionary buffer was used to generate model input data as a means of reducing spatial autocorrelation among covariates.

3.3 Results

The results from our classification demonstrate that it is possible to detect coastal ghost forests using Landsat imagery. The overall accuracy for all five classes was 92.2% for the Landsat 8 classifier, 82.5% for the Landsat 7 classifier and 82.3% for Landsat 5 classifier. The average producer accuracy and user accuracy for the ghost forest class is 88.8% and 85.5%, respectively. In the orthophotos used for training data, each point characterized as ghost forest contained approximately 20-40 visible snags or fallen tree trunks per Landsat pixel (about 220-440 dead trees per hectare). In a random sample of Landsat pixels classified as ghost forest, the mean number of snags and fallen trunks per pixel was lower (mean = 13, n = 50), which is likely due to bare ground reflectance which also contributes to the spectral characteristics of a ghost forest pixel. This may suggest a slight overfitting of the ghost forest class, however the overall accuracy for this class is still quite good (see Appendix B: Table 10). We assume that the overall accuracies are a good approximation of the accuracy of each map produced with the respective classifier. Lower accuracy from the older imagery is due in part to a lack of validation points within the ghost forest class (there simply were not as many ghost forests present at that time on which the classifier could be trained). We found that using both a winter and summer composite image greatly enhanced the classifier's ability to distinguish between the pine, deciduous and ghost forest categories; in summer the pine/deciduous distinction is more difficult to parse and in winter the deciduous/ghost forest signatures are similar, but combining summer and winter reflectance enables us to distinguish between all three. Overall, pine, deciduous and marsh were the most successfully distinguishable classes for the classifiers and shrub and ghost forest were more difficult to parse out (see complete confusion matrices in Appendix B: Table 11, Table 12, and Table 13).

In this 99,347 hectare (ha) study area, 77% (76,575 ha) was forested wetland in 1985. Over 35 years, the refuge has lost 1,151 ha of land (1.2%) to open water and had a net loss in forest cover of 15,811 ha (Table 2). Most strikingly, of the 76,575 ha that were forest in 1985, 21,097 ha (27.6%) transitioned to either shrub, marsh, ghost forest or open water by 2019. In fact, only 69.2% percent of this protected wildlife refuge has not experienced a vegetation transition over the last 35 years (shown in light gray in Figure 8A). Of the forest classes that transitioned to non-forest classes, 40.8% (8616 ha) went through a detectable ghost forest stage at some point during the study period (these are the pathways shown in red in Figure 8B). The majority (17,115 ha, 81%) of the forested area that transitioned is now categorized as shrubland. Parts of the Refuge have experienced forest regrowth (mainly from shrubland) totaling 5,287 ha. The marsh class has grown about 7% over the study period however its position on the landscape has shifted: marshes are moving inland to areas that were shrub and forest as the shoreline retreats. The conversion to marsh is occurring both with and without a ghost forest transition state (Figure 8B), which may indicate the relative contributions of multiple mechanisms driving vegetation change.

Table 2: Summary of net area change for each vegetation class (in hectares).

Class	1985	2019	Net Change
Pine	27,483	20,205	- 7,279
Deciduous	49,092	40,560	- 8,532
Ghost forest	66	2,051	+ 1,985
Shrub	13,798	25,850	+ 12,052
Marsh	8,907	9,530	+ 623
Open Water	0	1,151	+ 1,151

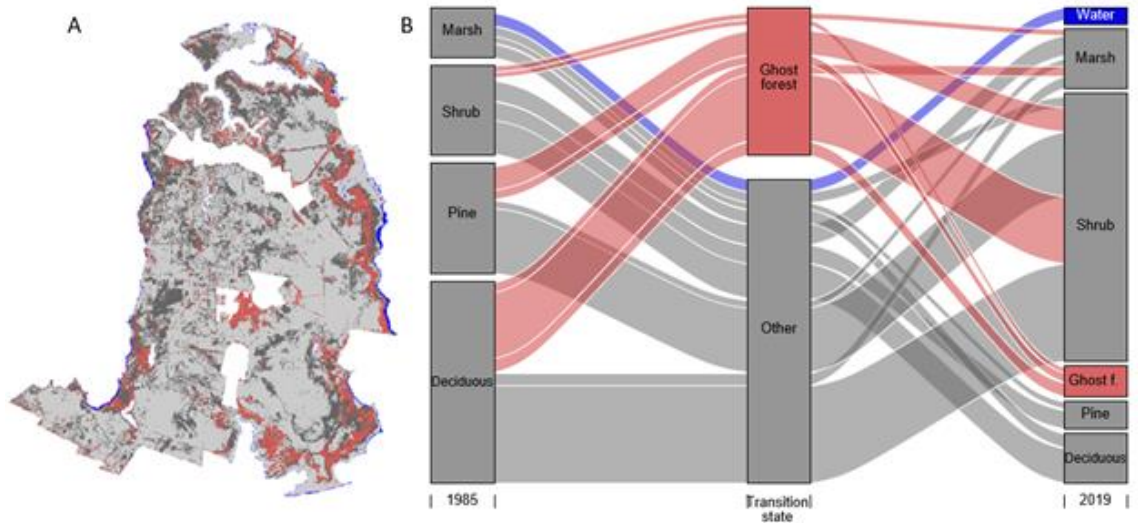


Figure 8: Areas of vegetation change in the Alligator River National Wildlife Refuge.

(A) Map of areas that have undergone change since 1985. Blue denotes the conversion from land to open water, red indicates transition through ghost forest at any point in time, dark gray are all other changing areas and light gray indicates no change. (B) For the changing pixels only, the alluvial plot shows the relative frequency of the various transition pathways.

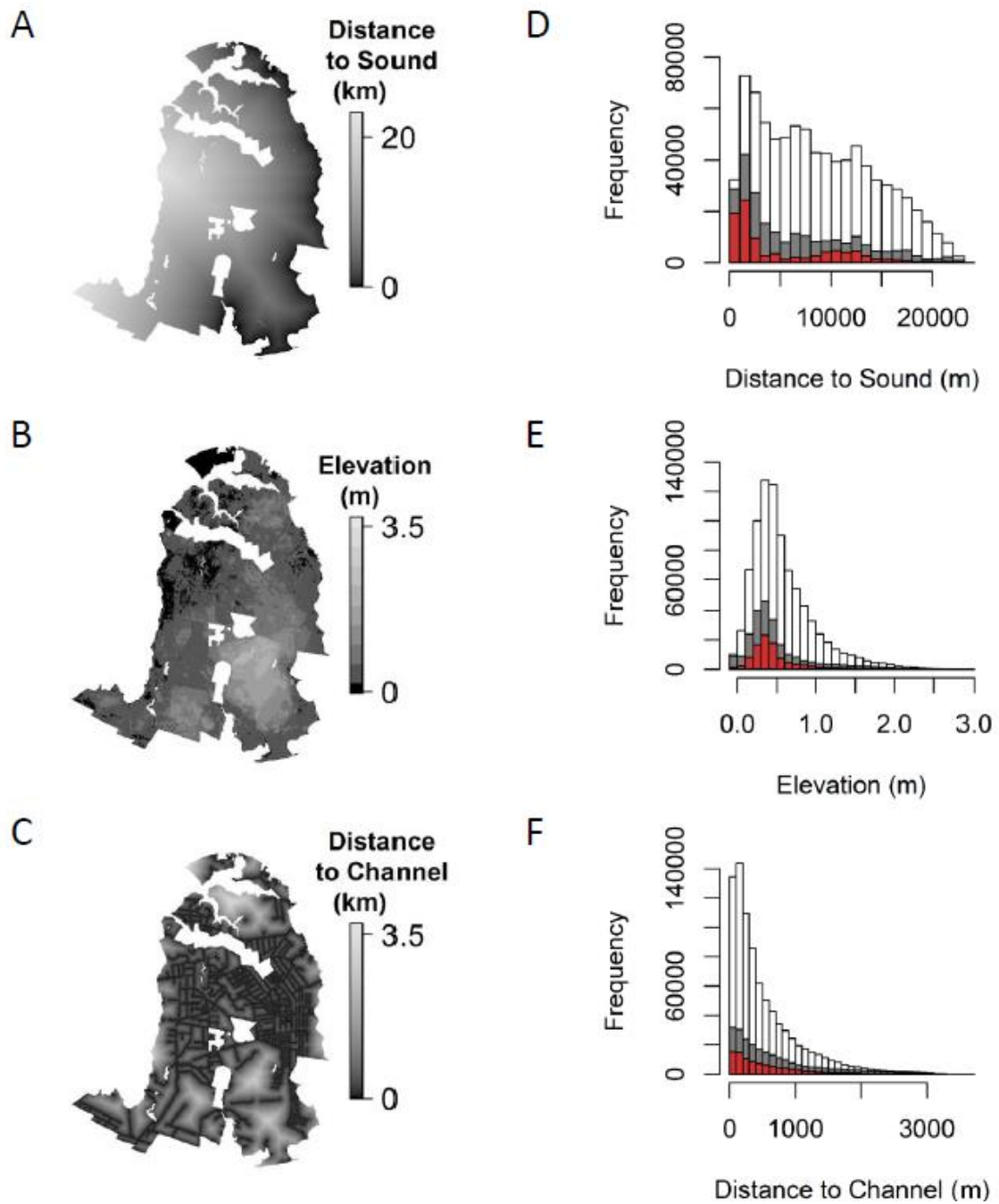


Figure 9: Maps of spatial predictors of vegetation change. (A) distance to the sound, (B) elevation above mean sea level, and (C) distance to a channel. Histograms of the distribution of forested pixels (white), pixels where forest cover was lost (gray), and forest pixels that went through a ghost forest state (red) across the same topographical parameters are shown in D-F.

The spatial distribution of change within the refuge is most heavily concentrated along the coasts, and the eastern side along the Sound is more severely affected than the western coast on the Alligator River (see the map in Figure 8 and histogram in Figure 9D). The distribution of forest loss is concentrated on the eastern side of the refuge, however 59% of forest loss is occurring in the interior part of the landscape (more than 1000 meters from either coast). The distribution of forest loss is more concentrated at low elevations (Figure 9E). The distribution of forested pixels and forest loss based on distance to channel is heavily right-skewed owing to the prevalence of channels in this landscape (Figure 9F).

Each of the topographic predictors in the spatial models of forest loss and ghost forest formation (binary response variables) are statistically significant (p values <0.001) drivers of these transitions except for distance to channel on ghost forest formation (p value = 0.11) (Figure 10). The spatial autocorrelation of some variables (e.g., topography) violates the assumption of independent observations, and reduces the effective sample size. However, using random subsets of the data reduces the effect of autocorrelation (Moran's I is reduced for each model from 0.86/0.71 to 0.39/0.21), and the subsequent impact on the p -values is negligible. Distance to the Sound (the eastern shore of the refuge) was the strongest predictor of both forest loss and ghost forest formation compared with elevation and distance to a channel. We standardized the predictor variables in the linear model such that the slope coefficients may be compared to determine the relative strength of each predictor on the outcome of a forested pixel. The coefficient estimate for distance to the Sound was -0.839 (95% CI -1.01 – -0.669) for forest loss and -0.906 (95% CI -1.12 – -0.689) for ghost forest formation. Negative coefficient estimates indicate that forests closer to the coast are more likely to undergo these types of transitions. The coefficient estimate for elevation was -0.673

(95% CI -0.862 – -0.485) for forest loss and -0.677 (95% CI -0.928 – -0.426) for ghost forest formation; forests at lower elevation are more likely to transition. The coefficient estimate for distance to a channel was +0.239 (95% CI 0.098 – 0.380) for forest loss and -0.170 (95% CI -0.357 – 0.018) for ghost forest formation. The effects of proximity to a channel are of lesser magnitude and are inconsistent: forested wetlands are less likely to be lost alongside channels, but the effect on ghost forest formation is not statistically significant. We speculate that adjacency to a channel may be associated with less drought risk for much of the area and for the possibility of event-based salinization and mortality for trees alongside canals nearest to the sound. The ghost forest response variable indicates a ghost forest was detected at any time during the time-series but modeling each year individually shows that the relative importance and even the direction of these relationships vary across the time series (see Appendix B: Figure 30).

The changing areas of Alligator River NWR are shown in Figure 11A for the entire period of study. The steady loss of land to open water is apparent in the blue wedge along the x-axis. In contrast to the linear pace of land conversion to open water, the vegetation classes fluctuate over time (10-20% of this fluctuation maybe attributed to classification error). The forested area (pine and deciduous classes combined) is declining over time and the shrubland is expanding. The formation of ghost forest happened most dramatically between 2011 and 2012 and although the rates of ghost forest formation remain high (Figure 11B), the total area of ghost forest on the landscape declines after peaking in 2012. We address the possible reasons for the observed timing of ghost forest formation in the discussion, but the direct hit of Hurricane Irene in the study region is a notable factor.

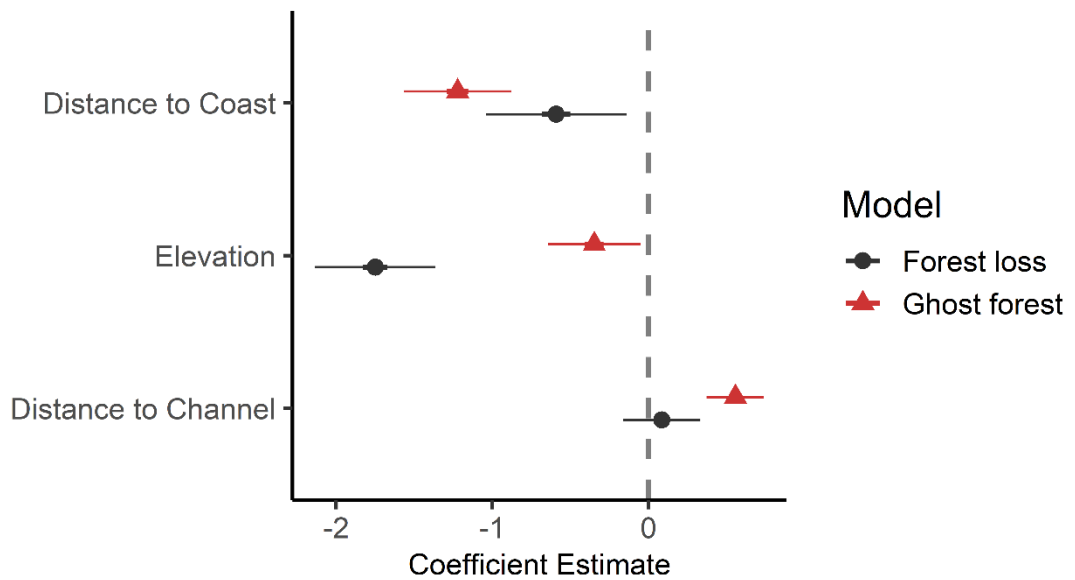


Figure 10: Model coefficient estimates for drivers of vegetation change. Distance to the Sound is the dominant controlling factor of ghost forest formation (red triangle) and forest loss (black dot) followed by elevation and distance to channel (coefficient estimates shown with 95% confidence interval). Predictors with negative coefficients increase the risk of forest loss and ghost forest formation.

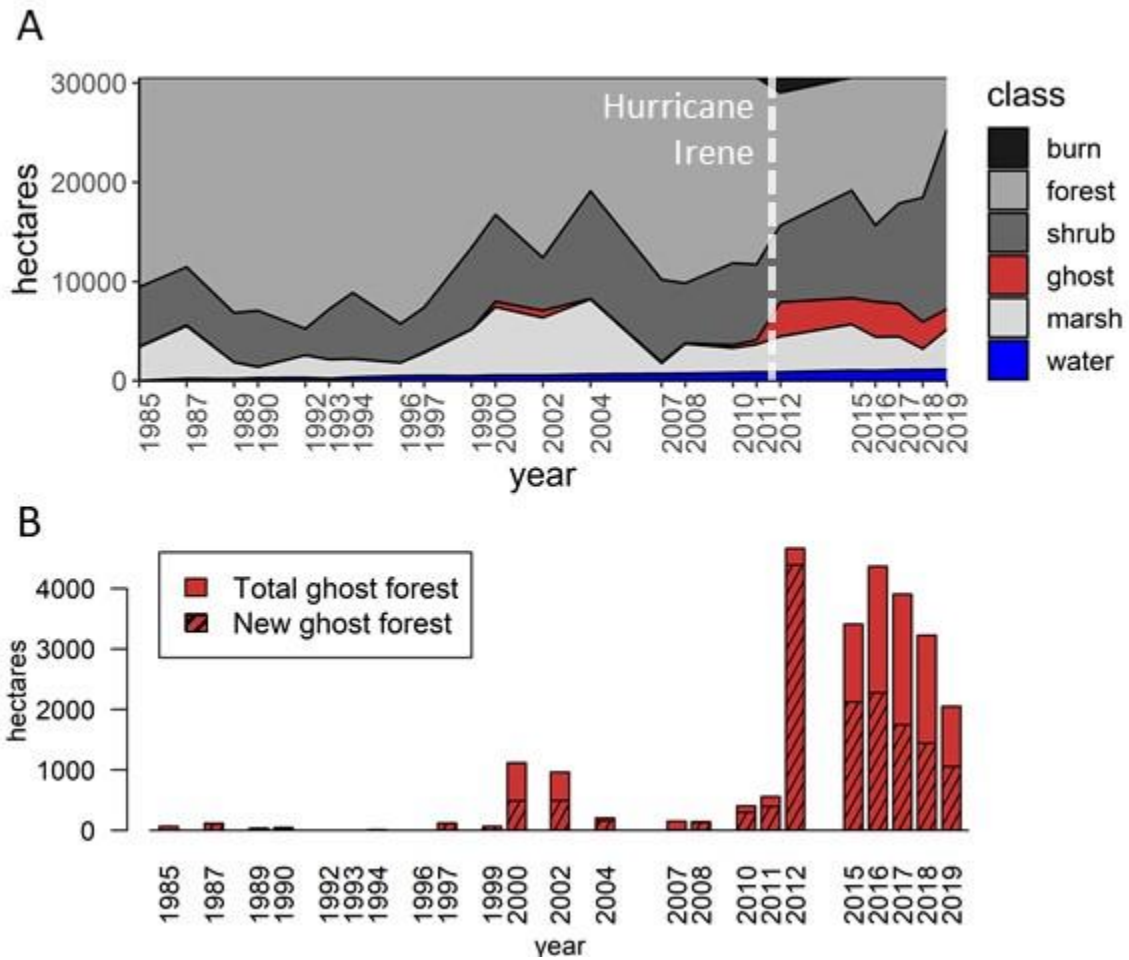


Figure 11: Timeseries of change in Alligator River National Wildlife Refuge. (A) Areas of the study region that changed vegetation class between 1985 and 2019 (pine and deciduous classes were combined to 'forest' and data was interpolated linearly across years missing data). The formation of ghost forest (red) shows a marked increase following Hurricane Irene. The Pains Bay Fire (summer 2011) left a large burn scar on the land which was visible in the 2012 imagery. (B) Extent of ghost forest observed each year with the hashed area representing areas not classified as ghost forest in the previous year and considered newly formed.

3.4 Discussion

Despite its protected status and the absence of any timber management, more than 19,000 ha of freshwater wetland forests have been lost from the Alligator River NWR since 1985. We determined that 30.8% of the landscape in our study region has experienced a transition of vegetation type within the last 35 years. The magnitude of forest cover lost is far greater than the amount of land lost outright to open water over the same time period (~1150 ha). Forest loss was concentrated in a band approximately 1 km inland from the coastal margin, and was greater in extent on the eastern, more saline shores of the Albemarle-Croatan-Pamlico Sound than on the western side along the Alligator River estuary. This forested wetland loss was not just on the shoreline, with more than half of all forest loss occurring in the interior of the refuge. While the trajectory of land loss in the study area was linear, forest loss was not. Instead, most of the ghost forest formation occurred within the last decade following a series of extreme events including 5 years of drought (2007-2011), a major fire and Hurricane Irene (both in 2011).

This analysis is the first reported attempt to use remote sensing to map the spatial and temporal distribution of coastal ghost forests. We were successful at training a classification algorithm to detect these unique transition states. Our analysis shows that ghost forests are both a prevalent and a transient feature in the Coastal Plain of North Carolina. We were surprised by the rapidity with which formerly forested patches transitioned through the ghost forest phase into shrublands or marsh, with pixels typically classified as ghost forests for no more than a few years. A portion (26.1 %) of the ghost forests detected earlier in the record (before 2010) have returned to a forested state, but for most pixels the ghost forest stage appears to represent a transition to non-forest vegetation cover. Most of the ghost forests

have become shrublands. We do not yet know whether the resulting increase in scrub-shrub wetlands represents an expansion of native plant communities that are characteristic of this habitat type or the creation of novel or random assemblages. The impact of these widespread ecosystem transitions on biodiversity and community composition deserves further study. A portion of forest becoming scrub-shrub does not transition through a ghost forest stage which we attribute to gradual tree mortality and forest thinning without replacement rather than mass tree mortality events that lead to large numbers of standing dead trees. The shrubland land-cover type is rapidly expanding in area and represents a major shift in ecosystem structure whose consequences for carbon storage and other ecosystem services have not yet been quantified.

If sea level rise were the primary driver of forested wetland loss, we would expect to see a linear rate of vegetation change and confinement of forest loss to shorelines. Instead, the spatial distribution of forested wetland loss appears more consistent with saltwater intrusion, while the timing suggests that extreme events are leading to forest mortality. In this landscape of low topographic relief and shallow groundwater, all hydrologically connected areas are potentially vulnerable to saltwater intrusion (Bhattachan *et al.* 2018; Zhang *et al.* 2018, 2019). Marine salts move inland as a result of diffusion and wind tides during droughts as well as during hurricane storm surges (Manda *et al.* 2014, 2018; Tully *et al.* 2019). The greatest period of ghost forest formation (2011-2012) followed Hurricane Irene which arrived after nearly 5 years of drought. While vegetation may still be in the recovery phase following these more recent disturbances, some areas may not recover, having been pushed too far into a new state. The combination of these two stressors may have been responsible for the increase in ghost forest formation, an interaction effect that may become more prevalent in the future as

climate is leading to an increased frequency of extreme events (Meehl *et al.* 2007; Miao *et al.* 2009).

Our study area represents only a small fraction of the 97,000 km² of palustrine forested wetland in the coastal plain of Eastern North America (NOAA 2016). By definition, these are low-lying coastal forests that are vulnerable to rising sea levels, saltwater intrusion and coastal storm damage. If the rates of change observed in this study are consistent across the entire North Atlantic Coastal Plain, climate deforestation could have already resulted in a tremendous loss of these unique ecosystems from North America. Field surveys have already documented dramatic losses of freshwater forested wetlands in the region (Desantis *et al.* 2007; White and Kaplan 2017; Taillie, Moorman, Poulter, *et al.* 2019; Kirwan and Gedan 2019; Ury *et al.* 2020). There is no reason to expect the east coast of North America to be an outlier in the vulnerability of its coastal forested wetlands. Indeed, a recent analysis suggested that parts of Northern Europe, Chile, Australia and particularly South East Asia will experience the most severe effects of climate driven losses of coastal plain wetlands (Blankespoor *et al.* 2014).

The extensive transformation of coastal plain vegetation we observed has taken place despite the protected status of the refuge and active management to maintain endemic and rare plant communities (Laderman 1989; Poulter and Halpin 2008). In many other coastal plains, historic drainage and deforestation have confined endemic forested wetlands to the limited areas where drainage is very costly. These remnant wetland forests, which maybe the last stronghold and seedbanks for threatened species such as the Atlantic white cedar (*Chamaecyparis thyoides*) (Laderman 1989), may now be especially vulnerable due to their landscape position. Already the loss of forested freshwater wetlands in coastal North Carolina has been linked to declines in bird diversity (Taillie, Moorman, Smart, *et al.* 2019).

Because freshwater forested wetlands are known to be important global carbon sinks (Brinson 1991), their conversion to shrublands may create positive feedbacks to climate change (Duarte *et al.* 2013; Spivak *et al.* 2019). Forested wetlands have far higher aboveground biomass than the shrublands that replace them (Kirwan and Gedan 2019). The effects of salinization on the carbon stocks stored in freshwater wetland sediments are less certain. Recent experiments in the Florida Everglades showed that salinization led to rapid declines in soil elevation and large soil carbon losses in freshwater and brackish wetlands (Charles *et al.* 2019), while gradient studies in North Carolina documented reductions in soil respiration and methane emissions during periods of saltwater intrusion (Helton *et al.* 2019).

We suggest that coastal forested wetland loss represents an important new class of climate change-driven ecological shifts akin to the desertification of drylands (Huang *et al.* 2016; Berdugo *et al.* 2020) and the shrubification of arctic tundra (Myers-Smith and Hik 2018; Pastick *et al.* 2019). Like these other examples, rising water tables and salinization ultimately will shift these formerly freshwater forests into a new ecosystem state (*sensu* Scheffer (2009)) since salinization and sulfidation of soils ultimately prevent the regeneration of shrubland back into coastal forests (Munns and Tester 2008; Fagherazzi *et al.* 2019).

Efforts to forecast the potential for global coastal wetland loss have focused almost entirely on sea level rise. Schuerch *et al.* (2018) estimated up to 30% of all coastal wetlands could be subsumed by the sea by 2100. Other recent papers suggest that an even larger proportion of coastal wetlands are vulnerable (Kirwan *et al.* 2016; Spencer *et al.* 2016). When we consider the likelihood of wetland loss in the coastal plain interior due to ecosystem salinization, these estimates are likely to increase in magnitude. Perhaps more importantly, considering both salinization and saltwater intrusion will require us to expand the range of

coastal wetland types that are vulnerable to climate change. Our analysis shows that ghost forest formation can be associated with *both* episodic disturbances (i.e., hurricanes) and the gradual progression of sea level rise and that landscape features such as drainage ditches can increase local vulnerability. We suggest that an analysis of coastal freshwater wetland vulnerability at a global scale is urgently needed. In addition to determining what proportion of interior freshwater forested wetland habitats have already been lost, new remote sensing technologies may enable us to detect vegetation stress and vulnerability prior to forest mortality, that could guide more effective and strategic protection and management.

4

Ecosystem carbon consequences of a four-year salt addition experiment in a coastal forested wetland

Emily A. Ury, Marcelo Ardón, Justin P. Wright, and Emily S. Bernhardt

4.1 Introduction

Sea level rise and salinization are impacting coastal wetlands and their ecological functions. Coastal wetlands provide a suite of ecosystem services, including coastal protection, habitat provisioning, water filtration and long-term carbon storage (Kirwan and Megonigal 2013). Coastal freshwater wetlands, whose plants and soils are not adapted to saline conditions, may experience a reduction of ecosystem services or collapse altogether as a result of sea level rise (Herbert *et al.* 2015; Tully *et al.* 2019). There is evidence of widespread landscape change in coastal regions as a consequence of sea level rise and salinization (Ury *et al.* 2021, White *et al.* in review). Landscape characteristics such as geomorphology, ditching, and agricultural legacies may exacerbate wetland vulnerability to sea level rise (Bhattachan *et al.* 2018). Yet there is considerable uncertainty and inconsistency in the literature on ecosystem responses to salinization in these potentially vulnerable systems.

Ecosystem responses to salinity are complex because sea water's many constituents (chloride, sulfate, sodium, other base cations, and trace minerals) have numerous direct and indirect effects on organisms and wetland chemistry. Salinity induces osmotic stress on plants and microorganisms, as well as changes the pH and redox status of wetland soils and porewater, affecting biochemical interactions and processes within the soil matrix (Rath and Rousk 2015; Herbert *et al.* 2015). Sulfidation, another result of seawater exposure in wetlands, is also harmful to many taxa, but may be of less concern in iron rich soils (Schoepfer *et al.* 2014). Base cation build-up following repeated exposure to salt water may alter the alkalinity status of soils further impacting soil microbial functioning (Kaushal *et al.* 2018). Additionally, there may be indirect effects of salinity and feedbacks between the different constituents within wetland ecosystems; in particular, responses of plant-soil feedbacks to the salinization of freshwater wetlands have not been well studied. Geographic context such as vegetation and edaphic factors may be mediating the effect of salinity on soil microbial functions, effects that are difficult to study in a laboratory setting or single location studies.

Previous salt addition experiments have shown a surprising degree of divergence in response to salinity, which may be in part due to a lack of understanding of key environmental covariates. Several salt addition experiments have shown salt suppression of carbon mineralization (Ardón *et al.* 2018; Doroski *et al.* 2019; Wen *et al.* 2019), while others show salt stimulation of soil respiration (Weston *et al.* 2006, 2011; Chambers *et al.* 2011; Neubauer *et al.* 2013). The interaction between salinization and carbon availability within soil porewater may indirectly affect carbon mineralization rates beyond the direct effects of osmotic stress on soil microbes (Neubauer 2013; Ardón *et al.* 2016). Vegetation, which may play an important role in the mediation of salinization effects on soil carbon processing, is often left out of

experimental design for the sake of reducing study complexity. Studies that do include vegetation are typically conducted in salt marshes or in mesocosms with herbaceous plants, occasionally saplings, but seldom if ever, with full grown trees. To date, no large-scale, long-term field salinization experiments have been conducted in forested freshwater wetlands, but these ecosystems are highly vulnerable to coastal change.

We established a large-scale salt addition experiment in a freshwater forested wetland in coastal North Carolina to address the question *how does salinization of a freshwater wetland affect ecosystem processes and how do these effects change over time?* Our aim was to study ecosystem responses to marine salt addition in a field setting in an area large enough to affect the entire rooting zone of numerous trees. Our specific objectives included tracking above- and belowground biomass responses to elevated salinity, as well as soil carbon dynamics, and quantifying both the spatial and temporal variability in the responses to salt additions. Prior work at our study site in small plots demonstrated salt suppression of carbon dioxide fluxes with elevated salinity, but the effect was contingent upon hydrologic context (Helton *et al.* 2019). We predicted that salinity would adversely affect plant growth and soil microbial activity leading to a reduction of both pools and fluxes of carbon within these wetlands.

4.2 Methods

4.2.1 Site description and experimental design

Salt addition plots were established in 2015 in the Timberlake Observatory for Wetland Restoration (see Ardón *et al.* (2010) for addition details about the property) located on the coastal plain of North Carolina. The property is a restored wetland on formerly agricultural land that underwent rewetting and revegetation in 2004 with the planting of 750,000 native

wetland tree saplings. The site is 8 km from the shore of the Albemarle Sound and surface water typically has very low salinity (<0.5 ppt). However, during major drought events, salinity in the channel has been observed to reach over 5 ppt due to saltwater incursion (Ardón *et al.* 2013). There are two main soil series on the property, Hyde loam and Ponzer muck and the dominant tree species are *Taxodium distichum*, *Pinus taeda*, *Salix nigra*, *Liriodendron tulipifera*, and several *Quercus sp.*

A set of salt and control treatment plots were established at three sites, spread out across the property (see Appendix C: Figure 31). A small elevation gradient exists across the property such that the sites at the northern end are more frequently inundated than the site at the southern end. Because of this variation in hydrology, we have monikered the sites as ‘dry’, ‘intermediate’ and ‘wet’, which refers to their average conditions relative to one another. Each salt treatment plot is 10 x 20 meters and was established at least 10 meters away from a control plot of the same size. Salt additions began in the fall of 2016 using Instant Ocean® marine aquarium salt mix, applied dry. Care was taken to ensure an even application of salt across the plot and salt was added at a rate of 68 grams per m² between 3-9 times each year (see Appendix C: Table 14 for a schedule of field activities). Sampling was conducted at least one month following the most recent salt application except for summer 2020 when travel restrictions due to Covid-19 forced us to sample only 4 days following the final salt application.

4.2.2 *Vegetation monitoring*

Prior to the first salt addition, trees within the treatment plots were identified, tagged, and measured (diameter at breast height, DBH) in fall 2015 (note that a maximum of 10 individuals of a single species within each plot were tagged and measured). Tagged trees were re-measured

(DBH) in January 2021. Roots collected in soil cores (described below) were cleaned, dried and weighed during each sampling period.

4.2.3 Soil Collection and analysis

Soil cores were collected from the salt and control plots four times during the last three years: May and July of 2018, June 2019, and August 2020. Each sampling consisted of 5 soils cores collected from a randomly selected transect across the plot. Soil cores, in plastic sleeves were capped and kept on ice during transport back to the lab where they were stored at 4 °C, processed and analyzed within 72 hours.

Soils cores were extruded from their sleeves and sectioned into two depth increments: 0-5 cm and 5-10 cm. The weight of each core section was recorded for estimation of bulk density. Each increment was passed through a 2 mm sieve to remove roots, rocks, and large organic debris. Sieved soil was homogenized and stored in sterile plastic bags. Subsamples of each soil sample were weighed on an analytical balance for the following analyses. Approximately 10 g of soil was weighed in an aluminum tin for measuring soil moisture and organic content by mass difference after 48 hours in a drying oven at 60 °C followed by 4 hours in a muffle furnace at 500 °C. A 5-gram subsample was weighed into a conical tube for measuring pH in a soil-water slurry with a 1:2 ratio using a calibrated hand-held probe device (Hach H260G pH Meter, Loveland, CO).

Five grams each were weighed into amber glass I-Chem™ vials for soil respiration and substrate induced respiration (SIR) assays (soil respiration assays conducted from July 2018 onward). Accumulated CO₂ was measured on LI-6250 flow-through gas analyzer (Li-core Inc., Lincoln, Nebraska, USA) following protocols modified from Fierer et al. (2003) and described in detail in Marinos and Bernhardt (2018). In brief, vials were sealed with a PFTE coated

silicon septa and gas was allowed to accumulate for 24 hours before sampling. The headspace was sampled with a 1-mL glass syringe and injected into the port of the flow-through analyzer. After sampling, vials were vented to prevent anoxia. Vials were recapped 24 hours prior to subsequent sampling on day 3 and 7 of the incubation period. SIR assays were conducted in the same way, with the addition of 10 mL autolyzed yeast solution. Vials remained sealed for the duration of the SIR assay and were kept aerated via mixing on a shaker table. One mL of CO₂ free air was injected into each vial prior to sampling to maintain positive pressure within the jar and samples were drawn and analyzed at 10 minutes, 2 hours, and 4 hours following substrate addition and sealing.

Four grams of soil was weighed into a conical tube for water extraction with a 10:1 water to soil ratio. Soil slurries were shaken on an end-over-end rotating table at 60 rpm for 4 hours. Slurries were allowed to settle overnight at 4 °C and then centrifuged at 3500 rpm for 15 minutes. The supernatant was carefully poured off and passed through a 0.7 µm glass fiber filter. Filtrates were analyzed for ion content and dissolved organic carbon and nitrogen at the Duke River Center on a Dionex ICS-2000 Ion Chromatograph (Sunnyvale, CA) and a TOC-V combustion analyzer (Shimadzu Corporation, Kyoto, Japan).

Filtrate was also analyzed for phenolic compounds using a colorimetric method described in Ohno and First (1998). In brief, 0.1 mL of Folin-Ciocalteu's Reagent and 0.30 mL of 0.5 M NaHCO₃ was added to 1 mL of soil water extract and gently mixed before allowing color to develop for 4 hours. UV-vis absorbance spectra were measured at 750 nm and calibrated against a vanillic acid standard (0 to 10 mg/L). The concentration of phenolic compounds is also reported as mg/mg DOC after normalizing for the concentration of DOC in each extract following Weishaar *et al.* (2003).

4.2.4 Statistical Analysis

Statistical analyses were conducted in the R statistical computing environment (R Development Core Team 2020) with the ‘tidyverse’ and ‘ggplot2’ packages. One-way Analysis of Variance (ANOVA) was used to determine statistically significant differences ($p < 0.05$) between salt and control treatments within a single sampling date, site, and depth increment.

4.3 Results

4.3.1 Direct effects of salt treatment

The salt treatment raised the overall salinity of our experimental plots, though the effect was variable across time and space (Figure 12A and Appendix C: Table 15A-J for significant treatment effects from one-way ANOVAs). In general, the intermediate site achieved the highest salinity levels, followed by the dry and wet sites, respectively. Soil salt content did not build up gradually over time as we had expected, nor was it highly contingent on soil moisture at the time of sampling (Figure 12B). We suspect that cumulative precipitation was driving temporal patterns in salinity in concert with edaphic factor variation between sites. July 2018 and August 2020 had the highest concentrations of salt ions, and June 2019, a much wetter month, had the lowest suggesting that hydrology (precipitation) is a strong driver of ion retention within the soil (see Appendix C: Figure 32).

The effect of the salt treatment also varied between the different constituents of the marine salt mixture being added, though each ion was significantly elevated in the salt plots compared to the controls (see Appendix C: Figure 33). Soils in the dry and intermediate sites retained more potassium and sulfate as a proportion of the amount of each ion added (Table 3). In the wet site, magnesium was retained more than any other ion. In August 2020, the

average total ion concentration across all salt treatment plots was $2370 \pm 555 \mu\text{g}/\text{gram}$ dry soil (gds) compared to only $82.4 \pm 5.9 \mu\text{g}/\text{gds}$ across all control plots (a 28-fold increase in ion content). The maximum total extractable ion content measured (site average) was $5200 \pm 1800 \mu\text{g}/\text{gds}$ at Site 3 in August 2020. This is approximately a salinity of 5 ppt, which was the target level in the experimental design, however this target was not achieved across all sites nor for the entire duration of the experiment.

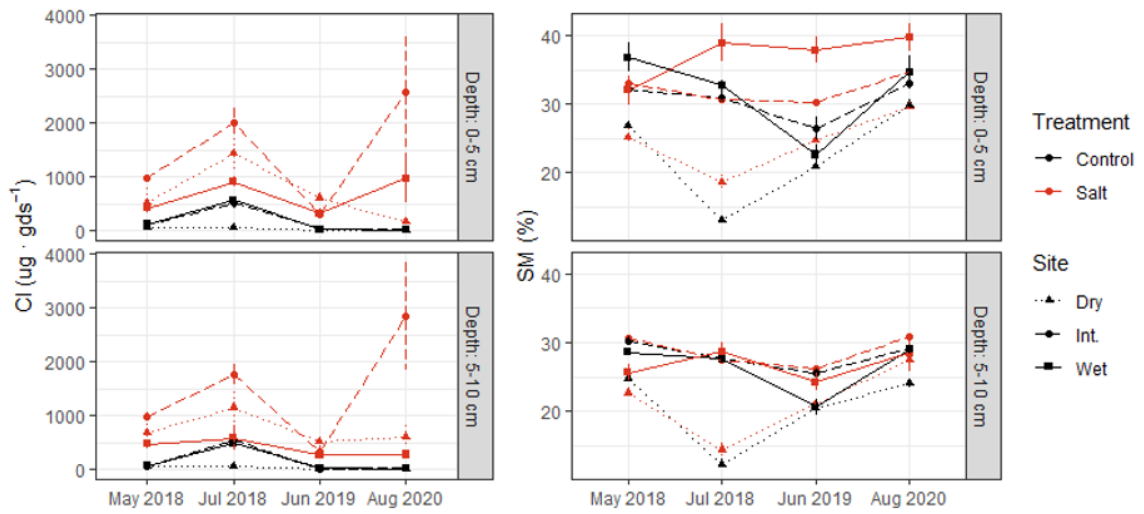


Figure 12. Soil chloride content (left) and soil moisture (right) on each sampling date across all sites (symbols), treatments (color) and depths (facets).

Table 3: Soil ion content in 2020 for all sites and depths (mean and standard error in parentheses) and percent recovery of each ion. Percent recovery is calculated as the ion concentration measured in 2020 (gram/gram dry soil) as a percentage of the total amount of salt added to the experimental plots over the duration of the experiment. Bulk density was used to convert the mass of salt applied on a per area basis, to a mass per gram soil, to a depth of 5 cm.

	2020		Recovery of total ion added (%) in the top 5 cm		
	Control	Salt	Dry	Int.	Wet
Cl ⁻	16.0 (2.93)	1240 (305)	1.1	15.1	5.3
SO ₄ ²⁻	14.7 (1.24)	206 (45.4)	4.3	21.7	6.08
Na ⁺	23.8 (2.30)	778 (177)	1.9	16.1	5.8
K ⁺	4.37 (0.774)	34.6 (6.50)	5.3	22.6	8.2
Ca ²⁺	22.1 (2.02)	38.2 (6.89)	0.64	14.8	4.37
Mg ²⁺	1.44 (0.249)	76.1 (19.2)	1.8	10.7	20.2

4.3.2 Indirect effects of salt treatment

We anticipated that the addition of marine salts would indirectly affect soil pH and other properties such as soil nutrient content. The range of pH observed in the experimental plots was 3.6 ± 0.05 (intermediate site in 2020) to $6.6 \pm$ (wet site in May 2018). While we expected the amendments of base cations would raise soil pH level in the salt treatment plots, we observed variable effects of the salt treatment on pH. At the driest site, the salt treatment lowered the pH relative to the control plots, but no consistent pattern was observed at the other two sites. Strikingly, we observed a strong decline in pH across all experimental sites over the course of the experiment that far exceeded the effect of the salt treatment (Figure 13).

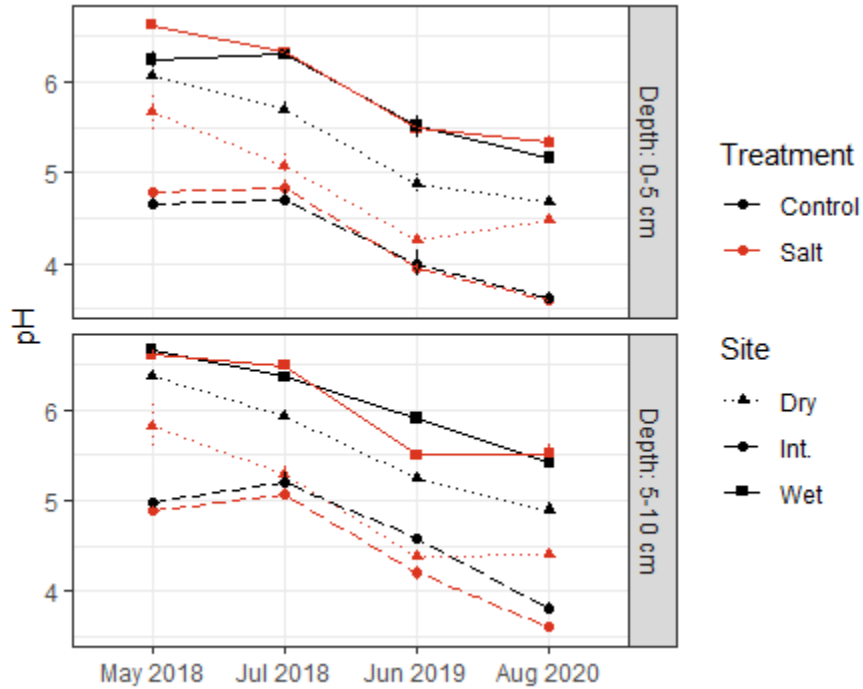


Figure 13: Average pH in experimental plots across all sampling dates, depths and sites (symbols). Salt treatment is shown in red.

We anticipated a release of nutrients due to ion exchange from the salt addition leading to a reduction in soil fertility over time. There was no significant effect of the salt treatment on soil nutrient content consistently across the entire experiment, though isolated effects were observed (see Appendix C: Figure 34). Total dissolved nitrogen (TDN) ranged from 0.47 to 4.36 mg/L across the experiment (plot averages) and was lower the salt treatment plots compared to the control plots, but only during 2020. Ammonium (NH_4^+) ranged from 0.08 to 3.5 $\mu\text{g/gds}$ across the experiment. Soil NH_4^+ content increased in the salt treatment plot of the wet site but had a mixed response in the dry site and no significant response in the intermediate site. Nitrate (NO_3^-) ranged from 0.23 to 20.3 $\mu\text{g/gds}$. The salt plot had less NO_3^- than the control plot in the dry site across all sampling dates except in 2020, but the intermediate and wet sites had elevated NO_3^- in

the salt treatment plots compared to the control in 2019 and 2020. Phosphate (PO_4^{2+}) ranged from 0.025 to 20.8 $\mu\text{g/gds}$ and the PO_4^{2+} response to the salt treatment was inconsistent across all sites and sampling dates (nutrient data courtesy of Matthew Stillwagon, unpublished data).

4.3.3 Salt effects on vegetation

We observed no significant effect of the salt treatment on either root biomass or tree growth over the duration of the experiment (Figure 14). Tree growth at the species level did not show any significant effect of the salt treatment, although the sample size was relatively small for most species (See Appendix C: Figure 35).

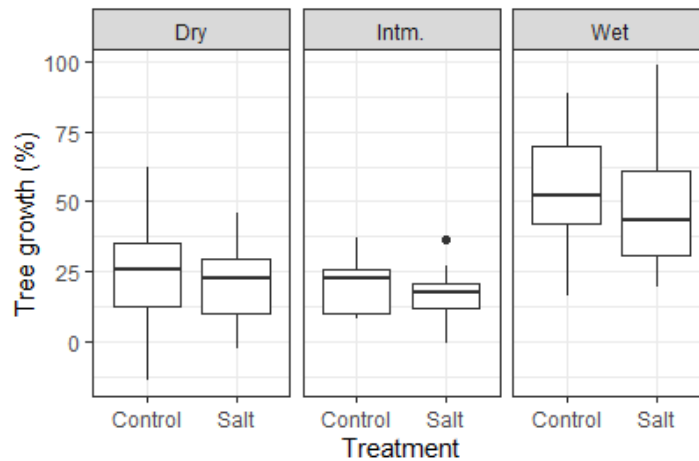


Figure 14: Growth (%) of trees in control versus salt treatment plots from November 2015 to January 2021. No significant difference between treatments within sites ($p_{\text{dry}} = 0.99$, $p_{\text{intermediate}} = 0.99$, $p_{\text{wet}} = 0.82$)

4.3.4 Salt effects on soil carbon

Microbial biomass (measured via substrate induced respiration, SIR) ranged from 0.17 to 9.8 $\mu\text{g C-CO}_2 \text{ hr}^{-1}$ per gram dry soil and 1.5 to 105 $\mu\text{g C-CO}_2 \text{ hr}^{-1}$ on a per gram carbon basis. The salt treatment generally reduced microbial biomass, but the effect was not statistically significant across all sites and sampling dates (Appendix C: Table 15G). The sample date with the most consistent reductions of microbial biomass across all sites was August 2020. Microbial biomass was consistently lower in the deeper soils. There was no consistent trend overtime across the experiment although sampling date is driving the majority of variation seen across all SIR results (Figure 15).

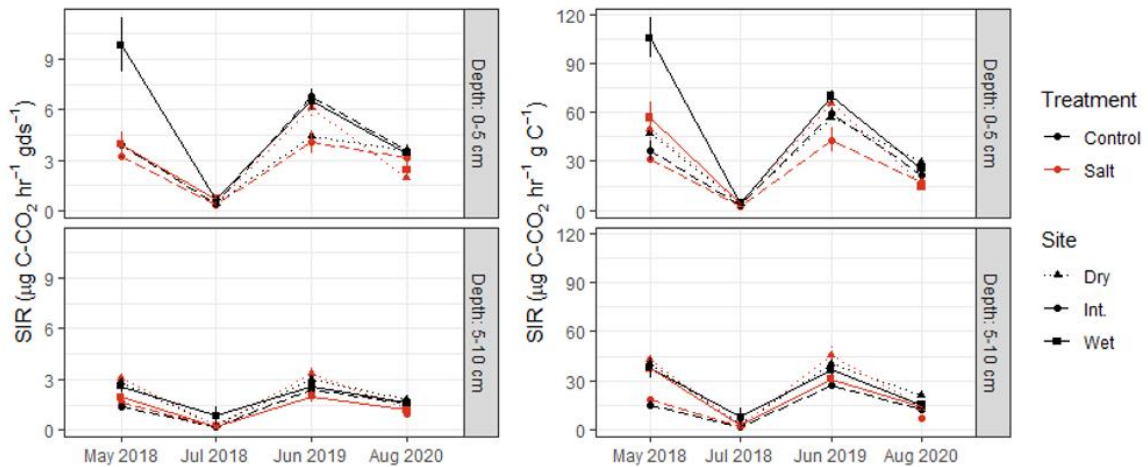


Figure 15: Substrate induced respiration (SIR) across all sites and sampling dates. Results normalized per gram of dry soil (gds) are shown on the left, results normalized per gram organic carbon content (g C) on the right.

Salinity suppressed soil respiration potential (carbon mineralization rates in lab incubations), but only in the final sampling period. Carbon mineralization rates ranged from 0.14 to 1.5 $\mu\text{g C-CO}_2 \text{ hr}^{-1}$ per gram dry soil and 1.5 to 14.0 $\mu\text{g C-CO}_2 \text{ hr}^{-1}$ on a per gram carbon basis. Respiration rates in soils from the deeper core section were consistently lower than the shallower depth. On a per gram soil basis, the salt treatment only produced a suppressing effect on soil respiration at the driest site. On a per gram carbon basis, there was a statistically significant suppression of carbon mineralization across all sites in 2020, but only in the upper depth increment. Carbon mineralization rates did not exhibit a temporal trend over the course of the experiment (Figure 16).

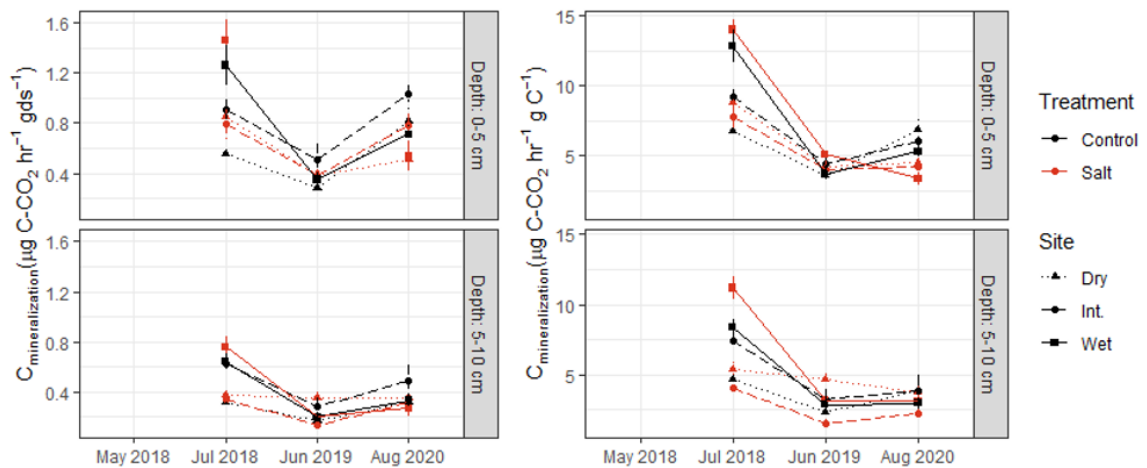


Figure 16: CO₂ flux from carbon mineralization assays across all sites and sampling dates. Results normalized per gram of dry soil (gds) are shown on the left, results normalized per gram organic carbon content (g C) on the right.

Salt treatments reduced water extractable dissolved organic carbon compared to control plots at all sites during the final sampling period, however the effect was not statistically significant across all depths (Appendix C: Table 15I). The overall range of DOC concentrations were 7.76 mg/L (August 2020, intermediate site, salt, 5-10 cm) to 36.8 mg/L (August 2020, dry site, control, 5-10 cm). We only observed consistent effects of the salt treatment across sites during the final sampling date. There does not appear to be a temporal trend of DOC changing over time (Figure 17).

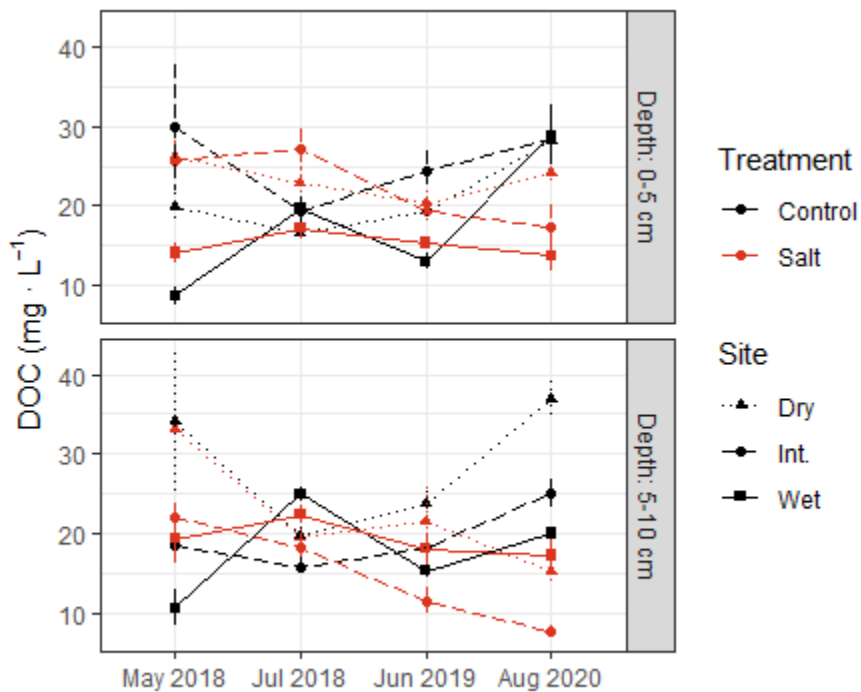


Figure 17: Dissolved organic carbon (DOC) across all sampling dates and sites.

Salt treatments suppressed the phenolic content of the soils during the August 2020 sampling period. The range of phenolic compound concentration observed is 0.59 mg/L (August 2020, intermediate site, salt, 5-10) to 7.68 (May 2018, dry, control, 0-5). Figure 18 shows a decline in the total concentration of phenolic compounds with salt treatment in 2020 (and in 2019 as well but only in the intermediate site). The decline in phenolic content is consistent with the trend observed for DOC suppression by salt in 2020. When normalizing for the DOC content of each sample (Figure 18), the proportion of phenolic compounds drops significantly over time but is not significantly affected by treatment. This pattern may be linked to the acidification of all sites observed over the lifetime of the experiment (Figure 13).

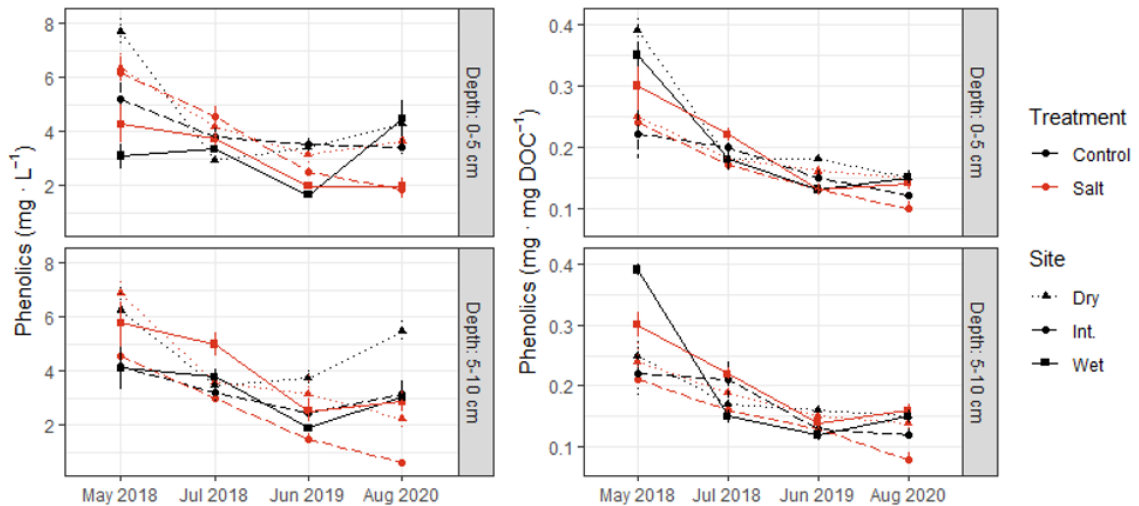


Figure 18: Phenolic compounds in soil water extracts shown as direct concentration (left) and as a proportion of DOC (right).

There was no effect of the salt treatment on total organic matter content of soils within the experiment, nor was there a significant pattern of organic matter development over time. Depth appears to be the most important driver of differences in organic matter content, with more organic matter in the shallower soils (Figure 19).

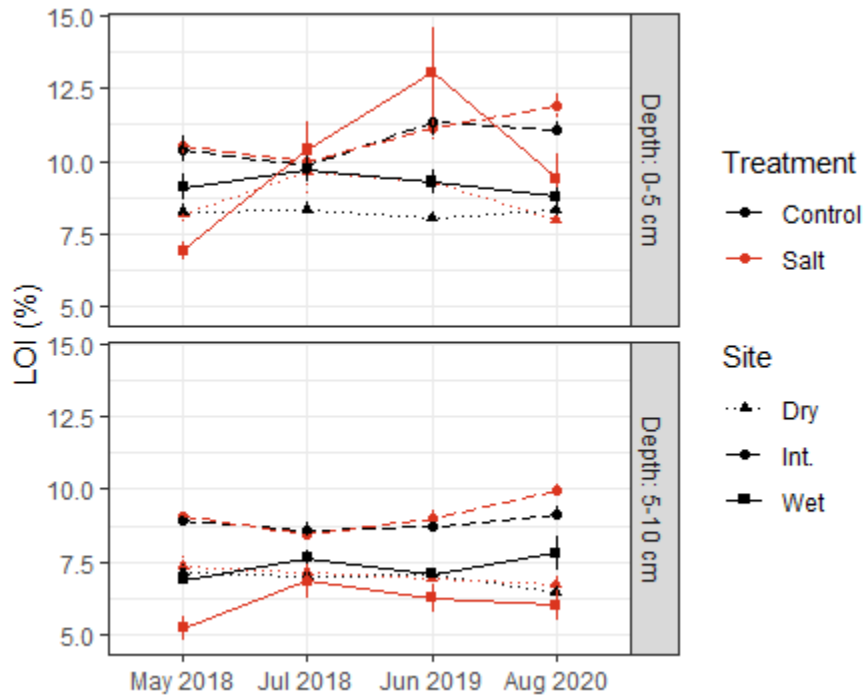


Figure 19: Soil organic content measured as loss on ignition (LOI).

4.4 Discussion

The carbon cycling process of this forested freshwater wetland proved surprisingly resistant to four years of marine salt additions. Smaller scale, manipulative experiments conducted previously in this study system have documented reduced DOC concentrations, microbial biomass, carbon mineralization, and soil CO₂ flux in response to salinization (Ardón *et al.* 2016,

2018; Helton *et al.* 2019). In this much larger, long-term study, there were few consistent impacts of salinization on ecosystem carbon stocks or fluxes. It was only on our final sampling date that we detected a significant decline in both DOC and phenolics, and a significant reduction in carbon mineralization in response to the salt treatment. Remarkably, there were no measurable effects of four years of salt enrichment on tree growth, root biomass, or soil carbon.

A primary motivation for conducting this large-scale and long-term field salinization experiment arose from divergent responses between laboratory and field experiments both across this site and elsewhere in the literature. Experimental salinization suppressed CO₂ flux in two prior incubation experiments conducted with intact soil columns from this field site, (Ardón *et al.* 2018; Helton *et al.* 2019). Yet in a small-scale field experiments, salinization had no effect on soil CO₂ fluxes (Helton *et al.* 2019). We had speculated that the difference in salinization impacts arose because soil-only incubations remove the potential plant-soil feedbacks and eliminate new inputs of recent photosynthate. In the Helton *et al.* (2019) experiment, salinization treatments were at a scale too small to impact trees, but our large-scale field experiment was designed to affect both vegetation and soil heterotrophs. We observed salt suppression of carbon mineralization only during the final year of our experiment, and there are three potential explanations for this, though it is not possible to distinguish between them. We hypothesize that it took considerable time for our salinization treatments to measurably alter soil chemistry. While we did not see a buildup of extractable ions in soil solution over time, we speculate that many of the added ions accumulated in soils and vegetation over time. We must acknowledge the alternative explanations that either the timing of sampling (soon after a salt addition) or site conditions on this final sampling date

(most consistent soil moisture across all treatment blocks of any sampling date, Figure 12) may have simply made it easier to detect a salinization impact. Previous work has shown that salt effects are highly contingent on hydrology in this region (Ardón *et al.* 2016, 2018; Helton *et al.* 2019) and that responses to elevated salinity are transient (Weston *et al.* 2011; Neubauer 2013).

We predicted a reduction in soluble organic carbon in the salt addition plots, due to flocculation caused by increased ionic strength and cation bridging (Shainberg and Letey 1984). Our results only matched these predictions on our final sampling date, and we are unable to distinguish between our alternative hypotheses that the salinization impact compounded over time vs. the possibility that it was easier to detect these treatment effects on a sampling date in which soils in all plots were near saturation. In prior research at our field site, Ardón *et al.* (2016) reported that both drought and salinization have equivalent and additive effects in reducing soil solution and surface water DOC concentrations.

We observed responses to salinity that varied over space and time, but this variability is consistent with results from previous studies. Salt addition experiments with long durations demonstrate temporal variability of CO₂ flux. In a field addition experiment by Neubauer (2013), salt suppressed CO₂ fluxes wetland plots, but only in the second year of this two year study. In a year-long soil core experiment, Weston and others (2011) found salt stimulated the production of CO₂, but only during the first six months of treatments. Both site and salt treatment level are also major sources of variability driving carbon flux responses to salinity. In a study using soil from three tidal wetlands in Georgia, the magnitude of the effect of salinity on soil respiration was variable across all three sites. At the low salt dose (2 ppt) there was consistently a positive relationship between salinity and CO₂ flux, but at the higher dose

(5 ppt), the treatment only stimulated CO₂ production at one of three sites while the other two were not significantly different from the control treatment (Marton *et al.* 2012).

Variability in carbon cycling responses to salt addition experiments is reflected throughout the literature. Several previous studies have reported increases in microbial respiration due to increased salinity (Table 4; (Weston *et al.* 2006, 2011; Chambers *et al.* 2011; Marton *et al.* 2012; Neubauer *et al.* 2013)). Unlike the work in this study, these experiments were mainly short-term studies with salt treatment applied in anoxic soil slurry assays. Longer term field studies and those conducted with intact soil cores were more likely to find salt suppression of CO₂ production (Neubauer *et al.* 2013; Ardón *et al.* 2018; Helton *et al.* 2019; Doroski *et al.* 2019), or no significant relationship (Chambers *et al.* 2014; Liu, Ruecker, *et al.* 2017). In the only study using the anoxic soil slurry method with soils from North Carolina, Wen *et al.* (2019) observed a decline in CO₂ with salinity, consistent with our results. A key commonality between these studies maybe local soil edaphic factors, in particular rich iron content that buffers soils from hydrogen sulfide toxicity (Schoepfer *et al.* 2014).

Table 4: Summary of experimental salt addition studies on the effects of salinity on CO₂ flux and extractable DOC. Arrows indicate the direction of the influence of salt treatment compared to freshwater controls.

Salt effect ¹ on CO ₂	Salt effect on DOC	Salinity, ppt ² (<i>effective</i>)	Method	Anaerobic	Duration	pH	Ecosystem	Location	Reference
↑ 24 %	--	2	Soil slurry	✓	2 days	--	Tidal freshwater marsh	SC	(Neubauer <i>et al.</i> 2013)
↑ 39 %	--	5	(1:1) ³						
↑	--	2	Soil slurry	✓	5 days	--	Tidal freshwater forest	GA	(Marton <i>et al.</i> 2012)
Variable	--	5	(1:2)						
↑ 20 %	--	3.5	Soil slurry	✓	2 weeks	6.8	Freshwater wetland	FL	(Chambers <i>et al.</i> 2011)
↑ 29 %	--	14	(1:1)						
↑ 32 %	--	35							
↑ ⁴	N.S.	10	Flow-through cores	✓	3 weeks	7.1	Unvegetated, intertidal freshwater creek bank	GA	(Weston <i>et al.</i> 2006)
↑ ⁵	N.S.	5	Intact soil cores	(✓) ⁶	1 year	--	Tidal freshwater marsh	NJ	(Weston <i>et al.</i> 2011)
N.S.	↑	15	Intact peat monoliths in outdoor mesocosms		6 weeks	7.8-8.0	Mangrove peat	FL	(Chambers <i>et al.</i> 2014)
N.S.	N.S.	1 (NaCl)	Soil slurry		60 days	5.0 ⁷	Forested wetland	SC	(Liu <i>et al.</i> 2017)
N.S.	N.S.	5 (NaCl)	(1:3)						
↓ ⁸	--	10.2 (2-5)	Field addition measured in situ		20 months		Tidal freshwater marsh	SC	(Neubauer 2013)
N.S.	--	18	Intact soil cores, measured directly		7 weeks		Tidal <i>Typha</i> wetland	CT	(Doroski <i>et al.</i> 2019)
↓	--	18 (-SO ₄)	Intact soil cores						
↓	--	18 (-SO ₄)	→ bottle assay						

Table 4 continued

Salt effect ¹ on CO ₂	Salt effect on DOC	Salinity, ppt ² (<i>effective</i>)	Method	Ana-robic	Duration	pH	Ecosystem	Loca-tion	Reference
↓ ↓	--	8 8 (-SO ₄)	Soil slurry (1:2)		11 weeks	4.35-6.73	Forested wetland	NC	(Wen <i>et al.</i> 2019)
↓ ↓	--	8 8 (-SO ₄)	Soil slurry (1:2)	✓					
↓ 76 %	↓ 49 %	5	Intact soil cores measured directly		16 weeks	--	Forested wetland	NC	(Ardón <i>et al.</i> 2018)
↓ ⁹ ↓ ⁹	--	5 5 (-SO ₄)	Intact soil cores measured directly		16 weeks	--			
N.S. N.S.	--	4 10	Field addition measured in situ		15 weeks	3-4	Forested wetland	NC	(Helton <i>et al.</i> 2019)
↓ ↓	--	4 10	Field addition → Soil slurry (1:2)						
49 %	↓	(2.1)	Field addition → Soil slurry	✓	3.5 years	--	Tidal freshwater marsh	SC	(Neubauer <i>et al.</i> 2013)
↓ ¹⁰	↓ ¹⁰	(1-3)	Field addition → bottle assay		4 years	4-6	Forested wetland	NC	This study

Notes: -- = Not measured or not reported; N.S. = no significant effect of treatment; -SO₄ = Artificial seawater without sulfate; ¹ Direction of effect of salt treatment on CO₂ flux, magnitude given for sources that reported an average percent change between salt treatment and control group; ² Target salinity treatment and the effective, or measured salinity shown in parentheses, where reported; ³ Soil to water/treatment solution ratio within the slurry; ⁴ Measured as DIC; ⁵ Significant effect of the treatment only the first six months of the experiment; ⁶ Cores were house in an artificial tide chamber on a 6-hour inundation cycle; ⁷ Reported increases in pH over the duration of the experiment; ⁸ Year two only (year one N.S.); ⁹ For intermittent flooding case only, permanently flooded cores showed no significant effect; ¹⁰ Significant effect of salt only in year four of the experiment.

We examined this body of literature on carbon flux responses to salt addition experiments to identify patterns driving the divergent outcomes. Site edaphic factors are likely an important source of variability, however lack of consistency in reporting edaphic factors makes it difficult to draw any conclusions. We hypothesized that our salt additions would raise ambient soil pH due to the contribution of base cations. Instead, we found a small acidifying effect of the salt treatments, but this response was eclipsed by a much larger trend of declining pH across all sites (including the control sites) over time (Figure 13). This striking pattern maybe driven by the natural acidifying processes that occur within wetlands as they establish given that this property was restored from prior agricultural land use in 2004. Soil pH and base cations affect the solubility of DOC; the shift in site pH as well as our salt treatments are likely working in concert to alter carbon form and fluxes – interactions which should be the subject of further investigation. In studies that measure soil organic matter content, extractable dissolved organic carbon, and other measures of carbon quality, these metrics are often reported as cofactors mediating CO₂ fluxes, rather than responses to salinity themselves (Chambers *et al.* 2014). Our results demonstrate suppression of bulk DOC and aromaticity in soil carbon due to salinity treatments. More work is need to understand the importance of this pathway in controlling soil respiration relative to the direct effects of salt on microbial function (Rath and Rousk 2015).

Disentangling the effects of salinization on wetland carbon cycling across time and space will require a concerted effort to standardize methods of study going forward. Consistency of methods will help facilitate comparison across studies from different locations. Edaphic factors, particularly pH and soil organic matter characteristics, are important covariate controls on carbon cycling and should be reported with salinity to understand these important

interactions. Future investigations should report both target and realized values for salinity treatments, as well as any changes to initial soil conditions such as pH or DOC. Finally, it is important that the results of short-term lab experiments be considered in concert with longer field studies. Only by challenging our phenomenological observations with environmental complexity do we further our understanding of how ecosystems are responding to multiple drivers of change.

5

Seawater is more than just salt: disentangling the effects of salinization and pH on coastal soil carbon cycling

Emily A. Ury, Marcelo Ardón, Justin P. Wright, and Emily S. Bernhardt

5.1 Introduction

The salinization of coastal wetlands due to sea level rise, storm surge and droughts is leading to forest mortality and substantial declines in biomass carbon stocks (Kirwan and Gedan 2019; Smart *et al.* 2020) (Ury *et al.* 2021). The consequences of soil salinization for below ground carbon cycling and sequestration are far less clear, with studies reporting both salt enhancement (Weston *et al.* 2006, 2011; Chambers *et al.* 2011; Neubauer 2013) and salt inhibition of microbial activity in coastal wetland soils (Ardón *et al.* 2016, 2018; Helton *et al.* 2019; Doroski *et al.* 2019; Wen *et al.* 2019). To understand these divergent responses, we must consider the multiple pathways by which salt affects microbial activity and the effects of salinity on properties of receiving soils. The addition of marine salts to soils does more than just increase the ionic strength of soil pore water; salt affects soil pH, base cation

concentrations, and introduces new terminal electron acceptors (Herbert *et al.* 2015, Tully *et al.* 2019). Additionally, the extent to which salinization alters soil carbon cycling is likely to be contingent on characteristics of the site itself (i.e., hydrology, soil properties), the level and duration of salt exposure, and prior exposure history.

There are multiple pathways by which salinity affects microbial activity in soil: directly by altering microbial activity, abundance, and community composition (Lozupone and Knight 2007; Dang *et al.* 2019; Rocca *et al.* 2020), and indirectly by affecting the quantity or quality of soil organic matter (Shainberg and Letey 1984; Jardine *et al.* 1989; Wichern *et al.* 2006; Mavi *et al.* 2012; Singh 2016). Increasing osmotic stress will lead to mortality for salt-sensitive microbes and major shifts in microbial community composition (Rocca *et al.* 2020). This may reduce rates of soil respiration or conversely, may stimulate the activity of salt-tolerant microbes through the release of labile organic matter following autolysis of less tolerant microbes (Wichern *et al.* 2006; Singh 2016). Salinity affects the solubility, and therefore availability, of organic carbon within soil matrices (Mavi *et al.* 2012). Dissolved organic carbon (DOC) becomes less soluble with rising ionic strength due to flocculation (Shainberg and Letey 1984), however this effect may be offset by cation exchange resulting in the desorption of DOC from soil particles following salt addition (Jardine *et al.* 1989; Mavi *et al.* 2012). These shifts in DOC availability might interact with the direct effects of salinization on microbial community composition and activity.

The effects of salinization on soil carbon cycling are also contingent on pH, though little attention has been paid to pH in the literature on wetland salinization. Salinity and pH interact in two ways. First, the introduction of marine salts may result in a shift of soil pH due to cation exchange and alkalization from base cations (Adams *et al.* 1984). Secondly, native

soil properties including pH, and other related characteristics such as cation exchange capacity and base saturation, may interact with the effect of introduced salinity (Bache 2008). Independently, pH is an important control on soil microbial processes (Lauber *et al.* 2009) though not always included as a parameter in ecosystem process models (Sulman *et al.* 2018). Given the importance of pH in moderating biochemical processes, we seek to investigate the interactions between salinity and pH in the context of wetland carbon cycling in the face of global change.

In this paper we conducted a laboratory soil salinization experiment in which we separately manipulated treatment salinity and pH. Our pH-modified salt solutions were added to two different wetland soils collected from sites in coastal North Carolina. Both soils were obtained from within a 440-ha restored wetland, with nearly identical land use history, but vary in pH and base saturation. Our goal was to tease apart the effects of increasing ionic strength and altered pH on soil carbon stocks, soil solution DOC concentration and composition, and rates of microbial respiration; and to determine whether these effects were contingent upon pre-existing edaphic factors. We expected that salinity would reduce the solubility of DOC and reduce the concentrations of high molecular weight phenolic and aromatic compounds. We anticipated that these effects would be partially mitigated in the higher pH treatments and in the soil with higher base saturation, due to the increased solubility of organic compounds. We predicted that rates of carbon mineralization would be suppressed by salinity but align with treatment effects on DOC. By investigating the effects of salinity on soil carbon availability and mineralization, we aimed to resolve some of the discrepancies observed in prior literature surrounding the effect of salinity on carbon fluxes from wetland soils.

5.2 Methods

5.2.1 Site description and sample collection

Soils were collected from the Timberlake Observatory for Wetland Restoration (TOWeR, see Ardón et al. (2010) for full site description) in Tyrrell County on the Albemarle-Pamlico Peninsula in Eastern North Carolina. The property was in agricultural production until 2004 when 440 hectares were restored to a 'preagricultural state' by way of extensive earth moving (ditch filling), rewetting, and planting 750,000 bare root saplings (wetland tree species). There are two major soil types at TOWeR, Ponzer Muck and Hyde Loam, which are the two predominant soil types of found across the entire Albemarle-Pamlico peninsula. For this experiment, we collected soils from a monitoring site within each soil type. Both soil types are characterized as very poorly drained, highly acidic, and rich in decomposing organic material. The Hyde series is a fine-silty, mixed, active, thermic Typic Umbraquults while the Ponzer series is a Loamy, mixed, dysic, thermic Terric Haplosaprists (Soil Survey Staff 2008, 2010).

There is a small elevation gradient across the property (less than 0.5 meters) that drives hydrologic variation between the two sampling locations. The planting schema of the original site restoration also follows the topography such that each site contains a different mix of planted trees. The Hyde loam site has a slightly lower surface elevation, is regularly flooded, and thus was planted predominantly with bald cypress (*Taxodium distichum*) as well as *Pinus taeda*, and *Salix nigra*. The Ponzer muck site has a slightly higher surface elevation, is less regularly inundated and so was planted mainly with species of oak (*Quercus nigra*, *Quercus phellos*, *Quercus falcate var pagodagfolia*, and *Quercus michauxii*). Natural recruitment of woody plants has been minimal at the Ponzer muck site, while an understory of *Acer rubrum* saplings and *Juncus effusus* is establishing at the Hyde Loam site.

Soils from both sites were collected on August 29th, 2020, to a depth of 5 cm and transported back to the lab on ice and stored overnight at 4 °C. The next day, soils were sieved (2 mm) to remove roots and homogenized prior to experimental set up. A subsample from each site was reserved for analysis (in triplicate) of soil moisture and soil organic matter content, used later for calculating normalized results.

5.2.2 Experimental set-up and treatment application

The lab experiment was designed to assess the effect of salinity on wetland soil carbon with a particular focus on the interaction between salinity and soil pH. To accomplish this, we applied salt treatments to soils with highly divergent soil pH status and measured soil carbon responses. We also manipulated the pH of the salinity treatments in a full factorial design to further disentangle the salinity by pH interaction. Treatment solutions were prepared with Instant Ocean® marine aquarium salt mixture (0, 2.5 and 10 ppt) and each solution was divided in three and titrated with either dilute acid (HCl) or base (NaOH) until the desired pH was reached for a total of nine treatments (see Table 5). The pH levels were chosen to match the actual pH of each solution at the respective salinity (i.e., solutions on the diagonal of Table 5 required no pH manipulation).

Table 5: Experimental treatment solution salinity and pH (in parentheses).

	pH manipulation		
Salinity	0 (5.5)	0 (7.2)	0 (8.8)
treatment	2.5 (5.5)	2.5 (7.2)	2.5 (8.8)
(ppt)	10 (5.5)	10 (7.2)	10 (8.8)

Note: Shading indicates treatments with no pH manipulation.

Soils were weighed into filter funnels lined with Grade 1 Whatman filter paper (see Figure 20 for a schematic of the experimental setup). Treatments were randomly assigned and soils were rinsed with treatment solutions in a 10:1 (volume:mass) ratio. Both the soil residue and the initial filtrate were used for further analysis. Filtrate solution was collected after approximately 25 minutes and the treated soils were allowed to air dry on the filter paper overnight. Half of the soil residue samples were transferred by mass into pre-weighed 40 mL amber glass I-ChemTM vials for carbon mineralization analysis (54 total) over a 21-day incubation period at 20 °C. The remaining set of soil samples were transferred to falcon tubes for an identical incubation period followed by water extraction (54 total) in order to measure extractable DOC, phenolics and solution absorbance at a wavelength of 254nm, SUVA₂₅₄, as a proxy for aromatic content.

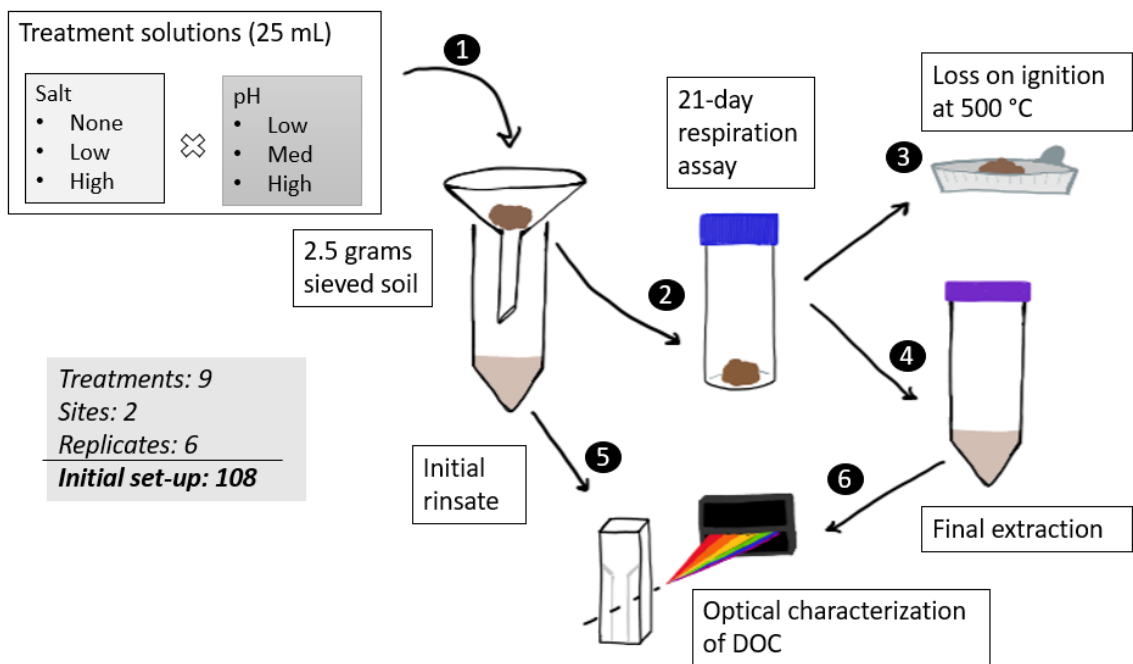


Figure 20: Schematic of experimental design. Setup began with (1) rinsing 2.5 grams of field-moist soil with 25 mL of treatment solution. (2) The treated soil was transferred (analytically) to a sealed jar for incubation and respiration assay for 21 days. (3) Following the incubation, half of the jars were ashed in a muffle furnace to determine the remaining fraction of organic matter. (4) Remaining jars were extracted with a 10:1 ratio of DI water. (5 and 6) Both the initial filtrate and final extract were characterized for optical properties of DOC (phenolic compounds and $SUVA_{254}$) and DOC was quantified using a TOC analyzer.

5.2.3 Response measurements

Soil respiration assay vials were sealed with caps fitted with a PTFE-lined silicone septum to allow for headspace gas sampling via syringe. We measured headspace CO₂ concentrations with a LI-6250 gas analyzer (Li-core, Inc., Lincoln, Nebraska, USA) on days 1, 2, 3, 5, 7, 11, 14, 17, and 21. Vials remained sealed during the first three days of the incubation, then vented to prevent anoxia. Vials were vented and resealed 24 hours prior to each subsequent measurement. The initial rate of potential C mineralization was calculated from the slope of the measurements over the first 3 days of the incubation and reported as $\mu\text{g C-CO}_2 \cdot \text{hr}^{-1} \cdot \text{g C}^{-1}$, having been also corrected for the initial soil organic C content. The cumulative CO₂ collected over all measurements is also reported as the total $\mu\text{g C-CO}_2 \cdot \text{g C}^{-1}$. Following the 21-day incubation period, the vials were oven dried at 60 °C for 48 hours to obtain a mass of dry soil for each assay and then heated in a muffle furnace at 500 °C for 4-hours to obtain an estimate of the organic matter content remaining in each sample by loss on ignition.

The second set of incubated soils were kept in the dark, loosely covered for 21 days and then extracted with nano-pure water. A 10:1 water:soil (by mass) ratio was used to extract soils, first by shaking the slurry on an end-over-end shaker at 60 rpm for 4 hours. Slurries were then allowed to settle over-night in the fridge and were then centrifuged at 3500 rpm for 15 minutes before being filtered through a 0.7 μm glass fiber filter. Both the initial filtrates and final extracts were analyzed for dissolved organic carbon (DOC), phenolic compounds, SUVA₂₅₄, pH, and conductivity. Water extractable dissolved organic carbon (DOC) was measured at the Duke River Center on a TOC-V combustion analyzer (Shimadzu Corporation, Kyoto, Japan). Solution pH and conductivity were measured with calibrated, hand-held probe devices (Hach

H260G pH Meter, Loveland, CO; Oakton Con6 Acorn Series Conductivity Meter, Vernon Hills, IL). All measurements were conducted within 48 hours of sample collection.

Phenolic compounds were measured using a colorimetric method (modified from Ohno and First (1998)). In a 24-well plate, 0.10 mL of Folin-Ciocalteu and 0.30 mL of 0.5 Molar NaHCO_3 was added to 1 mL of filtrate/extract, gently mixed and allowed to rest for color to develop for 4 hours. UV-vis absorbance spectra were measured on a BioTek Epoch™ 2 Microplate Spectrophotometer (Winooski, VT, USA) at 750 nm and calibrated against a standard curve made of vanillic acid ($0 - 10 \text{ mg} \cdot \text{L}^{-1}$). The concentration of phenolic compounds was normalized by the DOC concentration and reported in $\text{mg phenolics} \cdot \text{mg DOC}^{-1}$. SUVA_{254} was measured on the same spectrophotometer at 254 nm. Absorbance at 254 was normalized by the concentration of DOC in the sample as a characterization of the aromaticity of the carbon independent of the general level of organic matter and expressed as liters per mg DOC per meter ($\text{L} \cdot \text{mg DOC}^{-1} \cdot \text{m}^{-1}$) following Weishaar et al. (2003).

A second, separate set of soils collected previously from the same sites (July 2, 2020) were dried and sent to the North Carolina Division of Agriculture & Consumer Services for routine soil testing of macro- and micro-nutrients (P, K, Ca, Mg, S, Na, Mn, Cu and Zn; see <https://www.ncagr.gov/agronomi/stmethod.htm> for details) using Melich's standard methods (Mehlich *et al.* 1976; Mehlich 1984a; b).

5.2.4 Statistical Analysis

All statistical analysis were conducted using R 4.0.1 (R Development Core Team 2020) with 'tidyverse' (Wickham *et al.* 2019) and 'ggplot' (Wickham 2016) packages. One-way Analysis of Variance (ANOVA) followed by Tukey's HSD post-hoc test were used to determine

statistically significant ($p < 0.05$) differences between treatments groups within each site. Two-way ANOVA was used to test for an interaction between the treatment effect and site.

5.3 Results

5.3.1 Site characteristics

Sites were selected due to their known difference in soil pH, however chemical analysis revealed further differences (Table 6) including a surprisingly large difference in base saturation. The Hyde loam had more than 4x greater base saturation (79.5 ± 4.1 %) than the Ponzer Muck (17 ± 2.1), with calcium and magnesium levels in the Hyde loam more than 10x and 3x greater than the Ponzer muck, respectively. The cation exchange capacities of the two soils were similar, with the differences in base saturation perhaps due to differences in agricultural lime application or the hydrologic transport of lime during this site's prior history of agricultural use.

Table 6: Site characteristics and soil chemical properties.

General Site Characteristics		
Soil series	Ponzer muck	Hyde loam
Dominant tree species	<i>Quercus spp.</i>	<i>Taxodium distichum</i>
Hydrology	Periodically inundated	Frequently inundated
Soil properties measured on experimental soil		
Soil moisture (%)	32.4 ± 0.1	36.7 ± 0.25
Soil organic matter (%)	11.2 ± 0.04	8.1 ± 0.1
Soil properties measured by NCDA&CS		
Humic matter (%)	2.9 ± 0.2	2.2 ± 0.2
pH	4.0 ± 0.054	5.6 ± 0.13
Base saturation (%)	17 ± 2.1	79.5 ± 4.1
Cation exchange capacity (mEq/100cm ³)	6.28 ± 0.7	8.0 ± 0.50
Na (mEq/100cm ³)	0.2 ± 0.07	0.15 ± 0.089
Phosphorus (mg/dm ³)	62.4 ± 2.8	36.8 ± 3.1
Calcium (mg/dm ³)	101 ± 26	1026 ± 128
K (mg/dm ³)	69.8 ± 98.7	42.7 ± 3.8
Mg (mg/dm ³)	45 ± 5.7	145 ± 9.0
S (mg/dm ³)	36.8 ± 6.6	19.7 ± 2.4

Note: Means plus or minus the standard deviation of 5 replicates.

5.3.2 Treatment effects on soil salinity and soil pH

Both salinity and pH treatments significantly altered the carbon content and composition of the initial filtrate and the final soil water extracts (Figure 21). Our experimental pH treatments had far less of an effect on soil solution pH than our salinity treatment. Adding marine salts reduced the pH of the initial filtrate, relative to the control, by an average of 0.87 pH units ($p < 0.001$) for the 2.5 ppt treatment and by 0.65 ($p < 0.001$) for the 10 ppt treatment in the Ponzer Muck. In the Hyde loam the salinity treatment reduced the pH by an average of 0.78 pH units ($p < 0.001$) for the 2.5 ppt treatment and by 0.43 ($p < 0.001$) for the 10 ppt treatment. In both soils, our low salinity treatment had a larger effect on soil solution pH than our high salinity treatment.

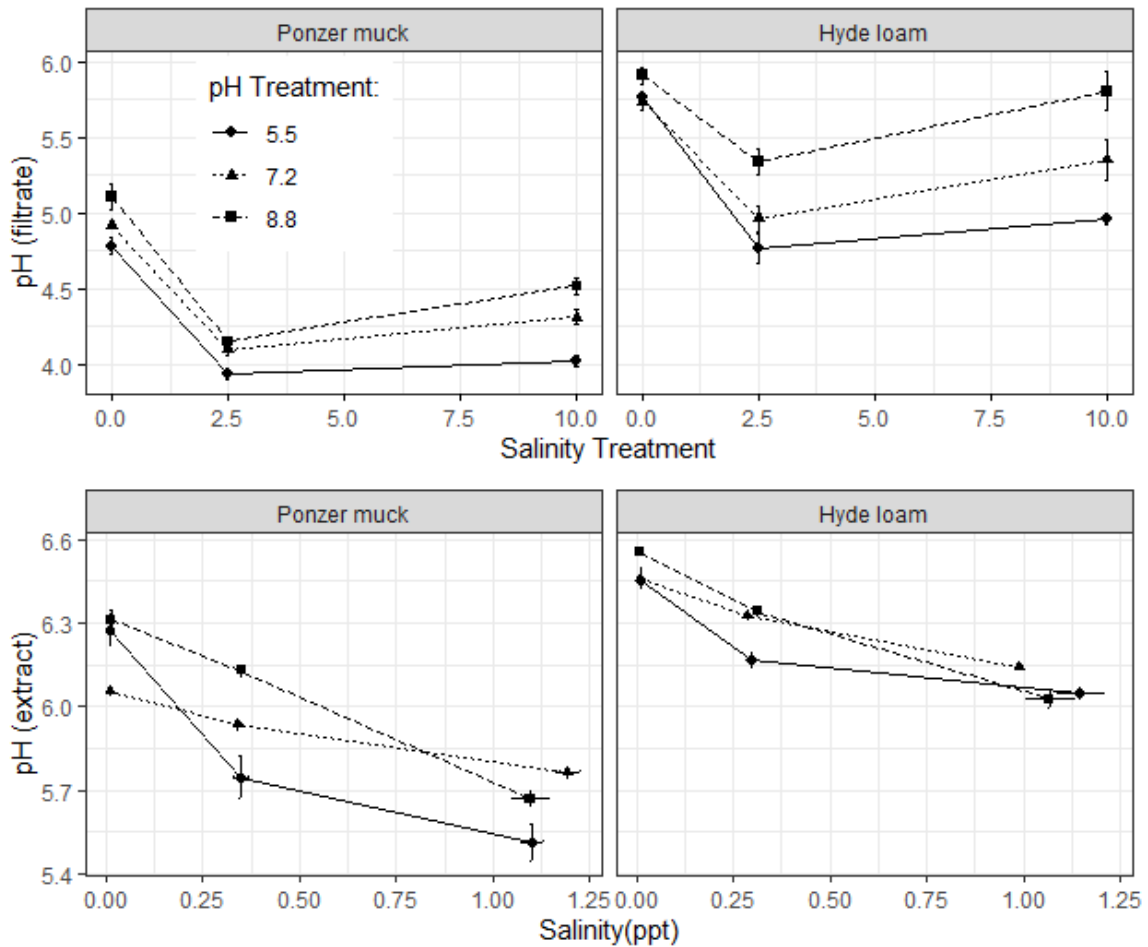


Figure 21: Measured salinity and pH of the initial filtrate (top) and the final soil water extract (bottom). The pH treatment groups (5.5, 7.2, 8.8) are indicated by symbol.

There were no statistically significant differences in pH of the final extract between pH treatment groups as determined by one-way ANOVA for either the Ponzer muck or the Hyde loam (respectively, $F(2,24) = 1.001$, $p = 0.38$ and $F(2,24) = 0.58$, $p = 0.57$). The salinity treatments significantly raise the salinity of the final soil extracts by an average of 0.31 ppt ($p < 0.001$) for the 2.5 ppt treatment and 1.1 ppt ($p < 0.001$) for the 10 ppt treatment. This indicates the effective salinity experienced within the soil samples may have been significantly

lower than target treatment levels, even when considering that some salt ions will bind to soil particles.

Our experimental manipulation of soil pH, in the absence of a salinity treatment had almost no measurable effects on any response variables. The single exception, was that our highly acidic treatment stimulated a significantly greater loss of total soil carbon in the Hyde Loam over the course of the experiment ($F(2,6) = 8.70$, $p = 0.0168$). Strong soil buffering clearly dampened the efficacy of our attempts to alter soil and soil solution pH. Given these findings, we focus the remainder of our results on the effect of salinity treatments on soil C response variables and the variation in these salinity effects across two soil types.

5.3.3 Salinity effects on soil carbon

Dissolved organic carbon in the filtrate of the initial treatment rinses was significantly ($p < 0.0001$) lower in the salt treatments as compared to the control by an average of $5.3 \text{ mg} \cdot \text{L}^{-1}$ and $5.1 \text{ mg} \cdot \text{L}^{-1}$ for the 2.5 ppt and 10 ppt salinity treatments, respectively (see Appendix D: Figure 36). The difference between the 2.5 ppt and 10 ppt treatments was not significantly different ($p = 0.243$). The amount of carbon removed from soil samples in this first rinse accounts for approximately 0.1 – 0.2 % of the total organic carbon content of the initial soils. Thus, although the salt treatments removed less C, we determine that the removal of organic material at this stage is negligible with respect to the remaining soil organic carbon (SOC) pool. This distinction is relevant for interpretation of subsequent experimental results.

The salinity treatments significantly reduced the initial (3-day) rate of C mineralization relative to the control in both soil types (Figure 22). The Hyde loam experienced a greater reduction in C mineralization rate (47.0 %) than the Ponzer muck (15.1 %) following the high salinity treatment and there was a significant site by treatment interaction effect ($F(2,48) =$

9.62, $p = 0.00031$). Carbon mineralization in the Ponzer muck is significantly suppressed by the 2.5 ppt salinity treatment ($p = 0.0496$) but the effect of the 10 ppt treatment is not significantly different from the control. The relationship between salinity treatment level and C mineralization in the Hyde loam exhibits a more linear decline.

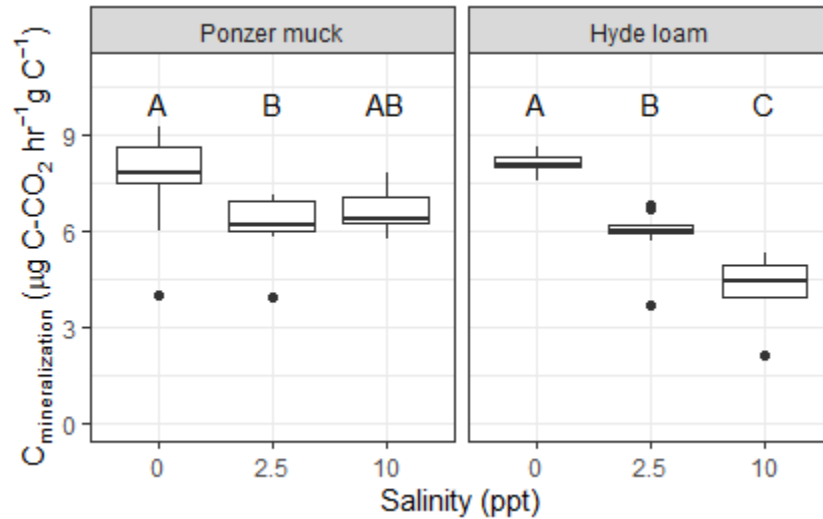


Figure 22: Initial C mineralization rate (first 3 days) from the soil incubation assays on a per gram carbon basis. C mineralization rate per gram of dry soil is reported in Appendix D: Figure 37. Letters indicate significant difference between treatment (Tukey's HSD test, $P < 0.05$).

Total C mineralization over the 21-day duration of the experiment shows a similar pattern to the initial C mineralization rates. There is a strong reduction in C mineralization over 21 days in the Hyde loam soil (24.1 % and 43.2 % for the 2.5 ppt and 10 ppt salinity treatments, respectively). We also measured a substantial reduction of C mineralization in the Ponzer muck with salinity (21.5 % and 27.4 % for the 2.5 ppt and 10 ppt salinity treatments, respectively), however the difference between the 2.5 ppt and 10 ppt treatment groups is not significant (Figure 23). Unlike the initial rate, there is not a significant interaction between

treatment and site on cumulative carbon mineralization over the entire 21-day incubation period (See Appendix D: Table 16 for ANOVA results).

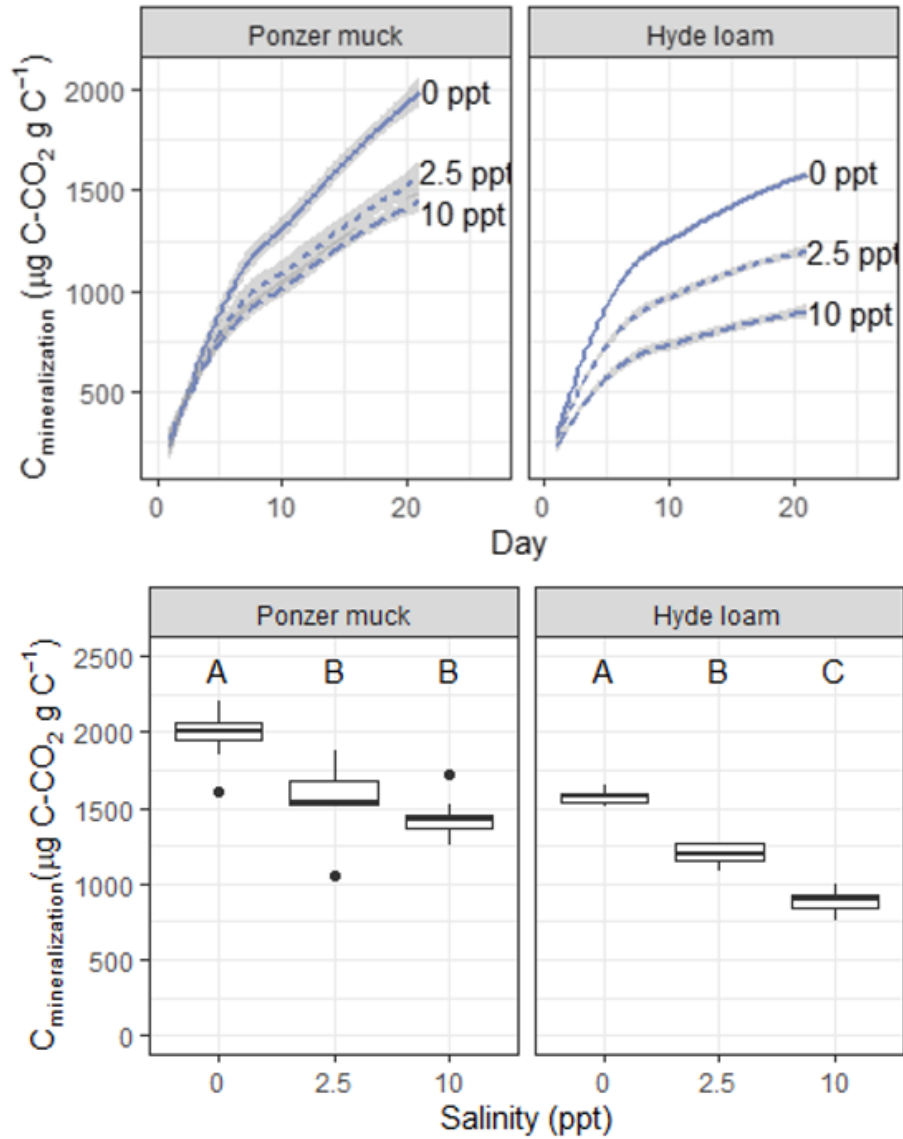


Figure 23: Accumulation curve (top panels) and cumulative CO₂ mineralization (bottom panels) from soil incubations over 21 days. Letters indicate significant difference between treatment (Tukey's HSD test, P < 0.05).

Adding marine salts significantly reduced water extractable DOC by the end of the incubation in both soil types (Figure 24). These treatment effects were more extreme in the more organic rich Ponzer Muck soils, where we measured a 62.5% reduction of DOC in the 2.5 ppt treatment and a 77.8 % reduction in the 10 ppt salinity treatment. The effects of salt addition on extractable DOC in the Hyde loam, were similar in direction but lower in magnitude, with a 33.9% reduction of DOC in the 2.5 ppt salinity treatment and 62.0% in the 10 ppt treatment. The divergent responses between the two soils led to a significant site by treatment interaction on the DOC response to salinity treatments ($p < 0.0001$). We predicted that the more aromatic constituents of DOC would be particularly affected by salinity, and indeed measured significant declines in the total concentration of phenolics and $SUVA_{254}$ and their relative contribution to total DOC in all salinity treatments ($p < 0.0001$). The effect of salinity on carbon quality is further demonstrated by the flattening of the slope of the relationship between phenolics and DOC (Figure 25). As we found for bulk DOC, these treatment effects were more extreme in the Ponzer muck than in the Hyde loam, leading to a significant interaction effect of site by salinity on phenolics ($F(2,48) = 3.341, p = 0.0438$) and $SUVA_{254}$ ($F(2,48) = 4.055, p = 0.0236$).

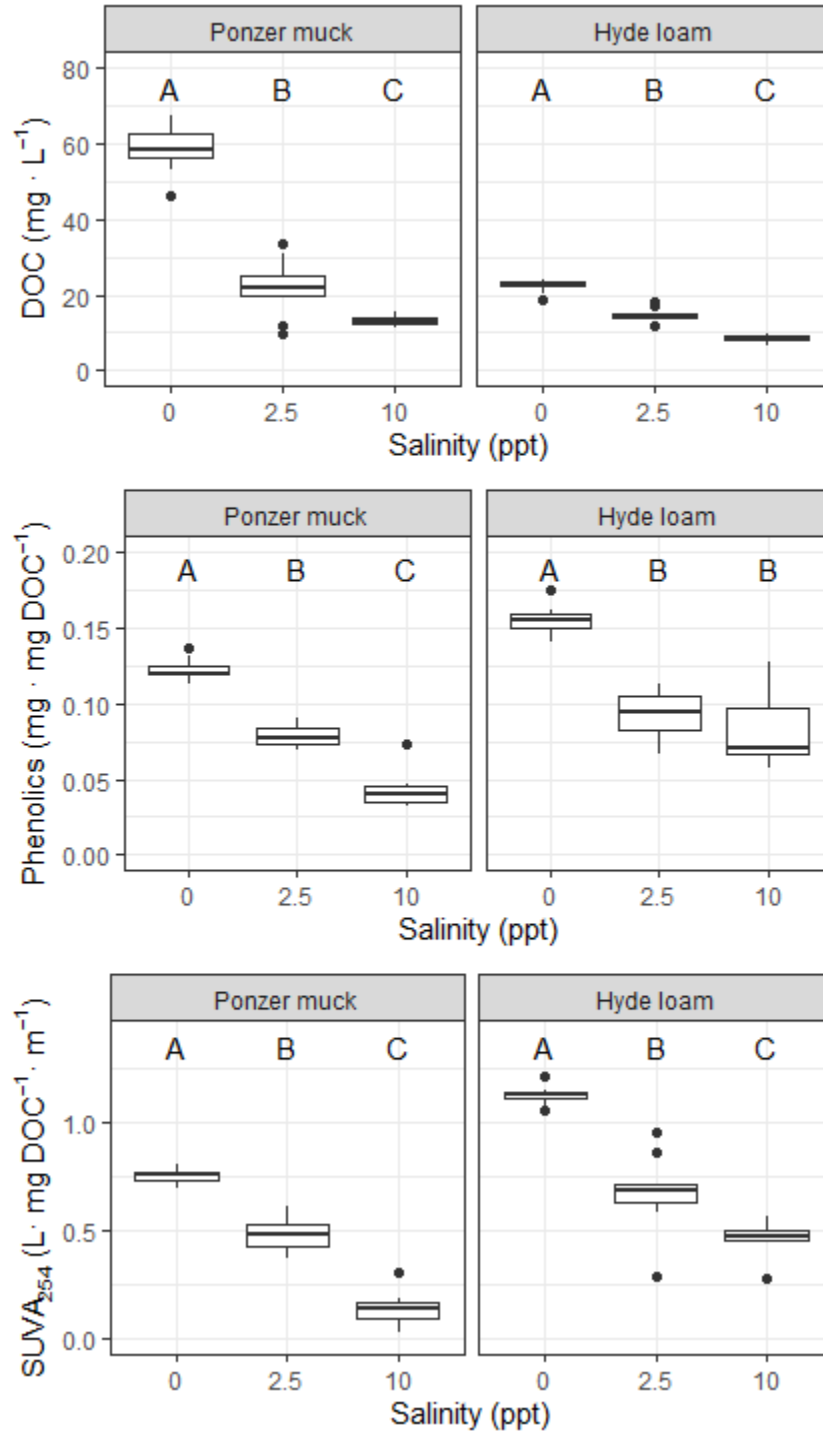


Figure 24: Effect of salinity treatment on DOC, phenolic compounds and SUVA₂₅₄. Letters indicate significant difference between treatment (Tukey's HSD test, P < 0.05). Absolute concentrations of phenolics compounds and SUVA₂₅₄ absorbance are shown in Appendix D: Figure 38.

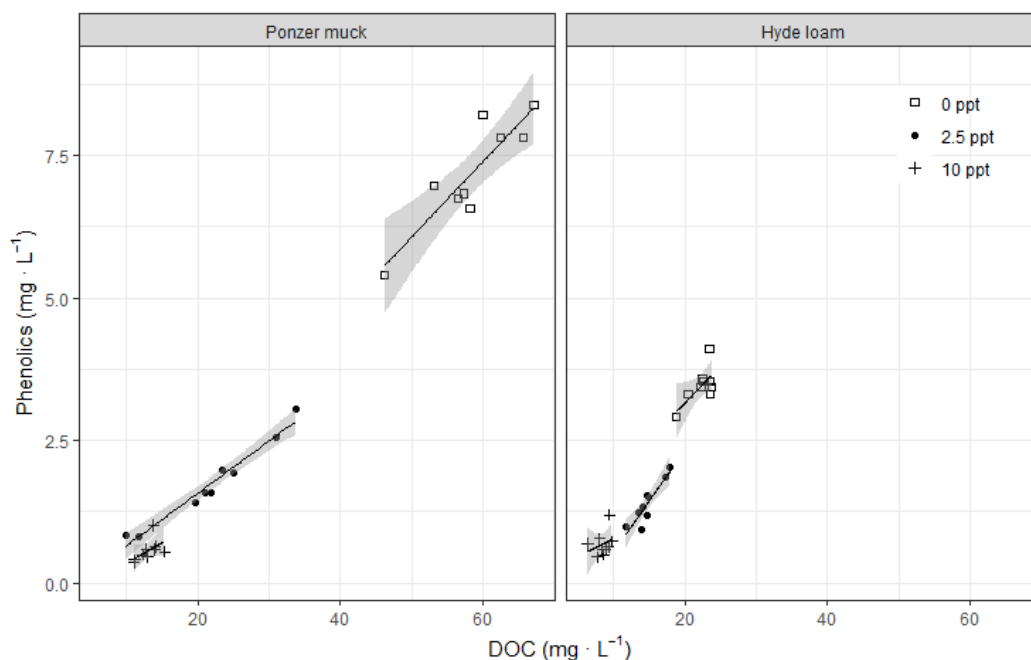


Figure 25: Effect of salinity on DOC and phenolics in relation to one another. The relationship between $SUVA_{254}$ and DOC exhibits a similar pattern (see Appendix D: Figure 39).

Finally, we examined the total organic matter content of soil samples following the 21-day incubation period. Salinity treatments resulted in greater retention of soil organic matter and all differences were statistically significant ($P < 0.0001$) as shown in Figure 26. The loss of organic matter was 11.6 % (Ponzer muck) and 14.6 % (Hyde loam) greater in the control treatment than the high salt treatment). The Hyde loam experienced a greater percent loss than the Ponzer muck under the control treatment, however under elevated salinity, soil organic matter losses were comparable across soil types. Salt suppression of organic matter loss is assumed to be primarily through suppression of microbial respiration. We did not detect an overall site by treatment interaction effect on final SOM content.

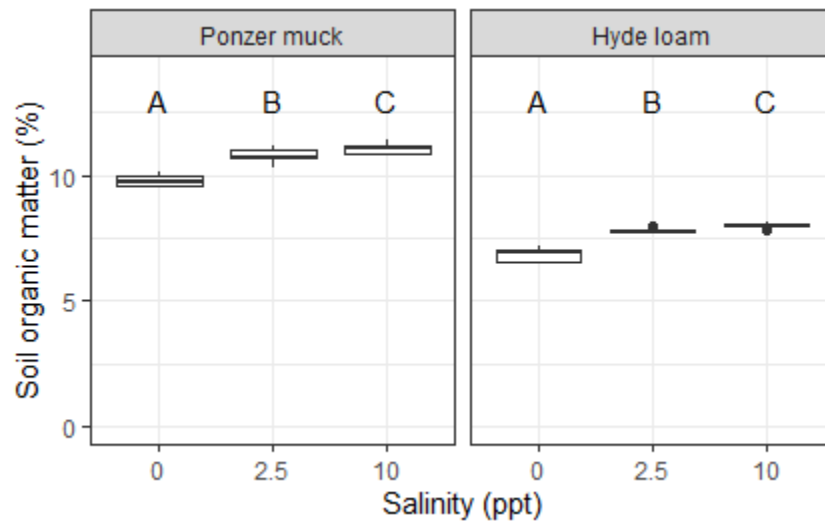


Figure 26: Total soil organic matter lost on ignition at 500 °C. Letters indicate significant difference between treatment (Tukey’s HSD test, $P < 0.05$).

5.4 Discussion

We found an overall slowing of soil organic carbon cycling in response to salinity that is strongly mediated by background soil conditions in this experimental manipulation of soil salinity and pH. Our findings support our initial predictions—the salinity treatments reduced microbial respiration, the solubility of organic carbon, and the aromaticity of DOC. Surprisingly, we also observed a significant effect of the salinity treatment on the total organic matter pool. At the conclusion of the 21-day incubation period, while the control soils have lost 12.8 % (Ponzer muck) and 15.7 % (Hyde loam) of their organic matter content, the highest salt treatment soils lost only 1 % of their organic matter content (both soil types). Given the short duration of the experiment, we did not expect to observe a significant effect on this relatively stable carbon pool.

The effects of our salinity treatments eclipsed the effect of the pH manipulation, and we found no evidence to support our prediction that increases in pH from seawater additions might offset the effects of the salinity treatments on carbon solubility. Indeed, our pH manipulations had minimal impact on soil pH in our experimental soils. The effective pH variation we achieved with our 5.5 to 8.8 pH manipulation treatments led to variation of less than 0.3 pH units across both soils due to extensive soil buffering. Measuring the effective pH of our treatments, revealed an unanticipated but important outcome of this experiment. Our salinity treatments affected soil pH itself (See Figure 21 and Appendix D: Figure 40, Figure 41, and Figure 42). Soil pH may either increase or decrease as a result of salinization (Adams *et al.* 1984; Kombo *et al.* 2005) and ecosystem responses may be contingent upon that pH change. Our results show a decline in pH of more than half a unit in both soils following the initial treatment application (Figure 21). A release of hydrogen ions may be stimulated by the exchange of cations from soil particles and organic matter following salt addition or a natural saltwater intrusion event (Adams *et al.* 1984; Kissel *et al.* 2009). Interestingly, the low salinity treatment (2.5 ppt) produced a greater pH decrease than the high salinity treatment (10 ppt). It is possible that at low salinity, protons are displaced, but at higher salinity, or after prolonged exposure, the base cations added in our treatment solution and released into solution through cation exchange may elevate soil pH over all, as observed in this study and in studies by Kombo *et al.* (2005) and Weissman and Tully (2020). This mechanism of pH alteration would be dependent on the initial conditions of soil base saturation. Base saturated soils (like the Hyde loam) may not exhibit an increase in acidity upon the introduction of marine salts, instead pH is elevated by the influx of base cation, as seen in our results (10 ppt treatment). The effective pH caused by inundation with seawater (pH of 8.1) can thus vary widely based on degree and

duration of exposure and initial soil conditions and may explain much of the variation in reports of salt effects on soil carbon dynamics.

Adding marine salts to our soils reduced the solubility of organic carbon, altering both the quantity and quality of DOC leached from soil samples and, presumably, the form and availability of the soil carbon removed from solution. These results are in agreement with previous work done on soils from this site in a study that demonstrated a similar reduction of DOC export due to salinization and drought at the landscape scale (Ardón *et al.* 2016). The salinity treatments also impact the chemical makeup of DOC by reducing the absolute concentrations of phenolic compounds and SUVA₂₅₄ absorbing compounds (see Appendix D: Figure 39) as well as their relative abundance within the total DOC pool (Figure 25). This suggests a potentially important change in the quality of soluble carbon following salinization, with large, aromatic compounds likely to be more susceptible to flocculation upon the addition of marine salts (Shainberg and Letey 1984). These changes to microbial carbon sources may have cascading impacts on soil carbon turnover and other biogeochemical processes (Creed *et al.* 2018).

Microbial respiration was significantly reduced by the addition of salt, although this effect was greater in the Hyde loam than in the Ponzer muck soil. While salinity's direct effect on microbial activity and community composition is almost certainly at play (Lozupone and Knight 2007; Dang *et al.* 2019; Rocca *et al.* 2020), there may also exist an indirect effect following the influence of salt on organic carbon solubility. Prior work by Liu *et al.* (2017) asserts that DOC is the main source of CO₂ from microbial respiration. Alterations to the form and availability of the DOC pool following salinity treatment, may indirectly mediate microbial respiration. The indirect effects of salinity on DOC as a control for microbial

respiration is not often discussed in the literature (Neubauer 2013), but provides a case for a more wholistic approach to investigating soil carbon dynamics. More work in this area is necessary to tease apart the contribution of the indirect effects of salinity on DOC versus the direct effects of salinity stress on soil microbes.

Our demonstration that salt suppressed microbial activity is consistent with several prior experiments (Ardón *et al.* 2016, 2018; Helton *et al.* 2019; Doroski *et al.* 2019; Wen *et al.* 2019), though numerous studies have observed the opposite trend (Weston *et al.* 2006, 2011; Chambers *et al.* 2011; Neubauer 2013). Mechanisms supporting enhanced respiration following salt exposure include the fertilization effect of low dose salt treatments and mobilization of nutrients and labile carbon following cell death (Wichern *et al.* 2006; Herbert *et al.* 2015). Explanation for these discrepancies within the literature may include geographic differences, experimental duration, treatment strength, and other experimental design conditions. We hypothesize that edaphic factors, in particular soil pH may be an important, and often overlooked, explanatory variable. Our study was not designed to tease apart the different potential mechanisms underpinning the observed site differences; however, this should be the subject of further research, particularly the effects of variable vegetation and hydrology. Vegetation may be driving soil organic matter content, which may in turn mediate soil respiration responses to salinization as discussed above. The presence of bald cypress at the Hyde loam site may be contributing to the abundance of phenolic compounds in the soil due to more recalcitrant leaves. The absence of living plants from our experimental design may also underpin certain results (Marinos and Bernhardt 2018). Prior work demonstrates the importance of the interaction between salinity and hydrology particularly in intermittently flooded soils (Helton *et al.* 2019). The Hyde loam site, which experienced greater suppression

of respiration following salinity, experiences more frequent inundation, however dry conditions typically exacerbate salt stress on microbes (Rath *et al.* 2017). These findings provide new avenues to pursue in future work.

Our experiment contributes to the expanding literature on coastal wetland salinization and helps tease apart a nuance of salinity that is often overlooked. Though pH and salinity cannot be independently manipulated, we show that salinity interrupts several processes within the carbon cycle. Our results show that salinity leads to a slowing of soil carbon cycling by reducing SOC solubility and suppressing microbial respiration. We also provide evidence that salinity induced changes in pH may drive the observed responses and that the effects of salinity are mediated by baseline soil properties, likely pH and base cation saturation. This experiment provides evidence that salinization of freshwater wetlands may lead to a slowing down of soil carbon cycling, however one must be careful not to extrapolate this result for carbon sequestration potential without examining how vegetation contributes to this cycle (Setia *et al.* 2012). Furthermore, carbon stocks in wetlands transitioning following salinization may take a long time to restabilize (Dang *et al.* 2019). Our experiment helps to shed light on some of the mechanisms at play within the soil matrix, a simplified system without hydrology or vegetation. Understanding how wetland carbon stocks will be affected by sea level rise depends on understanding these important drivers in concert. Nevertheless, we have shown how important site conditions and baseline soil properties are for mediating soil carbon cycling. Future experimental work on this subject should attempt to document baseline soil conditions and treatment effects on both salinity and soil pH, so that we may adequately compare between sites and synthesize a more complete understanding of coastal carbon dynamics in the context of sea level rise.

6

Conclusion

On the North Atlantic Coastal Plain, and in North Carolina in particular, sea level rise and salinization have had dramatically visible impacts on the landscape. Increasingly prevalent ghost forests and abandoned farmland are indicators that both ecological and human systems are retreating in the face of a growing threat. This dissertation addresses some of the questions and inconsistencies surrounding the effects of salinization on coastal landscapes as well as the spatial and temporal dynamics of these changes.

The first half of this dissertation examines vegetation change at the landscape scale. Using vegetation surveys, we found that tree growth was negatively correlated with soil salt content. Elevation was also correlated with tree growth, indicating low elevation may be unfavorable for forested wetlands. The most important finding was that the lowest, saltiest plots were where biomass loss occurred. Findings from these surveys suggest that significant changes to coastal vegetation may be imminent, but they also highlight a major drawback of classical survey methods. The time and effort required to collect this data and the paucity of associated statistical power does not match the scope of the changes occurring in coastal NC.

It became clear while writing this chapter that spot surveys could not provide answers to a bigger question. For this reason, we turned to remotely sensed data of regional vegetation to assess the extent to which these plant communities have already changed across the region as a whole.

The idea for Chapter 3 was driven by a need for answers we could not get with measurements taken on the ground. Where is the landscape changing? How much has it already changed? What is the current extent of salinization? How much more wetland area may be vulnerable to change? Satellite records allowed us to determine that 32 % of Alligator River National Wildlife Refuge has experienced a shift in land cover over the past 35 years. As a protected Refuge, free from development and other land uses, this finding provides strong evidence that climate change is the driver of these observed changes. This work is also the first to attempt to estimate the extent of ghost forests, a novel habitat type, and found that as much as 11 % of forested area within the refuge had a detectable ghost forest phase. Our analysis showed that that these novel ecosystems are highly transient, quickly giving way to the scrub-shrub habitats which, in this region, appear to persist far longer. This study advances our understanding of the pace and consequences of vegetation community changes in coastal wetlands.

The second half of this dissertation goes beyond vegetation change to investigate the other major carbon pool vulnerable to sea level rise: soil carbon. As sea levels rise, it is important that we understand how this large carbon pool will be affected by increasing salinity. In our field experiment we found that soil carbon responses to salt treatments were variable between site and sampling date. Only in the final year of the four-year effort did results match our prediction of salt suppressing soil respiration and solubility of organic carbon. The

primary stocks of carbon in this system, vegetation and total soil carbon, were unaffected by our four-year treatment, and provide evidence for substantial resistance of young wetland forests to low-level salt stress. The final chapter of this dissertation was designed to follow up on the site variability observed between soil carbon responses in the field experiment. Despite similar land use history, the two soil series on the TOWeR property showed remarkable differences in certain characteristics, chiefly pH and base saturation. We interrogated site interactions with salt treatment effects as well as the effect of an added pH manipulation. Soil carbon responses (respiration and DOC solubility) were suppressed by marine salts but not by the pH manipulation, and there was a significant site-by-treatment interaction on most response variables. Our results highlight the importance of edaphic variation on the outcomes of salinization, a factor often overlooked and underreported in the literature.

The goals of my dissertation were to examine the effects of salinization on freshwater ecosystems. I have explored landscape patterns of vegetation changes and show that sea level rise and extreme events are contributing to massive ecosystem turnover, even in protected areas. I have also furthered our understanding of the soil carbon responses to salinization through experimental work. The field experiment was designed to resolve discrepancies in past studies surrounding ecosystem responses to salinization. Instead, the results highlighted substantial variation in these responses, but importantly, this variation is helping to move our understanding of these processes forward. The temporal variation we observed across the study period emphasizes the importance of interannual variability controlling these processes. Variability we observed between nearby sites with similar land-use histories emphasize the importance of edaphic factors in controlling the impact of salinization. Improving our

understanding of factors that mediate ecosystem responses to salinization will contribute to better global systems models and may enhance outcomes of restoration and land management.

Appendix A – Supplementary materials for chapter 2

Table 7: Site information and physical characteristics

Site ID	Date	LONG	LAT	Soil Type	Elev- ation	Soil moisture	Loss on ignition	pH	Bulk density
					m	%	%		g/cm ³
GC11	10/20/2015	-76.90	35.48	Tarboro Sand	1.30	39	22	4.43	0.63
GC12	10/20/2015	-76.90	35.48	Arapahoe fine sandy loam	0.22	78	51	5.48	0.22
GC13	10/13/2015	-76.91	35.47	Arapahoe fine sandy loam	0.91	48	22	5.63	0.41
GC14	10/14/2015	-76.91	35.47	Arapahoe fine sandy loam	0.27	85	74	6.35	0.16
PP7	10/21/2015	-76.14	35.99	Tomotley fine sandy loam	0.47	56	16	6.33	0.65
PP8	10/22/2015	-76.14	35.99	Tomotley fine sandy loam	0.27	45	13	6.33	0.69
PP9	10/28/2015	-76.14	35.99	Tomotley fine sandy loam	0.30	50	15	6.47	0.56
PP10	10/28/2015	-76.14	35.99	Tomotley fine sandy loam	0.33	89	68	6.73	0.13
CS2*	6/23/2016	-76.40	35.44	Stockade mucky sandy loam	0.33	108	15	5.75	0.64
CS3*	6/23/2016	-76.72	35.43	Roanoke fine sandy loam	2.35	48	13	4.64	0.24
CS4*	6/24/2016	-75.98	35.53	Backbay mucky peat	0.12	177	21	4.89	0.29
CS5*	6/24/2016	-75.92	35.61	Scuppernong muck	0.61	774	90	3.29	0.08
CS7	7/15/2016	-76.08	35.73	Weeksville silt loam	0.31	81	17	5.48	0.89
CS8	7/15/2016	-76.06	35.72	Belhaven muck	0.25	147	16	5.08	0.40
CS9	7/21/2016	-75.91	35.67	Pungo muck	0.48	756	96	3.58	0.15
CS12	7/7/2016	-75.78	35.70	Pungo muck	0.54	411	80	4.85	0.19
CS13*	7/14/2016	-75.88	35.80	Pungo muck	0.31	1480	82	4.82	0.08
CS15	7/14/2016	-75.92	35.84	Pungo muck	0.08	944	77	4.94	0.09
CS17*	6/17/2016	-75.92	35.89	Hyde loam	0.40	91	16	4.71	0.73
CS19*	6/30/2016	-75.83	35.95	Pungo muck	0.31	1062	91	4.13	0.09
CS20	7/14/2016	-75.82	35.94	Pungo muck	0.46	889	75	6.03	0.11

Table 7 Continued

Site ID	Date	LONG	LAT	Soil Type	Elev- ation	Soil moisture	Loss on ignition	pH	Bulk density
					m	%	%		g/cm ³
CS21*	7/14/2016	-75.84	35.94	Pungo muck	0.33	881	96	4.42	0.09
CS22*	7/01/2016	-76.31	35.74	Pungo muck	1.35	388	93	3.33	0.14
CS23*	6/16/2016	-76.55	35.73	Pettigrew muck	3.83	63	21	5.32	0.52
CS24*	6/9/2016	-76.45	35.80	Fortescue mucky loam	3.25	105	8.8	4.84	0.60
CS25*	6/10/2016	-76.40	35.78	Perquimans loam	3.06	57	11	4.35	1.01
CS27*	6/9/2016	-76.36	35.87	Tomotley fine sandy loam	0.62	66	8.5	4.93	0.85
CS28*	6/10/2016	-76.35	35.87	Altavista loamy fine sand	0.34	49	6	4.7	0.97
CS29*	7/7/2016	-76.36	35.93	State loamy fine sand	2.19	22	9.7	4.83	0.91
CS30*	7/7/2016	-76.36	35.94	Conetoe loamy fine sand	1.38	13	8.5	4.38	0.72
CS31	7/7/2016	-75.83	35.62	Hyde loam	0.84	206	35	4.26	0.53
AR1	6/8/2016	-75.76	35.77	Belhaven muck	0.50	424	96	3.73	0.18
AR2	6/8/2016	-75.79	35.81	Pungo muck	0.20	183	24	4.8	0.39
AR3	7/20/2016	-75.81	35.80	Belhaven muck	0.70	702	88	4.24	0.15

*Data marked with an asterisk and in bold are sites included in the comparative analysis with the Carolina Vegetation Survey.

Table 8: Soil chemistry data

Site ID	Cl ⁻	SO ₄ ²⁻	Na ⁺	K ⁺	Mg ²⁺	Ca ²⁺	NH ₄ ⁺	NO ₃ ⁻
	µg/g	µg/g	µg/g	µg/g	µg/g	µg/g	µg/g	µg/g
GC11	94.9	51.6	19.4	14.1	5.2	8.3	0.8	2.4
GC12	1722.3	246.9	305.5	b.d	19.6	14.9	10.9	5.7
GC13	157.7	75.3	52.3	18.4	8.0	8.7	0.4	2.9
GC14	3793.1	427.7	465.4	b.d	65.8	31.2	5.8	0.8
PP7	109.5	34.2	99.0	14.2	9.2	6.8	1.0	0.5
PP8	188.7	21.2	99.6	11.7	8.6	4.2	2.5	1.8
PP9	656.8	46.2	270.9	21.3	22.4	11.6	2.6	2.2
PP10	8532.3	284.4	b.d.	b.d	215.3	101.6	29.6	12.7
CS2*	2835.5	282.4	884.6	51.3	54.2	22.4	10.5	2.4
CS3*	91.3	17.8	188.9	9.9	19.8	11.6	7.8	1.5
CS4*	9479.2	1417.6	2523.9	149.1	217.3	80.0	22.3	3.5
CS5*	114.9	1071.1	227.3	19.9	25.8	21.0	9.2	4.2
CS7	196.8	61.0	1117.2	25.7	157.7	157.7	b.d.	0.1
CS8	1135.7	129.7	262.1	37.4	16.9	16.9	12.6	0.7
CS9	310.8	190.0	1128.0	46.6	53.7	53.7	9.6	2.6
CS12	976.2	118.9	924.4	35.4	376.3	376.3	13.7	b.d
CS13*	1264.1	256.6	841.9	84.4	121.4	121.4	39.4	4.0
CS15	807.9	196.6	115.9	4.4	11.4	11.4	27.3	1.6
CS17*	123.4	24.5	233.4	13.7	27.7	12.6	2.5	1.6
CS19*	1836.7	139.2	444.4	27.4	54.5	50.9	14.3	12.0
CS20	15354.1	1793.7	444.4	27.4	54.5	50.9	44.2	3.2
CS21*	1444.4	178.4	444.4	27.4	54.5	50.9	12.7	b.d
CS22*	223.5	46.7	127.6	28.9	7.7	28.1	21.6	18.4
CS23*	60.7	12.4	81.0	6.3	8.4	36.7	1.6	37.0
CS24*	19.4	96.1	105.7	13.2	18.1	48.1	31.2	1.4
CS25*	11.3	12.0	87.9	12.7	8.7	17.0	6.5	9.7
CS27*	24.4	55.0	97.8	4.0	3.3	12.0	23.2	0.6
CS28*	12.8	50.0	68.8	2.1	1.9	7.1	16.5	0.7
CS29*	63.2	8.4	103.8	7.6	6.6	9.6	4.8	1.2
CS30*	52.3	6.4	66.1	2.8	1.4	11.1	4.2	1.1
CS31	180.2	15.5	119.3	23.1	17.9	17.9	b.d.	0.4
AR1	205.8	68.1	314.3	13.0	12.1	12.1	16.0	5.9
AR2	212.7	31.4	335.9	10.1	39.2	39.2	13.5	2.9
AR3	192.2	125.5	264.5	29.0	46.6	46.6	29.7	8.4

Table 9: Vegetation Summary

Site ID	Total basal area	Major species	basal area (percent change in basal area from CVS survey)
	m ² /hectare		m ² /hectare (%)
CS2*	14.9	Pinus t.	14.8 (-39)
CS3*	230	Liriodendron t., Pinus t.	66.7 (+750), 53.6 (+786)
CS4*	3.1	Juniperus v.	3.0 (-61)
CS5*	136	Pinus s., Gordonia l.	75.3 (+360), 35.0 (+140)
CS13*	16.3	Chamaecypari t., Nyssa b.	0 (-100), 9.6 (+245)
CS17*	171	Pinus t., Liquidambar s.	63.3 (+63), 47.3 (+267)
CS19*	65.9	Persea p., Pinus s.	46.3 (179), 14.3 (-11.9)
CS21*	35.3	Pinus s., Persea p.	23.6 (0.04), 11.6 (-26.7)
CS22*	200	Nyssa b., Magnolia v.	118 (651), 37.6 (1250)
CS23*	225	Liriodendron t., Liquidambar s.	182 (561), 34.7 (159)
CS24*	533	Taxodium d.	487 (122)
CS25*	221	Liquidambar s., Ilex o.	129 (303), 44.6 (753)
CS27*	177	Liriodendron s., Pinus t.	81.2 (289), 36.9 (318)
CS28*	127	Quercus a., Fagus g.	54.8 (995), 35.2 (199)
CS29*	223	Quercus n., Liriodendron t.	71.9 (404), 57.3 (1062)
CS30*	166	Pinus t.	80.1 (981)

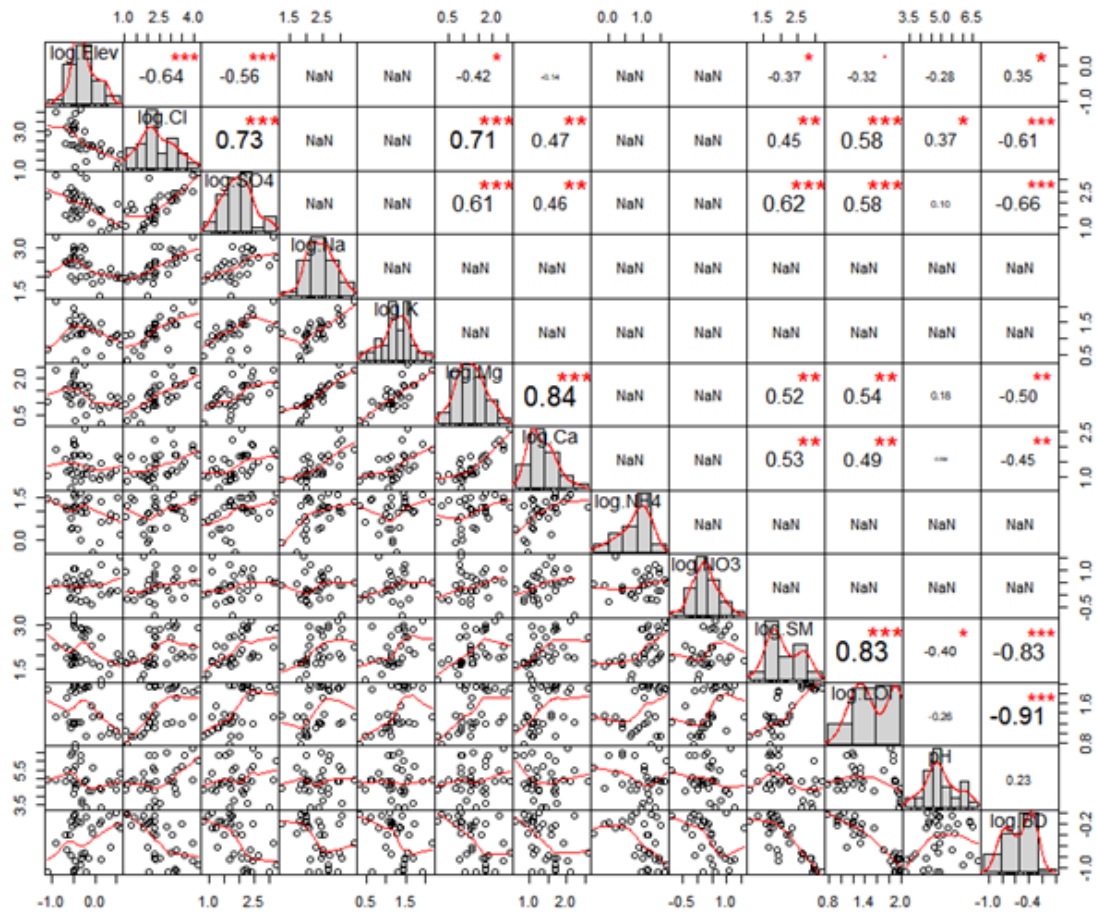


Figure 27: Full correlation matrix. Correlation plots of all environmental characteristics (log transformed) measured at each site. (Elev = elevation, SM = soil moisture, LOI = loss on ignition, and BD = bulk density). Significance codes are: * < 0.05, ** < 0.01, *** < 0.001.

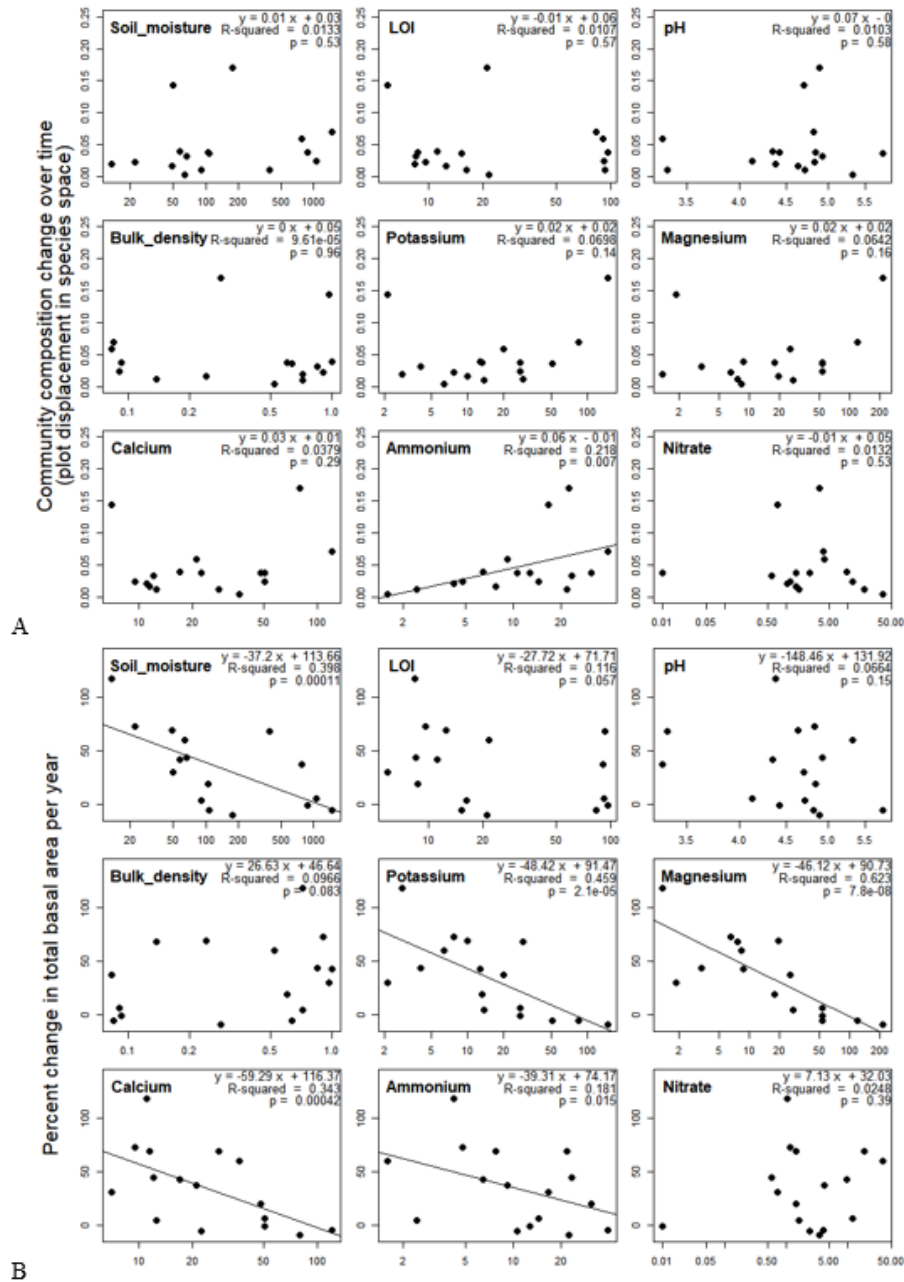
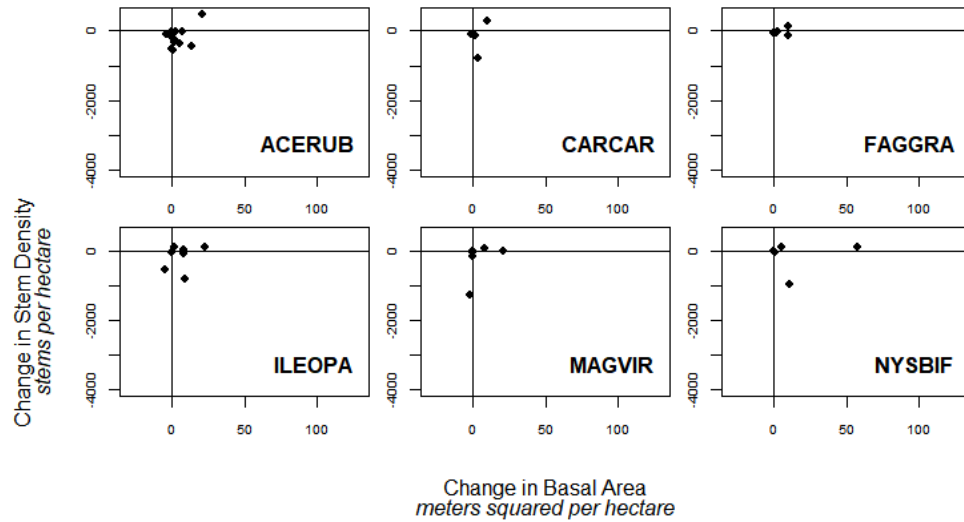
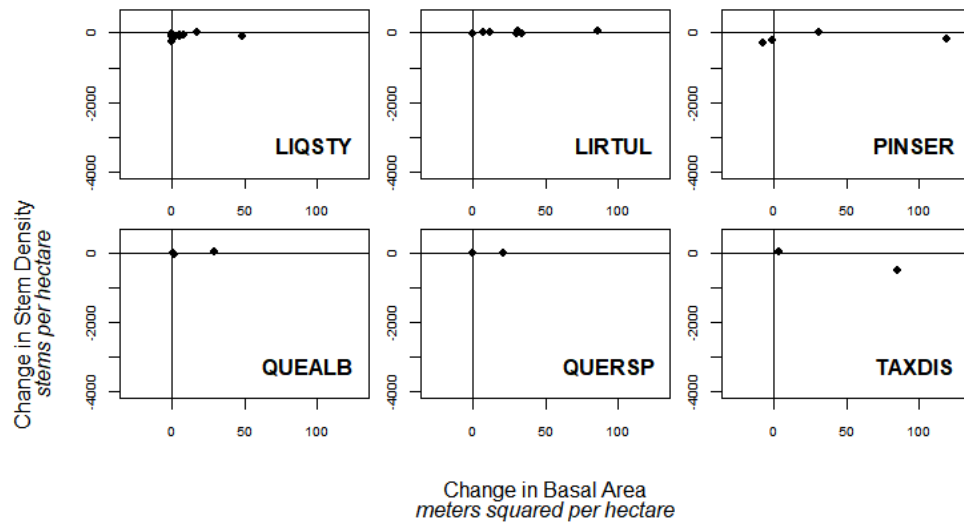


Figure 28: Normalized correlation plots. (A) Community composition change (y-axis is the length of the arrows in Figure 3, normalized over time). (B) Percent change in total basal area per year compared to environmental characteristics. Soil ion content ($\mu\text{g}/\text{gram}$ dry soil), soil moisture (SM, %), loss on ignition (LOI, %), and elevation (meters) data is shown on log scales.

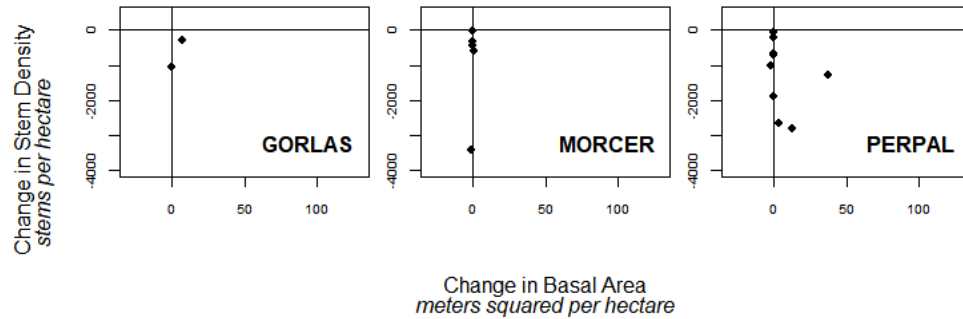
Group 1: Variable, these species are gaining basal area in some plots and losing stems in others.



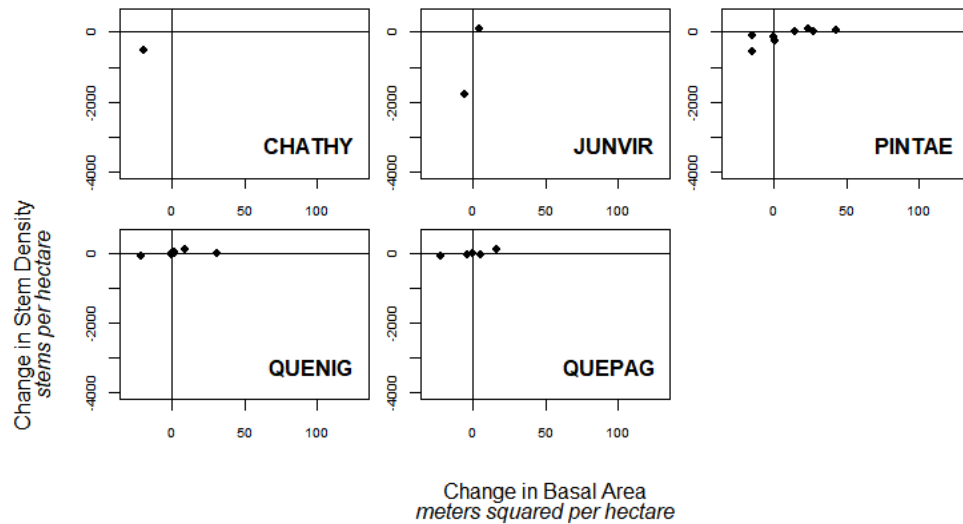
Group 2: These species are generally gaining basal area with little gain or loss of stems



Group 3: These species are losing stem density with little change in basal area.



Group 4: These species are losing basal area in some plots (plot #2, 4, 13, 17 are the plots experiencing the most loss overall. In plot #4, which was dominated by *Juniperus virginiana*, nearly all stems have died; this plot is transitioning to shrub/scrub dominated community).



Group 5: Species experiencing little change in most plots.

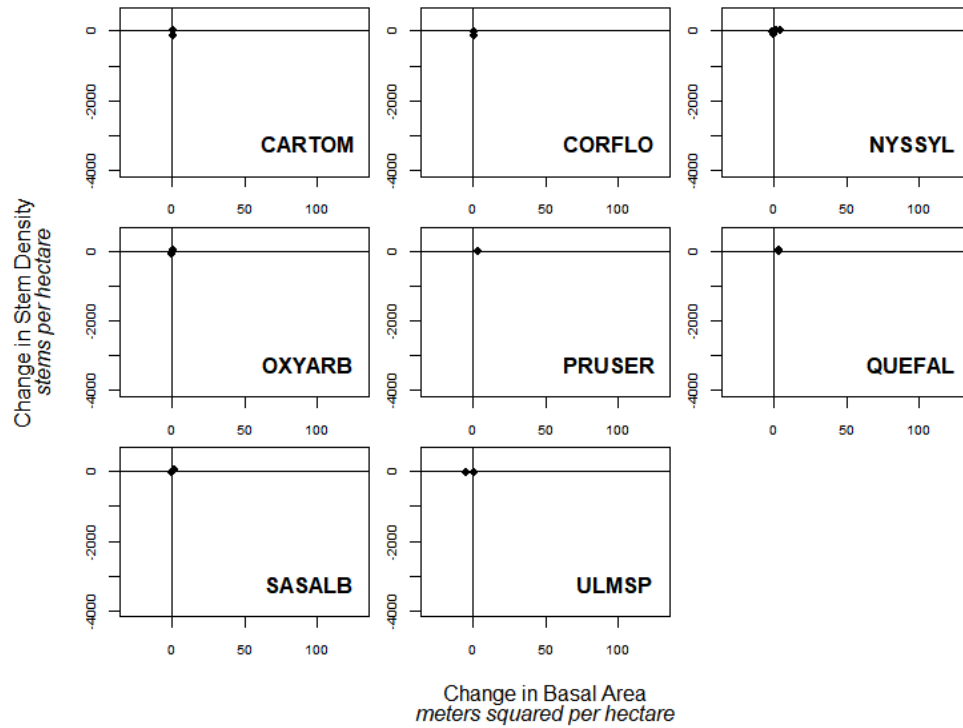


Figure 29: Species change plots. For each species surveyed, the change in basal area and change in stem density over time is plotted showing how communities on the Coastal Plain of NC are shifting. Species have been categorized qualitatively into five general groupings.

Appendix B – Supplementary materials for chapter 3

Table 10: Accuracy Assessment for classifications.

Landsat 8 (2017)			
Class	Validation Points	Producer Accuracy	User Accuracy
Pine	166	91.9%	95.2%
Deciduous	164	98.1%	93.3%
Marsh	136	93.2%	93.2%
Ghost	91	88.8%	85.5%
Shrub	158	87.7%	90.5%
Overall	715		92.2%

Landsat 7 (2012)			
Pine	179	89.5%	85.5%
Deciduous	165	89.5%	87.9%
Marsh	171	86.4%	88.9%
Ghost	90	69.0%	77.5%
Shrub	147	68.1%	62.6%
Burn	46	91.8%	97.8%
Dry pine	78	91.5%	96.2%
Overall	876		82.5%

Landsat 5 (2010)			
Pine	188	86.1%	88.8%
Deciduous	195	89.6%	88.7%
Marsh	175	89.2%	95.4%
Ghost	29	76.9%	34.5%
Shrub	157	80.9%	80.9%
Overall	744		82.3%

Table 11: Confusion matrix for the Landsat 8 classifier

Landsat 8 (2017)

<i>observed</i>	<i>predicted</i>						<i>% error</i>
	pine	deciduous	marsh	ghost	shrub		
pine	157	1	2	2	4		5.73
deciduous	6	153	0	2	3		7.19
marsh	1	0	123	2	6		7.32
ghost	3	1	1	71	7		16.90
shrub	4	2	6	3	143		10.49
<i>% error</i>	8.92	2.61	7.32	12.68	13.99		

Table 12: Confusion matrix for the Landsat 7 Classifier

Landsat 7 (2012)

<i>observed</i>	<i>predicted</i>							<i>% error</i>
	pine	deciduous	marsh	ghost	shrub	burn	dry pine	
pine	153	9	0	4	13	0	0	16.99
deciduous	10	145	0	0	9	1	0	13.79
marsh	0	0	152	4	13	0	2	12.50
ghost	1	0	7	69	8	0	4	28.99
shrub	7	8	17	20	92	2	1	59.78
burn	0	0	0	1	0	45	0	2.22
dry pine	0	0	0	2	0	1	75	4.00
<i>% error</i>	11.76	11.72	15.79	44.93	46.74	8.89	9.33	

Table 13: Confusion matrix for the Landsat 5 Classifier

Landsat 5 (2010)

<i>observed</i>	<i>predicted</i>					<i>% error</i>
	pine	deciduous	marsh	ghost	shrub	
pine	167	11	0	1	9	12.57
deciduous	16	173	0	0	6	12.72
marsh	1	0	166	0	7	4.82
ghost	4	0	7	10	8	190.00
shrub	6	9	13	2	127	23.62
<i>% error</i>	16.17	11.56	12.05	30.00	23.62	

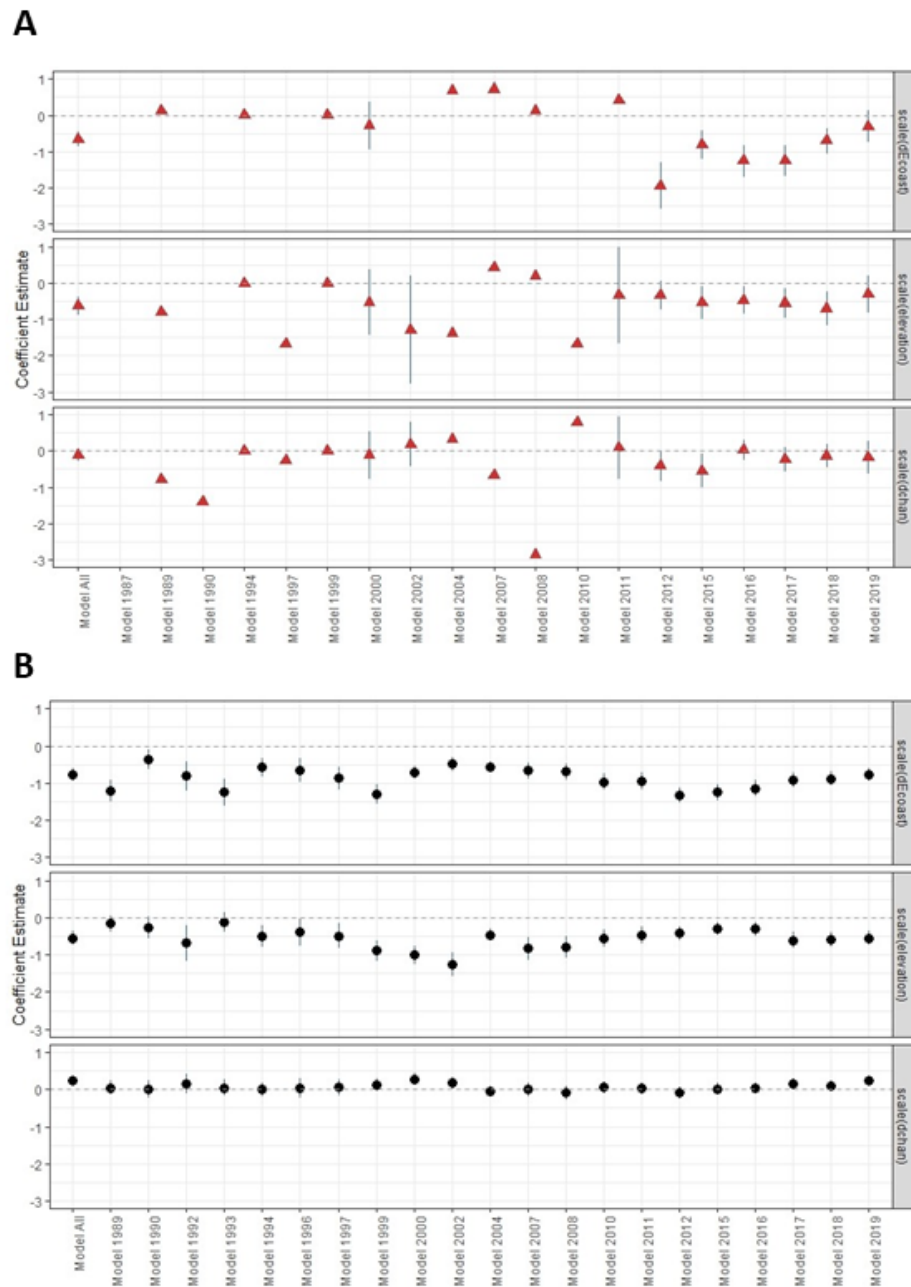


Figure 30: Coefficients of environmental predictors over time. (A) Ghost forest formation and (B) forest loss for each year in the time series (missing years indicate that the model did not converge).

Appendix C – Supplementary materials for chapter 4

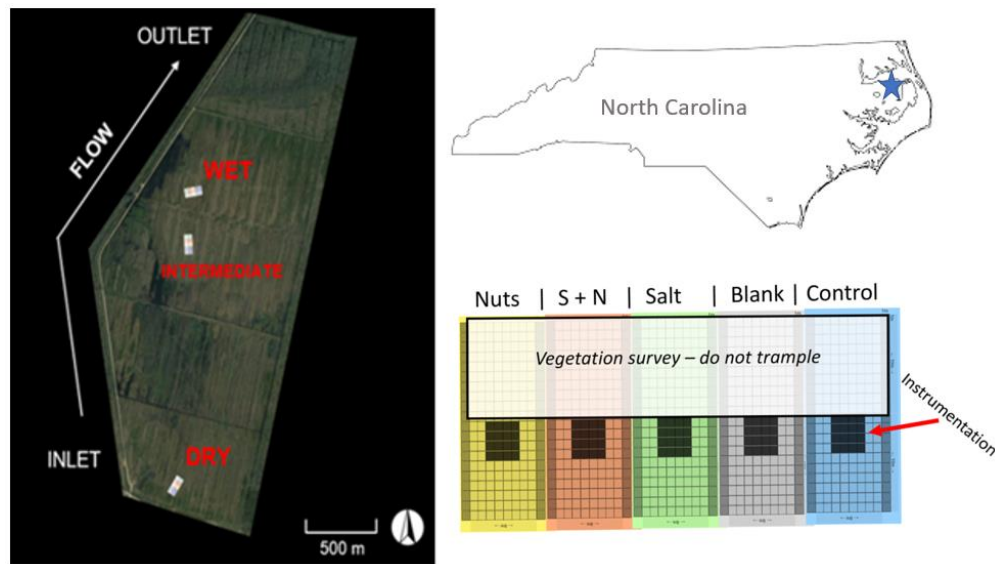


Figure 31: Timberlake property map with site locations (left). Location in North Carolina (top right) and schematic layout of salt and nutrient addition plots (bottom right).

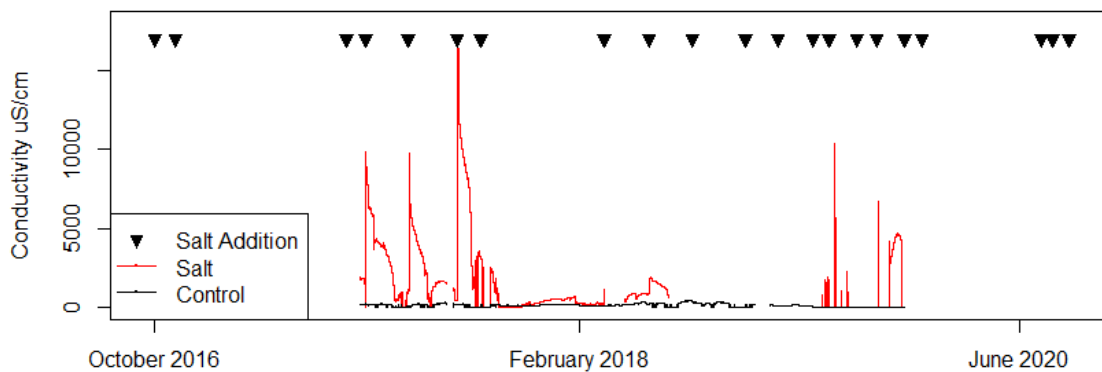


Figure 32: Timeline of salt additions (black triangle) beginning in Fall 2016 through summer 2020. Conductivity data from wells illustrating the effect of the treatments on porewater (gaps in the data indicate water level dropped below sensor depth or sensor failure).

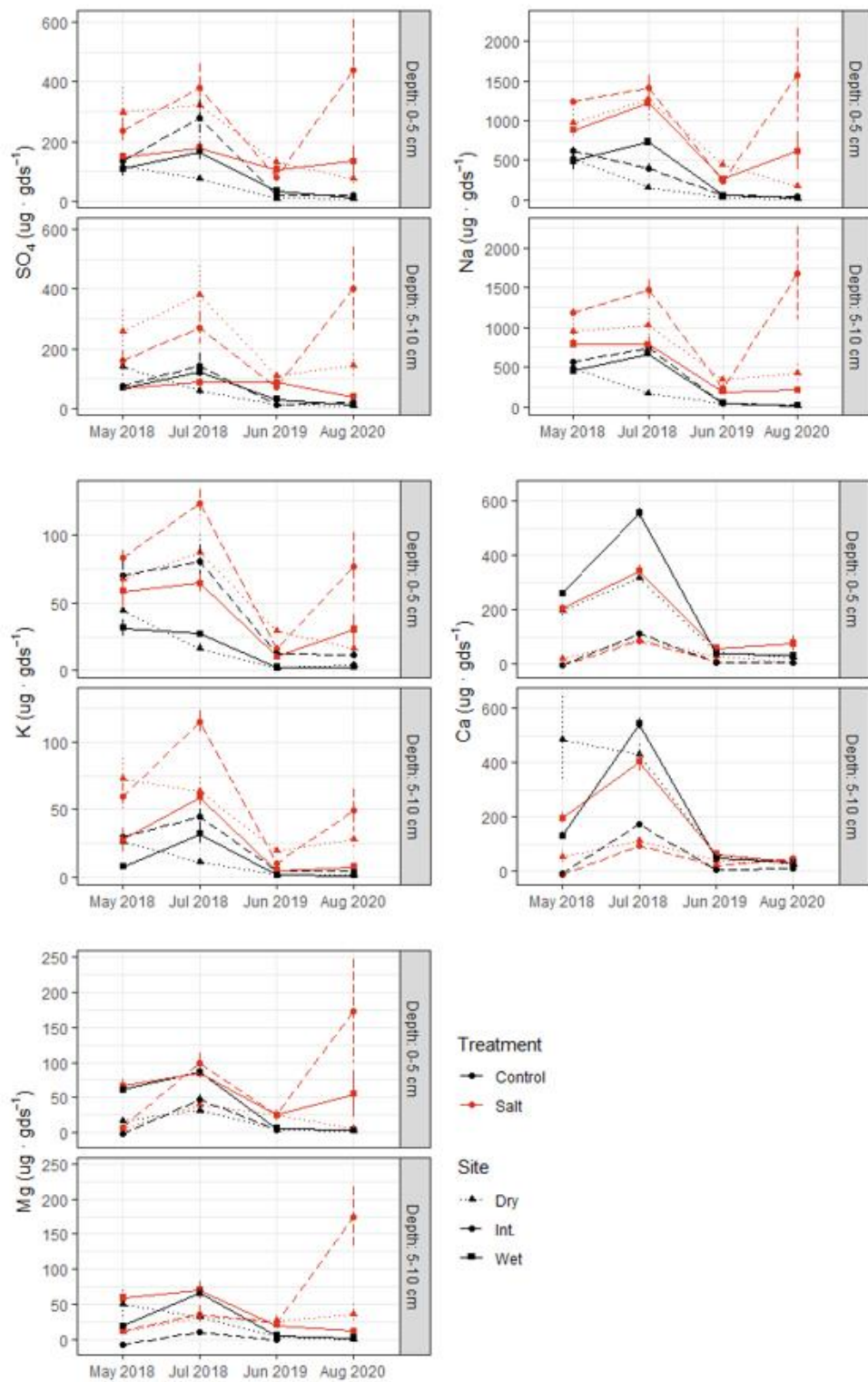


Figure 33: Soil extractable ion concentrations across all sites, treatments, depths and sampling dates.

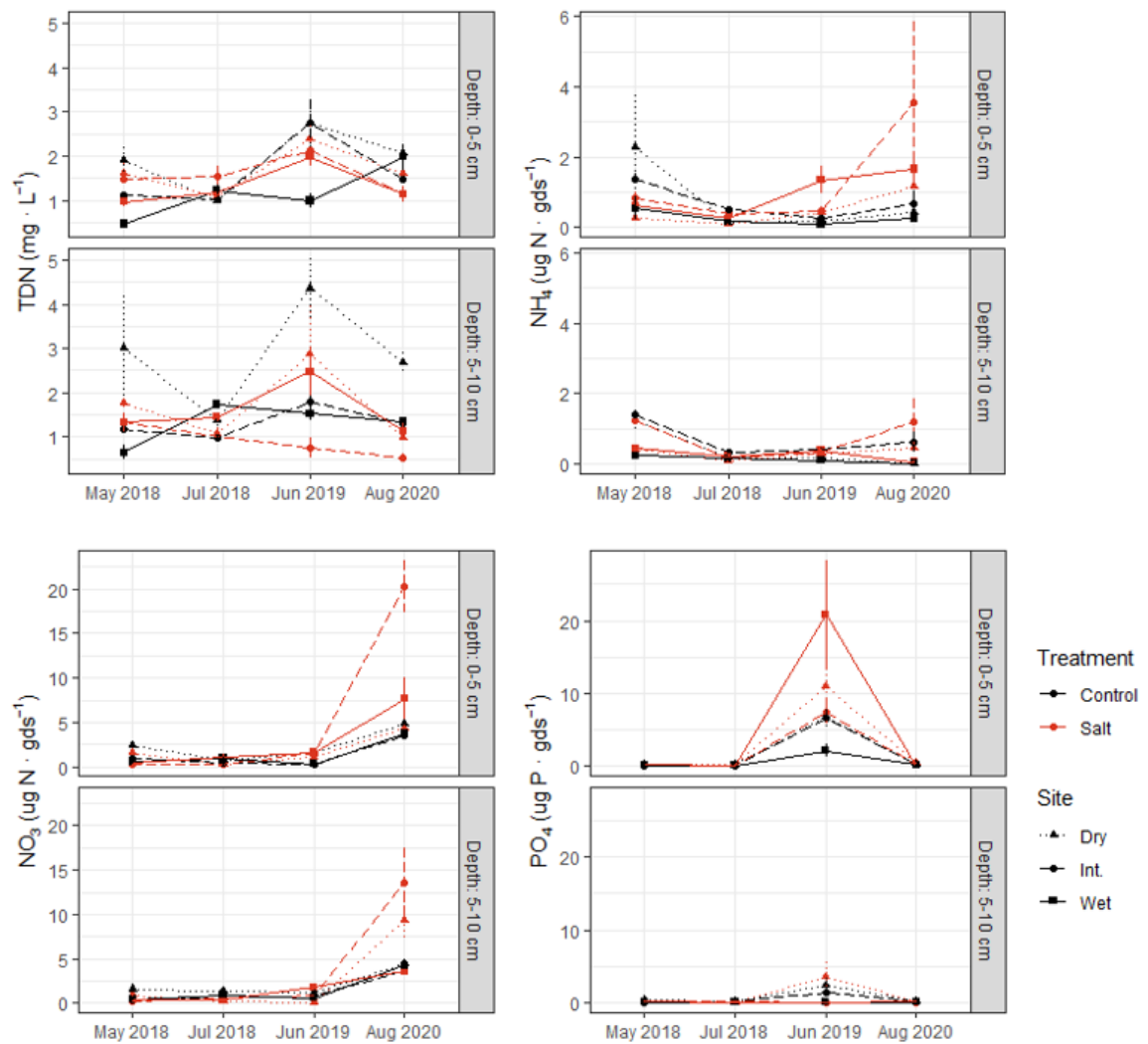


Figure 34: Soil extractable nutrient concentrations across all sites, treatments, depths and sampling dates.

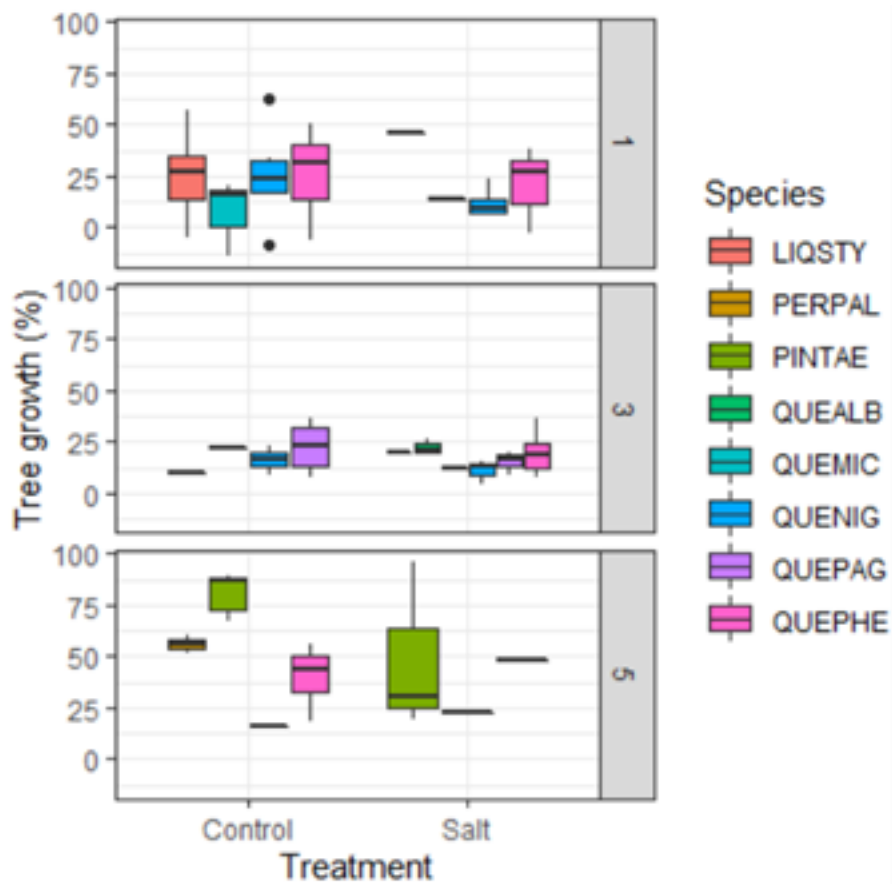


Figure 35: Tree growth (%) from 2015-2021 by species (species with fewer than 3 occurrences excluded).

Table 14: Salt addition and sampling schedule

Year	Date	Activity
2015	November	Sites established; trees measured
2016	October 5	Salt additions begin
	November 3	Salt addition
2017	March 7	Salt addition
	May 4	Salt addition
	July 5	Salt addition
	October 15	Salt addition
	April 9	Salt addition
2018	May 10	<i>First soil sampling</i>
	June 11	Salt addition
	July 10	<i>Second soil sampling</i>
	August 8	Salt addition
	October 27	Salt addition
	February 28	Salt addition
	March 29	Salt addition
	April 30	Salt addition
2019	May 21	Salt addition
	June 20	<i>Third soil sampling</i>
	June 30	Salt addition
	July 22	Salt addition
	August 19	Salt addition
	September 28	Salt addition
	October 12	Salt addition
2020	June 26	Salt addition
	July 13	Salt addition
	August 5	Salt addition
	August 8	<i>Fourth soil sampling</i>
2021	January 16	Trees measured

Table 15: Supplementary data tables for Chapter 4. A: Water extractable soil ion content (Cl, SO₄, Na) by site, treatment, depth, and date, reporting mean (standard error, n = 5). Bolding indicates a statistically significant difference between salt and control ($\alpha = 0.05$).

	Depth	Site 1		Site 3		Site 5	
		Control	Salt	Control	Salt	Control	Salt
Cl ⁻ (µg/gds)							
May 10th, 2018	(0-5)	64.3 (10.27)	532.3 (265.82)	105.25 (6.68)	975.71 (45.2)	123.92 (23.98)	419.8 (28.15)
	(5-10)	59.73 (10.97)	685.0 (367.37)	67.13 (12.3)	978.51 (79.57)	58.36 (11.96)	467.82 (74.2)
July 10th, 2018	(0-5)	63.63 (9.83)	1444.7 (371)	511.31 (104.4)	2019.2 (259.9)	572.26 (36.82)	910.45 (98.9)
	(5-10)	47.24 (5.11)	1148.6 (273)	532.54 (50.37)	1756.7 (184.2)	476.5 (17.49)	575.87 (227.8)
June 20th, 2019	(0-5)	6.2 (0.82)	616.07 (99.8)	28.13 (8.48)	306.1 (94.34)	31.04 (5.84)	328.17 (64.9)
	(5-10)	7.44 (1.38)	511.68 (82.1)	5.21 (0.56)	336.93 (99.05)	20.73 (9.15)	261.37 (17.1)
August 8th, 2020	(0-5)	10.02 (1.44)	170.5 (35.5)	35.31 (14.02)	2571.8 (1033)	11.43 (2.08)	972.8 (455.8)
	(5-10)	7.23 (1.08)	601.1 (199.8)	22.78 (4.38)	2848.6 (1001)	9.37 (1.02)	273.16 (81.1)
SO ₄ ²⁻ (µg/gds)							
May 10th, 2018	(0-5)	117.84 (17.17)	298.47 (81.04)	136.46 (26.37)	238.59 (38.39)	109.6 (25.83)	148.97 (9.2)
	(5-10)	137.84 (27.87)	256.28 (74.02)	76.78 (2.34)	160.54 (33.09)	68.8 (9.63)	67.67 (6.62)
July 10th, 2018	(0-5)	76.35 (12.29)	323.21 (72.2)	277.31 (63.55)	379.51 (82.17)	166.91 (26.13)	177.55 (27.41)
	(5-10)	57.01 (10.61)	380.24 (95.4)	143.26 (43.37)	268.4 (52.63)	121.46 (15.84)	86.14 (13.02)
June 20th, 2019	(0-5)	11.17 (0.18)	132.39 (15.0)	20.8 (4.29)	79.98 (18.24)	35.08 (4.9)	106.25 (23.7)
	(5-10)	13.81 (1.16)	109.23 (10.3)	13.8 (1.13)	70.54 (13.85)	30.52 (11.77)	87.31 (17.1)
August 8th, 2020	(0-5)	10.09 (0.62)	78.27 (18.34)	23.48 (3.14)	441.56 (167.7)	12.75 (0.91)	134.33 (52.75)
	(5-10)	8.94 (0.51)	141.75 (38.4)	21.61 (2.6)	400.6 (141.28)	11.57 (0.63)	38.08 (12.43)
Na ⁺ (µg/gds)							
May 10th, 2018	(0-5)	522.48 (58.04)	966.07 (184.1)	618.85 (43.08)	1232.53 (30.4)	492.22 (115.7)	879.03 (19.3)
	(5-10)	490.9 (12.45)	949.34 (224.5)	567.59 (13.59)	1187.1 (44.4)	456.23 (28.9)	789.87 (52.5)
July 10th, 2018	(0-5)	160.14 (11.73)	1264.7 (265)	399.14 (53.67)	1408.66(161.8)	731.61 (24.17)	1219.7 (77.5)
	(5-10)	168.98 (3.24)	1033.9 (197)	739.54 (40.96)	1482.15(114.1)	667.83 (6.97)	784.95 (93.1)
June 20th, 2019	(0-5)	34.1 (2.54)	444.82 (57.9)	57.57 (6.37)	241.72 (56.2)	56.74 (4.39)	261.72 (31.2)
	(5-10)	35.55 (2.26)	347.53 (37.9)	47.17 (2.75)	238.83 (57.26)	44.57 (5.57)	187.56 (12.2)
August 8th, 2020	(0-5)	14.5 (0.89)	167.05 (25.0)	44.3 (5.96)	1573.71 (594)	22.33 (1.55)	615.09 (240)
	(5-10)	12.18 (0.23)	416.7 (121.3)	32.23 (1.83)	1680.75 (595)	17.02 (1.12)	212.53 (39.2)

Table 15B. Water extractable soil ion content (K, Ca, Mg) by site, treatment, depth, and date, reporting mean (standard error, n = 5). Bolding indicates a statistically significant difference between salt and control ($\alpha = 0.05$).

	Depth	Site 1		Site 3		Site 5	
		Control	Salt	Control	Salt	Control	Salt
K⁺ (μg/gds)							
May 10 th , 2018	(0-5)	43.89 (2.7)	67.52 (11.9)	70.53 (9.99)	83.4 (5.8)	31.51 (6.14)	58.24 (12.15)
	(5-10)	25.96 (4.87)	72.45 (15.67)	30.24 (5.34)	60.06 (9.69)	7.99 (1.38)	27.67 (8.64)
July 10 th , 2018	(0-5)	16.55 (3.29)	86.57 (13.81)	80.18 (12.61)	123.63 (10.05)	27.19 (1.26)	64.54 (6.36)
	(5-10)	11.14 (0.51)	63.07 (11.07)	44.45 (5.97)	115.17 (8.08)	31.98 (6.63)	58.99 (5.72)
June 20 th , 2019	(0-5)	2.04 (0.22)	28.88 (3.05)	12.11 (1.75)	15.93 (3.5)	2.23 (0.36)	10.39 (2.43)
	(5-10)	1.72 (0.07)	19.69 (1.14)	4.47 (0.62)	10.07 (2.39)	1.6 (0.19)	4.88 (0.77)
August 8 th , 2020	(0-5)	3.82 (0.84)	16.06 (2.74)	11.74 (2.48)	76.31 (25.19)	2.59 (0.27)	30.17 (11.03)
	(5-10)	1.68 (0.19)	27.67 (7.03)	5.1 (0.57)	49.42 (15.91)	1.28 (0.12)	7.9 (1.17)
Ca²⁺ (μg/gds)							
May 10 th , 2018	(0-5)	194.95 (25.58)	18.98 (5.94)	4.04 (4.04)	b.d.	260.51 (12.32)	204.47 (15.1)
	(5-10)	484 (159.33)	52.47 (23.09)	0.3 (0.29)	b.d.	129.78 (12.72)	195.4 (17.48)
July 10 th , 2018	(0-5)	319.28 (7.51)	91.42 (21.36)	111.44 (13.36)	84.17 (9.57)	555.71 (19.21)	341.64 (24.5)
	(5-10)	428.12 (36.62)	112.52 (15.1)	170.61 (12.12)	92.39 (4.31)	541.77 (21.71)	401.46 (31.5)
June 20 th , 2019	(0-5)	44.88 (6.26)	28.6 (5.12)	8.48 (1.63)	11.25 (1.45)	39.73 (1.92)	57.38 (14.27)
	(5-10)	62.14 (4.48)	38.67 (7.28)	6.97 (0.47)	17.88 (1.61)	46.81 (4.48)	60.98 (3.84)
August 8 th , 2020	(0-5)	26.37 (1.11)	5.65 (0.63)	6.99 (1.15)	37.29 (16.12)	32.76 (3.95)	76.13 (29.12)
	(5-10)	25.98 (1.03)	28.34 (8.53)	9.22 (1.03)	46.38 (12.27)	31.24 (1.11)	35.19 (8.13)
Mg²⁺ (μg/gds)							
May 10 th , 2018	(0-5)	15.9 (1.5)	6.37 (2.67)	0.67 (0.45)	8.56 (2.26)	61.11 (5.06)	66.07 (10.02)
	(5-10)	49.59 (21.19)	11.44 (4.2)	0 (0)	12.79 (4.92)	18.93 (4.44)	59.42 (5.96)
July 10 th , 2018	(0-5)	31.91 (1.53)	40.5 (7.61)	46.65 (7.43)	99.99 (13.78)	86.27 (5.35)	84.23 (7.14)
	(5-10)	31.5 (5.24)	32.27 (9.55)	11.01 (3.9)	36.69 (11.81)	66.43 (3.34)	70.54 (12.73)
June 20 th , 2019	(0-5)	3.42 (0.44)	25.73 (6.19)	3.44 (0.98)	24.86 (7.42)	5.81 (0.54)	24.82 (8.46)
	(5-10)	3.96 (0.29)	27.13 (6.5)	0.04 (0)	22.92 (7.35)	5.51 (1.71)	20.55 (2.85)
August 8 th , 2020	(0-5)	1.64 (0.18)	6.59 (1.83)	0.27 (0.18)	172.62 (73.97)	3.41 (0.42)	55.16 (32.67)
	(5-10)	0.66 (0.2)	35.58 (14.12)	0 (0)	174.89 (41.81)	2.66 (0.24)	11.79 (4.86)

Table 15C. Water extractable soil nutrients (TDN, NO₃, NH₄) by site, treatment, depth, and date, reporting mean (standard error, n = 5). Bolding indicates a statistically significant difference between salt and control ($\alpha = 0.05$).

	Depth	Site 1		Site 3		Site 5	
		Control	Salt	Control	Salt	Control	Salt
TDN (mg/L)							
May 10th, 2018	(0-5)	1.89 (0.31)	1.6 (0.25)	1.11 (0.09)	1.49 (0.17)	0.47 (0.07)	0.97 (0.1)
	(5-10)	3 (1.17)	1.78 (0.19)	1.18 (0.1)	1.33 (0.09)	0.65 (0.17)	1.33 (0.21)
July 10th, 2018	(0-5)	0.99 (0.05)	1.08 (0.08)	1.04 (0.11)	1.55 (0.21)	1.23 (0.11)	1.18 (0.1)
	(5-10)	1.39 (0.15)	1.07 (0.13)	0.98 (0.08)	1.02 (0.13)	1.73 (0.11)	1.45 (0.1)
June 20th, 2019	(0-5)	2.74 (0.54)	2.38 (0.57)	2.76 (0.5)	2.14 (0.36)	0.99 (0.15)	1.98 (0.16)
	(5-10)	4.36 (0.68)	2.86 (1.08)	1.8 (0.24)	0.76 (0.23)	1.53 (0.15)	2.48 (0.54)
August 8th, 2020	(0-5)	2.06 (0.21)	1.6 (0.07)	1.49 (0.06)	1.17 (0.08)	1.98 (0.29)	1.14 (0.19)
	(5-10)	2.69 (0.21)	0.99 (0.12)	1.3 (0.07)	0.54 (0.07)	1.35 (0.05)	1.13 (0.17)
NO ₃ ⁺ (µg/gds)							
May 10th, 2018	(0-5)	2.4 (0.18)	1.63 (0.38)	0.99 (0.29)	0.29 (0.11)	0.51 (0.3)	0.5 (0.08)
	(5-10)	1.6 (0.17)	0.95 (0.15)	0.36 (0.08)	0.28 (0.08)	0.44 (0.05)	0.42 (0.07)
July 10th, 2018	(0-5)	0.69 (0.22)	0.23 (0.14)	0.35 (0.21)	0.34 (0.12)	0.98 (0.17)	1.05 (0.35)
	(5-10)	1.29 (0.33)	0.27 (0.03)	0.49 (0.1)	0.53 (0.07)	0.88 (0.23)	0.43 (0.06)
June 20th, 2019	(0-5)	1.53 (0.32)	1.12 (0.2)	0.32 (0.08)	1.52 (0.24)	0.3 (0.18)	1.57 (0.34)
	(5-10)	1.25 (0.21)	0.13 (0.05)	0.87 (0.28)	0.9 (0.13)	0.62 (0.21)	1.78 (0.33)
August 8th, 2020	(0-5)	4.79 (0.64)	4.32 (0.33)	3.48 (0.15)	20.3 (2.93)	3.73 (0.16)	7.66 (2.38)
	(5-10)	4.5 (0.38)	9.35 (2.13)	3.69 (0.29)	13.49 (3.96)	4.22 (0.11)	3.57 (0.22)
NH ₄ ⁺ (µg/gds)							
May 10th, 2018	(0-5)	2.28 (1.48)	0.27 (0.05)	1.35 (0.19)	0.83 (0.18)	0.53 (0.32)	0.61 (0.13)
	(5-10)	1.21 (0.29)	0.4 (0.07)	1.4 (0.12)	1.22 (0.16)	0.23 (0.07)	0.43 (0.03)
July 10th, 2018	(0-5)	0.14 (0.01)	0.1 (0)	0.48 (0.11)	0.36 (0.2)	0.16 (0.03)	0.24 (0.02)
	(5-10)	0.16 (0.02)	0.08 (0.01)	0.31 (0.03)	0.17 (0.03)	0.15 (0.02)	0.21 (0.02)
June 20th, 2019	(0-5)	0.17 (0.01)	0.4 (0.17)	0.26 (0.08)	0.46 (0.12)	0.09 (0.02)	1.33 (0.39)
	(5-10)	0.15 (0.01)	0.28 (0.04)	0.4 (0.05)	0.31 (0.07)	0.09 (0.03)	0.36 (0.03)
August 8th, 2020	(0-5)	0.4 (0.19)	1.16 (0.43)	0.65 (0.39)	3.55 (2.3)	0.25 (0.1)	1.65 (0.49)
	(5-10)	0 (0)	0.44 (0.12)	0.62 (0.29)	1.2 (0.63)	0 (0)	0.04 (0.04)

Table 15D. Water extractable soil PO₄ by site, treatment, depth, and date, reporting mean (standard error, n = 5). Bolding indicates a statistically significant difference between salt and control ($\alpha = 0.05$).

	Depth	Site 1		Site 3		Site 5	
		Control	Salt	Control	Salt	Control	Salt
PO ₄ ³⁻ (µg/gds)							
May 10th, 2018	(0-5)	0.19 (0.04)	0.16 (0.02)	0.11 (0.02)	0.17 (0.01)	0.12 (0.04)	0.16 (0.04)
	(5-10)	0.27 (0.13)	0.17 (0.07)	0.04 (0.01)	0.08 (0.01)	0.03 (0.01)	0.08 (0.01)
July 10th, 2018	(0-5)	0.23 (0.04)	0.13 (0.01)	0.08 (0.01)	0.11 (0.02)	0.08 (0.01)	0.09 (0.01)
	(5-10)	0.13 (0.01)	0.07 (0.01)	0.1 (0.02)	0.09 (0.01)	0.06 (0.01)	0.05 (0)
June 20th, 2019	(0-5)	6.78 (1.08)	10.88 (4.08)	6.5 (1.12)	7.38 (1.8)	2.06 (0.89)	20.82 (7.45)
	(5-10)	2.33 (0.99)	3.51 (1.97)	1.36 (0.85)	b.d.	b.d.	b.d.
August 8th, 2020	(0-5)	0.27 (0.02)	0.38 (0.06)	0.24 (0.02)	0.22 (0.06)	0.14 (0.05)	0.12 (0.08)
	(5-10)	0.17 (0.01)	0.11 (0.04)	0.21 (0.06)	b.d.	b.d.	0.1 (0.04)

Table 15E. Soil properties (pH, soil moisture, bulk density) by site, treatment, depth, and date, reporting mean (standard error, n = 5). Bolding indicates a statistically significant difference between salt and control ($\alpha = 0.05$).

	Depth	Site 1		Site 3		Site 5	
		Control	Salt	Control	Salt	Control	Salt
pH							
May 10th, 2018	(0-5)	6.06 (0.05)	5.66 (0.19)	4.66 (0.07)	4.78 (0.04)	6.24 (0.09)	6.62 (0.04)
	(5-10)	6.36 (0.05)	5.82 (0.24)	4.98 (0.04)	4.88 (0.09)	6.66 (0.02)	6.6 (0.05)
July 10th, 2018	(0-5)	5.68 (0.09)	5.08 (0.12)	4.7 (0.1)	4.84 (0.07)	6.3 (0.03)	6.32 (0.02)
	(5-10)	5.92 (0.05)	5.28 (0.09)	5.2 (0.1)	5.06 (0.07)	6.36 (0.04)	6.48 (0.06)
June 20th, 2019	(0-5)	4.88 (0.11)	4.25 (0.07)	4 (0.14)	3.94 (0.08)	5.51 (0.12)	5.49 (0.01)
	(5-10)	5.25 (0.04)	4.39 (0.07)	4.58 (0.04)	4.2 (0.07)	5.9 (0.05)	5.5 (0.04)
August 8th, 2020	(0-5)	4.67 (0.08)	4.48 (0.06)	3.62 (0.07)	3.6 (0.05)	5.16 (0.05)	5.33 (0.07)
	(5-10)	4.9 (0.04)	4.4 (0.07)	3.82 (0.05)	3.62 (0.04)	5.41 (0.05)	5.51 (0.1)
Soil moisture (%)							
May 10th, 2018	(0-5)	26.82 (0.39)	25.16 (1.29)	32.26 (0.98)	33.02 (0.59)	36.78 (2.16)	32 (2.11)
	(5-10)	24.8 (0.49)	22.69 (0.45)	30.14 (0.62)	30.56 (0.39)	28.55 (0.48)	25.63 (1.18)
July 10th, 2018	(0-5)	13.1 (0.56)	18.55 (1.21)	31.01 (1.06)	30.76 (0.53)	32.73 (0.81)	38.93 (2.76)
	(5-10)	12.28 (0.69)	14.42 (0.92)	27.75 (0.86)	27.45 (0.29)	27.59 (0.51)	28.63 (1.27)
June 20th, 2019	(0-5)	20.97 (0.69)	24.76 (0.56)	26.4 (1.69)	30.17 (0.35)	22.62 (1.51)	37.83 (1.89)
	(5-10)	20.38 (0.47)	21.04 (0.51)	25.62 (0.49)	26.21 (0.1)	20.58 (1.08)	24.2 (1.28)
August 8th, 2020	(0-5)	29.8 (0.81)	29.56 (0.67)	32.99 (0.65)	34.64 (0.69)	34.62 (2.46)	39.73 (2.01)
	(5-10)	24 (0.55)	27.38 (1.49)	29.15 (0.35)	30.8 (0.44)	28.97 (0.56)	28.48 (2.61)
Bulk Density (g/cm ³)							
May 10th, 2018	(0-5)	1.36 (0.05)	1.21 (0.05)	1.41 (0.03)	1.3 (0.04)	1.31 (0.05)	1.56 (0.1)
	(5-10)	1.55 (0.04)	1.46 (0.04)	1.49 (0.02)	1.48 (0.02)	1.54 (0.01)	1.6 (0.03)
July 10th, 2018	(0-5)	1.08 (0.03)	1.02 (0.05)	1.38 (0.02)	1.45 (0.04)	1.23 (0.03)	1.31 (0.03)
	(5-10)	1.38 (0.03)	1.36 (0.02)	1.47 (0.03)	1.53 (0.04)	1.52 (0.02)	1.48 (0.05)
June 20th, 2019	(0-5)	1.27 (0.06)	1.15 (0.03)	1.14 (0.07)	1.27 (0.04)	0.95 (0.05)	0.98 (0.09)
	(5-10)	1.42 (0.06)	1.45 (0.07)	1.49 (0.03)	1.45 (0.02)	1.3 (0.06)	1.49 (0.07)
August 8th, 2020	(0-5)	1.48 (0.03)	1.49 (0.03)	1.43 (0.02)	1.42 (0.02)	1.5 (0.06)	1.42 (0.08)
	(5-10)	1.55 (0.02)	1.44 (0.05)	1.5 (0.02)	1.45 (0.03)	1.52 (0.01)	1.53 (0.08)

Table 15F. Vegetation measurements by site, treatment, depth, and date, reporting mean (standard error, n = 5). Bolding indicates a statistically significant difference between salt and control ($\alpha = 0.05$).

	Depth	Site 1		Site 3		Site 5	
		Control	Salt	Control	Salt	Control	Salt
Roots (g)							
May 10 th , 2018	(0-5)	0.97 (0.63)	0.45 (0.21)	0.52 (0.15)	0.33 (0.11)	0.51 (0.07)	0.39 (0.09)
	(5-10)	0.05 (0.02)	1.35 (0.75)	0.37 (0.26)	0.49 (0.33)	0.49 (0.32)	0.14 (0.11)
July 10 th , 2018	(0-5)	0.43 (0.08)	0.38 (0.03)	0.81 (0.15)	0.87 (0.18)	0.53 (0.14)	1.13 (0.17)
	(5-10)	0.22 (0.1)	0.28 (0.03)	1.18 (0.47)	0.86 (0.41)	0.05 (0.02)	0.8 (0.47)
June 20 th , 2019	(0-5)	0.5 (0.21)	0.54 (0.19)	0.73 (0.34)	1.24 (0.29)	0.49 (0.07)	1.34 (0.55)
	(5-10)	0.39 (0.14)	0.36 (0.07)	1.92 (1.51)	0.58 (0.22)	0.31 (0.08)	0.39 (0.26)
August 8 th , 2020	(0-5)	0.18 (0.04)	0.31 (0.1)	0.91 (0.18)	0.72 (0.13)	0.6 (0.1)	1.24 (0.75)
	(5-10)	1.08 (0.83)	0.79 (0.31)	0.79 (0.33)	0.26 (0.15)	0.04 (0.02)	0.24 (0.08)
Tree diameter (percent growth)							
November 2015 - January, 2021		23.6 (4.3) n=23	21.3 (4.3) n = 12	20.5 (3.2) n = 11	16.9 (1.6) n = 27	54.7 (6.0) n = 15	47.3 (4.7) n = 12

**Table 15G. Substrate induced respiration (SIR) by site, treatment, depth, and date, reporting mean (standard error, n = 5).
 Bolding indicates a statistically significant difference between salt and control ($\alpha = 0.05$).**

	Depth	Site 1		Site 3		Site 5	
		Control	Salt	Control	Salt	Control	Salt
SIR (ugC-CO2/hr/goC)							
May 10th, 2018	(0-5)	46.87 (2.47)	49.33 (5.83)	36.34 (6.22)	30.82 (1.82)	105.5 (11.98)	56.7 (9.97)
	(5-10)	40.09 (2.88)	42.8 (2.95)	15.17 (2.34)	18.04 (1.66)	37.7 (5.88)	37.54 (5.58)
July 10th, 2018	(0-5)	4.22 (0.11)	3.72 (0.31)	2.85 (0.13)	2.51 (0.6)	4.5 (0.3)	3.97 (0.15)
	(5-10)	3.59 (0.09)	2.87 (0.14)	1.96 (0.11)	1.5 (0.08)	7.71 (4.97)	2.31 (0.31)
June 20th, 2019	(0-5)	57.01 (3.54)	65.56 (4.48)	59.47 (3.24)	42.45 (8.29)	69.67 (3.92)	NA (4.29)
	(5-10)	40.58 (2.47)	45.04 (5.69)	27.49 (1)	NA (5.45)	36.74 (3.57)	30.8 (3.19)
August 8th, 2020	(0-5)	29.65 (1.99)	16.71 (1.09)	21.54 (0.61)	16.94 (2.54)	25.41 (1.83)	14.69 (2.42)
	(5-10)	20.71 (1.39)	13.64 (0.62)	12.26 (1.94)	6.74 (1.06)	14.87 (1.01)	13.86 (1.04)
SIR (ugC-CO2/hr/gds)							
May 10th, 2018	(0-5)	3.87 (0.27)	4 (0.38)	3.86 (0.7)	3.25 (0.24)	9.8 (1.61)	3.93 (0.71)
	(5-10)	2.85 (0.22)	3.1 (0.13)	1.35 (0.19)	1.64 (0.17)	2.58 (0.37)	1.93 (0.28)
July 10th, 2018	(0-5)	0.41 (0.02)	0.45 (0.08)	0.41 (0.03)	0.37 (0.1)	0.65 (0.06)	0.7 (0.11)
	(5-10)	0.29 (0.01)	0.24 (0.02)	0.23 (0.02)	0.17 (0.01)	0.84 (0.56)	0.22 (0.03)
June 20th, 2019	(0-5)	4.4 (0.19)	6.11 (0.6)	6.75 (0.44)	4.09 (0.69)	6.51 (0.59)	NA (1.38)
	(5-10)	2.96 (0.16)	3.32 (0.37)	2.41 (0.11)	NA (0.42)	2.6 (0.26)	1.98 (0.34)
August 8th, 2020	(0-5)	3.54 (0.32)	1.91 (0.16)	3.57 (0.12)	3.11 (0.53)	3.4 (0.2)	2.39 (0.59)
	(5-10)	1.76 (0.12)	1.27 (0.09)	1.56 (0.2)	0.96 (0.14)	1.61 (0.09)	1.2 (0.18)

**Table 15H. Soil carbon mineralization rates by site, treatment, depth, and date, reporting mean (standard error, n = 5).
 Bolding indicates a statistically significant difference between salt and control ($\alpha = 0.05$).**

	Depth	Site 1		Site 3		Site 5	
		Control	Salt	Control	Salt	Control	Salt
C mineralization (ugC-CO2/hr/goC)							
May 10th, 2018	(0-5) (5-10)						
July 10th, 2018	(0-5) (5-10)	6.73 (0.37) 4.64 (0.22)	8.79 (0.21) 5.4 (0.5)	9.25 (0.43) 7.4 (0.49)	7.81 (0.94) 4.03 (0.27)	12.82 (1.18) 8.34 (0.58)	14 (0.67) 11.17 (0.82)
June 20th, 2019	(0-5) (5-10)	3.6 (0.27) 2.35 (0.07)	4.25 (0.44) 4.65 (0.4)	4.41 (0.91) 3.22 (0.75)	4.07 (0.67) 1.5 (0.33)	3.74 (0.43) 2.86 (0.48)	5.11 (0.29) 3.17 (0.15)
August 8th, 2020	(0-5) (5-10)	6.9 (0.72) 3.83 (0.4)	4.49 (0.51) 3.79 (0.4)	6.09 (0.32) 3.86 (1.12)	4.24 (0.38) 2.22 (0.38)	5.34 (0.43) 2.95 (0.41)	3.37 (0.48) 3.09 (0.43)
C mineralization (ugC-CO2/hr/gds)							
May 10th, 2018	(0-5) (5-10)						
July 10th, 2018	(0-5) (5-10)	0.56 (0.03) 0.32 (0.02)	0.85 (0.08) 0.38 (0.02)	0.91 (0.08) 0.63 (0.04)	0.79 (0.12) 0.34 (0.02)	1.26 (0.16) 0.64 (0.06)	1.46 (0.16) 0.76 (0.08)
June 20th, 2019	(0-5) (5-10)	0.28 (0.01) 0.17 (0.01)	0.39 (0.04) 0.35 (0.05)	0.51 (0.12) 0.28 (0.07)	0.39 (0.04) 0.14 (0.03)	0.35 (0.04) 0.2 (0.04)	0.49 (0.15) 0.2 (0.02)
August 8th, 2020	(0-5) (5-10)	0.82 (0.1) 0.32 (0.03)	0.51 (0.05) 0.35 (0.03)	1.03 (0.07) 0.49 (0.13)	0.78 (0.09) 0.32 (0.05)	0.71 (0.03) 0.33 (0.05)	0.54 (0.12) 0.27 (0.06)

Table 15I. Water extractable DOC and soil organic content (by loss in ignition) by site, treatment, depth, and date, reporting mean (standard error, n = 5). Bolding indicates a statistically significant difference between salt and control ($\alpha = 0.05$).

	Depth	Site 1		Site 3		Site 5	
		Control	Salt	Control	Salt	Control	Salt
DOC (mg/L)							
May 10th, 2018	(0-5)	19.81 (1.82)	26.21 (3.41)	29.81 (7.89)	25.67 (2.37)	8.79 (1.12)	14.09 (1.23)
	(5-10)	34.03 (8.71)	33.06 (8.55)	18.63 (1.1)	21.95 (1.91)	10.71 (2.29)	19.37 (2.96)
July 10th, 2018	(0-5)	16.67 (0.78)	22.99 (1.88)	19.39 (1.34)	27.11 (2.62)	19.59 (1.61)	17.22 (1.48)
	(5-10)	19.76 (2.04)	19.47 (2.03)	15.9 (1.12)	18.41 (1.54)	24.95 (0.88)	22.41 (1.19)
June 20th, 2019	(0-5)	19.45 (1.54)	20.31 (2.56)	24.49 (2.3)	19.45 (1.3)	13.04 (0.99)	15.36 (0.52)
	(5-10)	23.82 (1.6)	21.49 (4.45)	18.25 (1.49)	11.6 (1.56)	15.34 (0.79)	18.13 (2)
August 8th, 2020	(0-5)	28.24 (2.75)	24.18 (1.12)	28.43 (2.53)	17.46 (2.65)	28.83 (3.81)	13.8 (2)
	(5-10)	36.81 (2.3)	15.32 (1.88)	25.06 (1.68)	7.76 (0.73)	20.04 (0.61)	17.31 (2.02)
Organic matter (% LOI)							
May 10th, 2018	(0-5)	8.24 (0.26)	8.21 (0.34)	10.41 (0.47)	10.49 (0.21)	9.09 (0.45)	6.93 (0.3)
	(5-10)	7.12 (0.26)	7.32 (0.39)	8.94 (0.13)	9.04 (0.19)	6.89 (0.11)	5.23 (0.42)
July 10th, 2018	(0-5)	8.32 (0.25)	9.61 (0.72)	9.81 (0.42)	10 (0.3)	9.72 (0.44)	10.39 (0.95)
	(5-10)	6.99 (0.07)	7.14 (0.29)	8.55 (0.3)	8.46 (0.08)	7.63 (0.23)	6.83 (0.59)
June 20th, 2019	(0-5)	8.07 (0.16)	9.26 (0.32)	11.37 (0.52)	11.12 (0.38)	9.28 (0.41)	13.04 (1.54)
	(5-10)	7.06 (0.21)	6.91 (0.13)	8.74 (0.13)	9 (0.3)	7.09 (0.17)	6.27 (0.48)
August 8th, 2020	(0-5)	8.31 (0.17)	7.99 (0.19)	11.1 (0.25)	11.9 (0.41)	8.77 (0.31)	9.4 (0.83)
	(5-10)	6.46 (0.11)	6.75 (0.27)	9.15 (0.22)	9.96 (0.22)	7.81 (0.59)	6.01 (0.52)

Table 15J. Water extractable soil phenolic content (total and per gram DOC) by site, treatment, depth, and date, reporting mean (standard error, n = 5). Bolding indicates a statistically significant difference between salt and control ($\alpha = 0.05$).

	Depth	Site 1		Site 3		Site 5	
		Control	Salt	Control	Salt	Control	Salt
Phenolics (mg/L)							
May 10th, 2018	(0-5)	7.68 (0.51)	6.34 (0.56)	5.2 (0.62)	6.17 (0.59)	3.1 (0.46)	4.27 (0.7)
	(5-10)	6.25 (0.85)	6.85 (0.48)	4.19 (0.37)	4.57 (0.48)	4.1 (0.78)	5.77 (0.8)
July 10th, 2018	(0-5)	2.96 (0.13)	4.16 (0.39)	3.78 (0.35)	4.54 (0.38)	3.35 (0.14)	3.74 (0.24)
	(5-10)	3.45 (0.34)	3.59 (0.32)	3.17 (0.3)	2.96 (0.26)	3.77 (0.27)	4.98 (0.41)
June 20th, 2019	(0-5)	3.44 (0.3)	3.16 (0.4)	3.54 (0.22)	2.53 (0.14)	1.65 (0.13)	1.98 (0.08)
	(5-10)	3.75 (0.24)	3.16 (0.67)	2.43 (0.14)	1.48 (0.2)	1.89 (0.14)	2.52 (0.39)
August 8th, 2020	(0-5)	4.29 (0.41)	3.67 (0.17)	3.45 (0.32)	1.85 (0.32)	4.47 (0.68)	1.98 (0.32)
	(5-10)	5.47 (0.36)	2.2 (0.42)	3.15 (0.49)	0.59 (0.09)	3.03 (0.1)	2.87 (0.38)
Phenolics (mg/ mg DOC)							
May 10th, 2018	(0-5)	0.39 (0.02)	0.25 (0.02)	0.22 (0.04)	0.24 (0.01)	0.35 (0.02)	0.3 (0.04)
	(5-10)	0.25 (0.07)	0.24 (0.03)	0.22 (0.01)	0.21 (0.01)	0.39 (0.01)	0.3 (0.02)
July 10th, 2018	(0-5)	0.18 (0)	0.18 (0)	0.2 (0.03)	0.17 (0)	0.18 (0.02)	0.22 (0.01)
	(5-10)	0.17 (0)	0.19 (0.01)	0.21 (0.03)	0.16 (0)	0.15 (0.01)	0.22 (0.01)
June 20th, 2019	(0-5)	0.18 (0)	0.16 (0)	0.15 (0.01)	0.13 (0)	0.13 (0)	0.13 (0.01)
	(5-10)	0.16 (0)	0.15 (0)	0.13 (0)	0.13 (0)	0.12 (0.01)	0.14 (0.01)
August 8th, 2020	(0-5)	0.15 (0)	0.15 (0)	0.12 (0)	0.1 (0.01)	0.15 (0.01)	0.14 (0.01)
	(5-10)	0.15 (0.01)	0.14 (0.01)	0.12 (0.01)	0.08 (0.01)	0.15 (0.01)	0.16 (0.01)

Appendix D – Supplementary materials for chapter 5

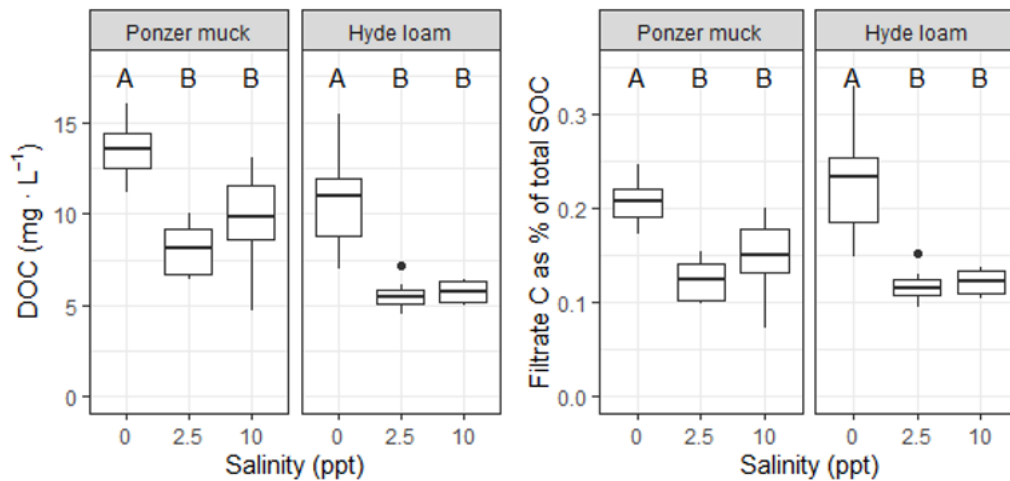


Figure 36: Treatment effect on DOC in the initial filtrate (left) and as an approximate percent of the total SOC pool (right). Letters indicate significant difference (Tukey's HSD, $p < 0.05$). Salinity treatments remove significantly less organic carbon from the soil than control, however the removal efficiency is sufficiently small enough that the effect on the total carbon stock remaining is negligible.

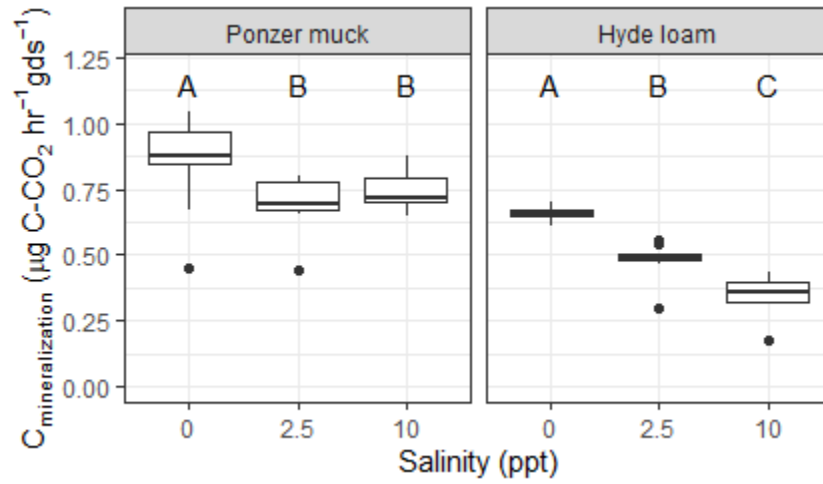


Figure 37: Initial C mineralization rate from the soil incubation assays on a per gram dry soil basis (first three days). Letters indicate significant difference between treatment (Tukey's HSD test, $P < 0.05$).

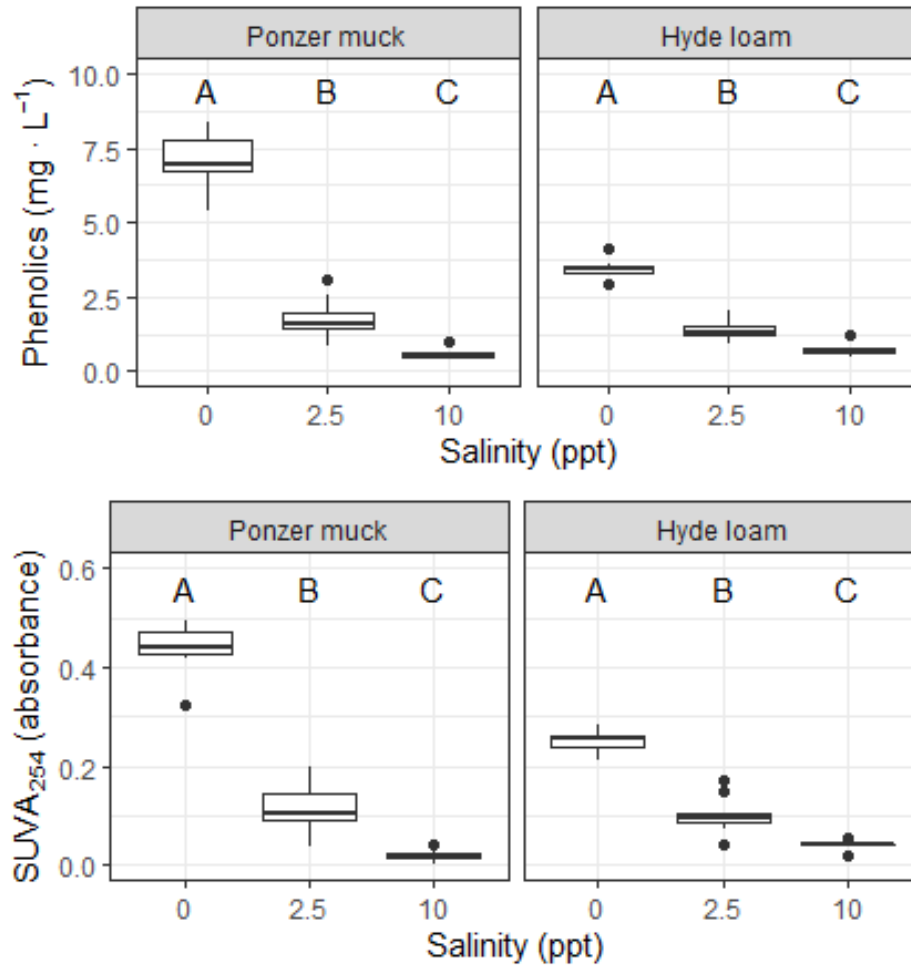


Figure 38: Phenolic concentration (above) and UV absorbance at 254 nanometers (below) of the final soil extract. Reduction of these compounds is highly correlated with the reduction in overall DOC solubility caused by the salinity treatments.

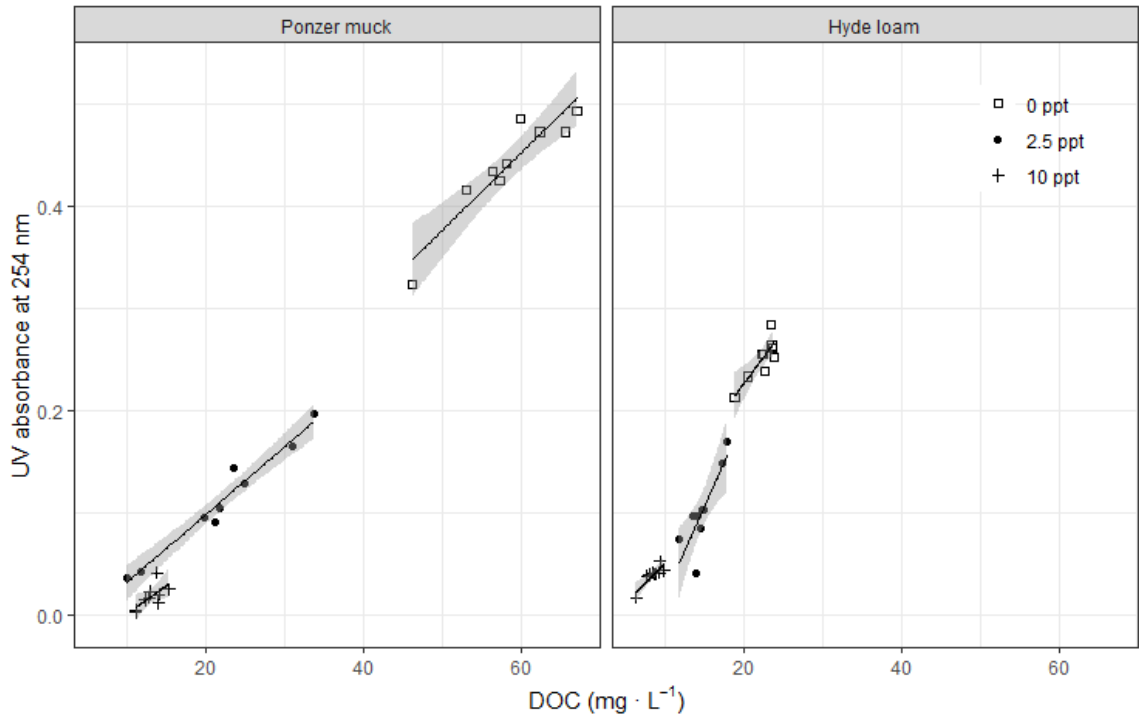


Figure 39: Effect of salinity on DOC and SUVA₂₅₄ in relation to one another. The overall relationship between DOC and SUVA₂₅₄ is linear and tightly correlated, but within treatment groups it is evident that there is a reduction in the strength of the relationship at higher salinity levels (blue) as indicated by a flattening of the slope. The 10 ppt salinity treatment yields the largest suppression of DOC solubility and reduces even further the solubility of aromatic compounds.

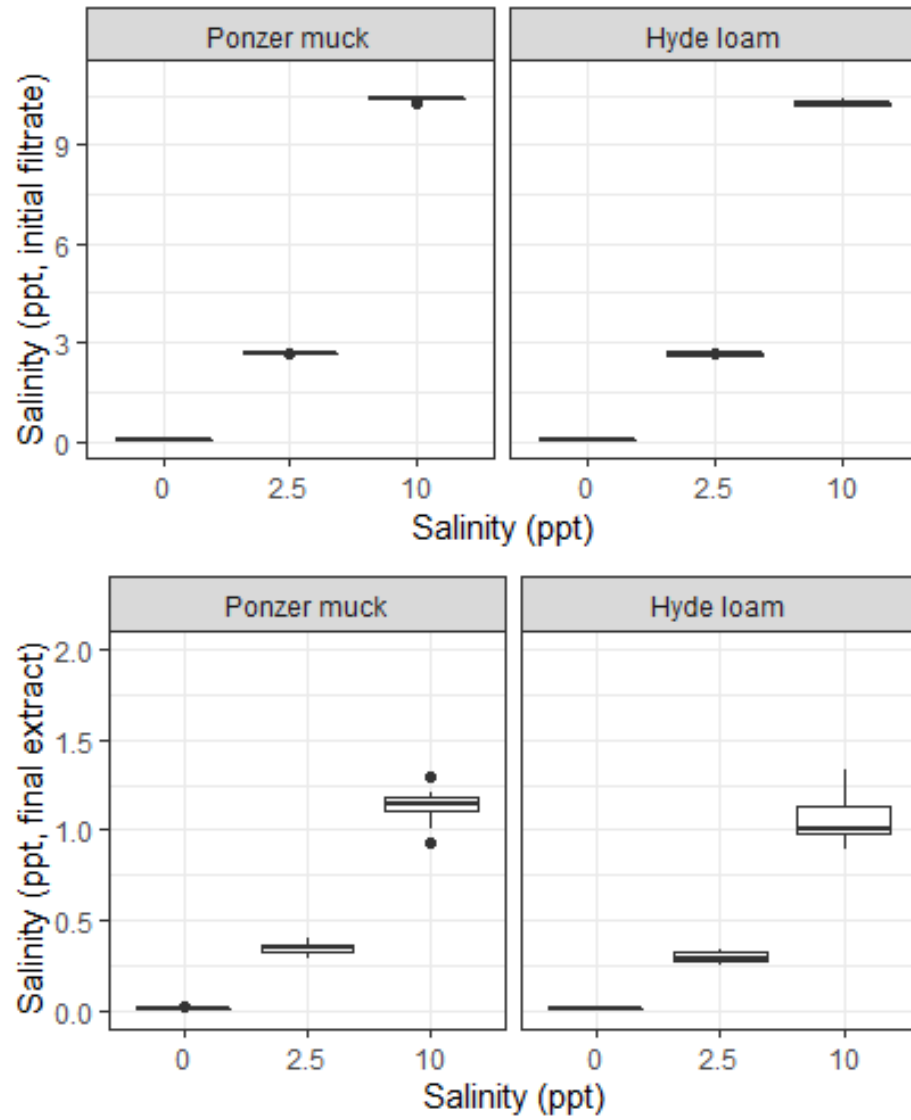


Figure 40: Effective salinity in the initial filtrate (top) and final extract (bottom).

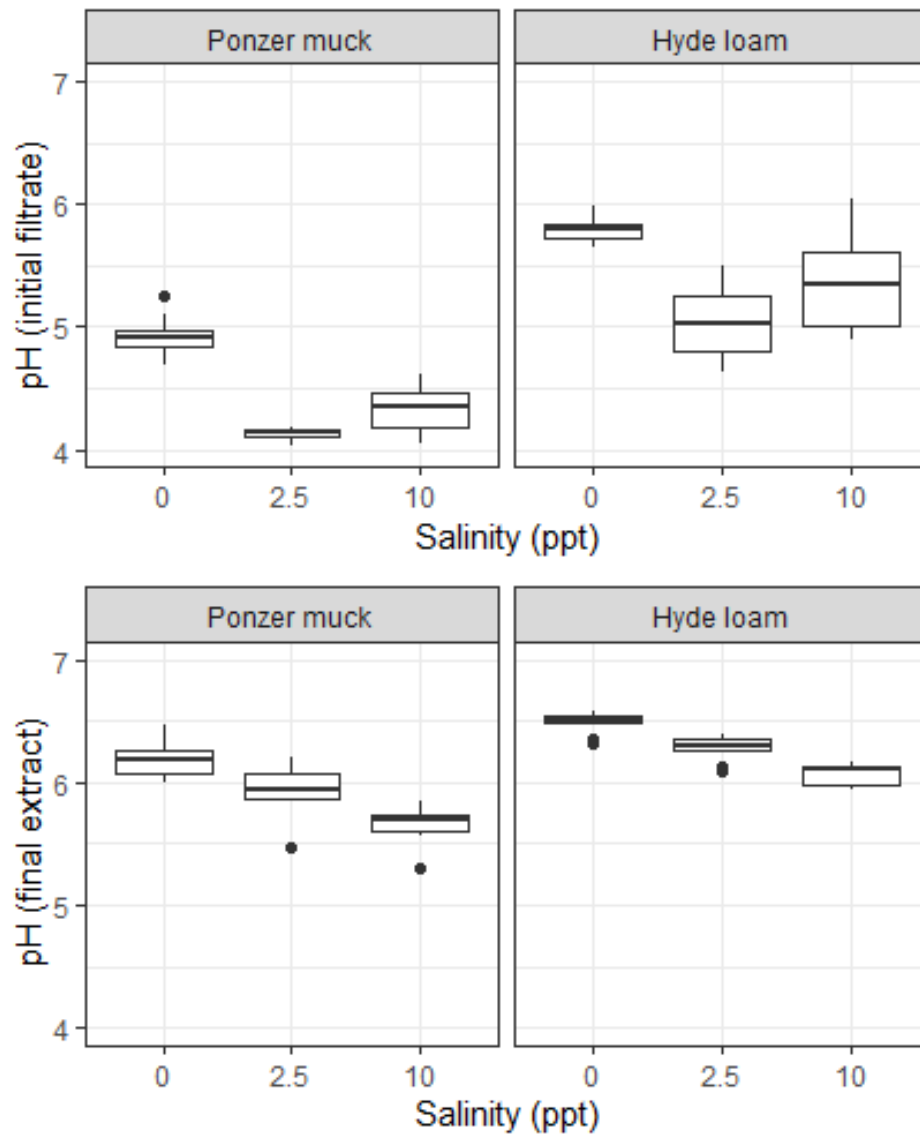


Figure 41: Effective pH by salinity treatment in the initial filtrate (top) and final extract (bottom).

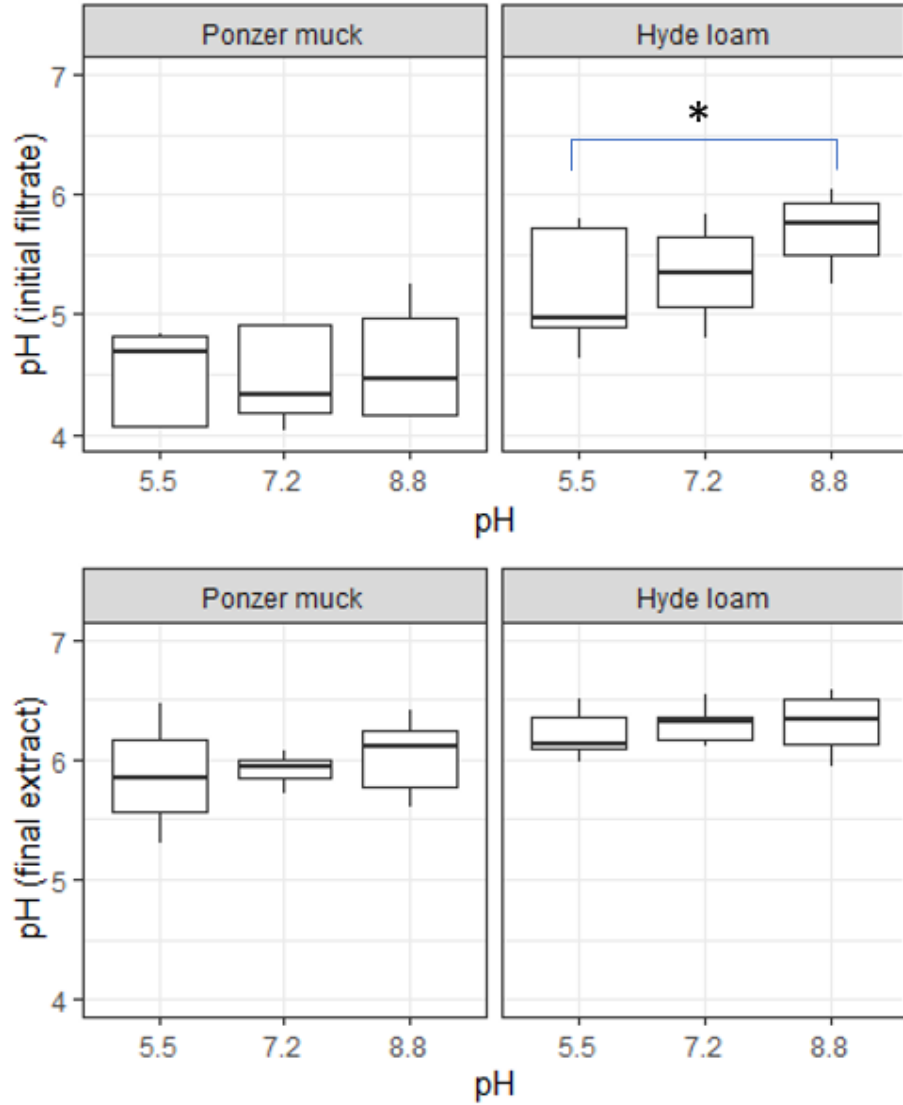


Figure 42: Effective pH by pH treatment of initial filtrate (top) and final extract (bottom).

Table 16: ANOVA results for all response variables.

Response	Data		Df	Sum sq	Mean sq	F Value	Pr (>F)		
Salinity (filtrate)	Ponzer Muck	Treatment	2	522.6	261.3	313923	< 0.0001 ***		
		Residuals	24	0.0	0.0				
	Hyde loam	Treatment	2	510.0	255	91679	< 0.0001 ***		
		Residuals	24	0.1	0				
	All Sites	Treatment	2	1032.6	516.3	285728.71	< 0.0001 ***		
		Site	1	0.0	0.0			21.55	< 0.0001 ***
		Treatment*Site	2	0.0	0.0			10.78	< 0.0001 ***
		Residuals	48	0.1	0.0				
	Salinity (extract)	Ponzer Muck	Treatment	2	5.937	2.9687	717.4	< 0.0001 ***	
			Residuals	24	0.099	0.0041			
Hyde loam		Treatment	2	5.381	2.6903	368.9	< 0.0001 ***		
		Residuals	24	0.175	0.0073				
All Sites		Treatment	2	11.309	5.654	989.277	< 0.0001 ***		
		Site	1	0.018	0.018			3.175	0.0811
		Treatment*Site	2	0.009	0.005			0.794	0.4578
		Residuals	48	0.274	0.006				
pH (filtrate)		Ponzer Muck	Treatment	2	3.723	1.8614	62.65	< 0.0001 ***	
			Residuals	24	0.713	0.0297			
	Hyde loam	Treatment	2	2.757	1.3783	16.29	< 0.0001 ***		
		Residuals	24	2.031	0.0846				
	All Sites	Treatment	2	6.372	3.186	55.723	< 0.0001 ***		
		Site	1	12.809	12.809			224.031	< 0.0001 ***
		Treatment*Site	2	0.107	0.054			0.939	0.398
		Residuals	48	2.744	0.057				
	pH (extract)	Ponzer Muck	Treatment	2	1.4282	0.7141	22.91	< 0.0001 ***	
			Residuals	24	0.7481	0.0312			
Hyde loam		Treatment	2	0.7813	0.3906	46.89	< 0.0001 ***		
		Residuals	24	0.1999	0.0083				
All Sites		Treatment	2	2.1609	1.0805	54.707	< 0.0001 ***		
		Site	1	1.6120	1.6120			81.621	< 0.0001 ***
		Treatment*Site	2	0.0458	0.0243			1.229	0.302
		Residuals	48	0.9480	0.0197				
C _{min} (3-day)		Ponzer Muck	Treatment	2	9.39	4.693	3.414	0.0496*	
			Residuals	24	32.99	1.375			
	Hyde loam	Treatment	2	66.34	33.17	54.26	< 0.0001 ***		
		Residuals	24	14.67	0.61				
	All Sites	Treatment	2	56.62	28.308	28.508	< 0.0001 ***		
		Site	1	6.85	6.848			6.896	0.0116 *
		Treatment*Site	2	19.11	9.554			9.681	0.000307 ***
		Residuals	48	47.66	0.993				

Table 16 continued

Response	Data		Df	Sum sq	Mean sq	F Value	Pr (>F)		
C _{min.} (21 day)	Ponzer Muck	Treatment	2	1465488	732744	22.74	< 0.0001 ***		
		Residuals	24	773441	32227				
	Hyde loam	Treatment	2	2090399	1045200	250.4	< 0.0001 ***		
		Residuals	24	100193	4175				
	All Sites	Treatment	2	3474389	1737195	95.447	< 0.0001 ***		
		Site	1	2546188	2546188			139.895	< 0.0001 ***
		Treatment*Site	2	81498	40749			2.239	0.118
		Residuals	48	873634	18201				
	DOC (final extract)	Ponzer Muck	Treatment	2	10458	5229	150.1	< 0.0001 ***	
			Residuals	24	836	35			
Hyde loam		Treatment	2	866.1	433.1	176.5	< 0.0001 ***		
		Residuals	24	58.9	2.5				
All Sites		Treatment	2	8553	4276	229.39	< 0.0001 ***		
		Site	1	3436	3436			184.32	< 0.0001 ***
		Treatment*Site	2	2771	1386			74.33	< 0.0001 ***
		Residuals	48	895	19				
Phenolics (per DOC)		Ponzer Muck	Treatment	2	0.0288	0.0144	164	< 0.0001 ***	
			Residuals	24	0.00210	0.00009			
	Hyde loam	Treatment	2	0.0283	0.0142	46.87	< 0.0001 ***		
		Residuals	24	0.00725	0.00030				
	All Sites	Treatment	2	0.05578	0.027888	143.084	< 0.0001 ***		
		Site	1	0.01087	0.010872			55.779	< 0.0001 ***
		Treatment*Site	2	0.00130	0.000651			3.341	0.0438*
		Residuals	48	0.00936	0.000195				
	SUVA ₂₅₄ (per DOC)	Ponzer Muck	Treatment	2	1.7040	0.852	171.1	< 0.0001 ***	
			Residuals	24	0.1195	0.005			
Hyde loam		Treatment	2	2.0344	1.017	72.83	< 0.0001 ***		
		Residuals	24	0.3352	0.014				
All Sites		Treatment	2	3.661	1.8307	193.239	< 0.0001 ***		
		Site	1	1.199	1.1991			126.567	< 0.0001 ***
		Treatment*Site	2	0.077	0.0384			4.055	0.0236*
		Residuals	48	0.455	0.0094				
Soil organic matter		Ponzer Muck	Treatment	2	8.204	4.102	69.39	< 0.0001 ***	
			Residuals	24	1.419	0.059			
	Hyde loam	Treatment	2	7.081	3.541	110.4	< 0.0001 ***		
		Residuals	24	0.770	0.032				
	All Sites	Treatment	2	15.26	7.63	167.324	< 0.0001 ***		
		Site	1	120.99	120.99			2653.490	< 0.0001 ***
		Treatment*Site	2	0.03	0.01			0.289	0.751
		Residuals	48	2.19	0.05				

Table 16 Continued

Response	Data		Df	Sum sq	Mean sq	F Value	Pr (>F)	
C _{min.} (per gram dry soil)	Ponzer	Treatment	2	0.1179	0.05897	3.42	0.0493*	
		Muck	Residuals	24	0.4138			0.01724
	Hyde loam	Treatment	2	0.4355	0.21773	54.24	< 0.0001 ***	
		Residuals	24	0.0963	0.00401			
	All Sites	Treatment	2	0.4471	0.2235	21.033	< 0.0001 ***	
		Site	1	0.9766	0.9766	91.892	< 0.0001 ***	
		Treatment*Site	2	0.1063	0.0532	5.003	0.0106	
		Residuals	48	0.5101	0.0106			
	Phenolics (mg L ⁻¹)	Ponzer	Treatment	2	224.77	112.39	228.3	< 0.0001 ***
			Muck	Residuals	24	11.82		
Hyde loam		Treatment	2	37.47	18.733	198.7	< 0.0001 ***	
		Residuals	24	2.26	0.094			
All Sites		Treatment	2	222.59	111.29	379.43	< 0.0001 ***	
		Site	1	23.55	23.55	80.29	< 0.0001 ***	
		Treatment*Site	2	39.66	19.83	67.60	< 0.0001 ***	
		Residuals	48	14.08	0.29			
SUVA ₂₅₄ (abs.)		Ponzer	Treatment	2	0.8848	0.4424	235.6	< 0.0001 ***
			Muck	Residuals	24	0.0451		
	Hyde loam	Treatment	2	0.21213	0.10606	161.3	< 0.0001 ***	
		Residuals	24	0.01578	0.00066			
	All Sites	Treatment	2	0.9803	0.4901	386.68	< 0.0001 ***	
		Site	1	0.0473	0.0473	37.31	< 0.0001 ***	
		Treatment*Site	2	0.1166	0.0583	46.01	< 0.0001 ***	
		Residuals	48	0.0608	0.0013			

Significance codes: 0 < *** < 0.001 < 0.01 < * < 0.05 < . < 0.1

References

- Adam E, Mutanga O, Rugege D. 2010. Multispectral and hyperspectral remote sensing for identification and mapping of wetland vegetation: A review. *Wetlands Ecology and Management* 18: 281–296.
- Adams F, Thomas GW, Hargrove WL. 1984. The chemistry of soil acidity In: *Soil Acidity and Liming*. American Society of Agronomy, Crop Science Society of America, Soil Science Society of America, .
- Antonellini M, Mollema P, Giambastiani B, *et al.* 2008. Salt water intrusion in the coastal aquifer of the southern Po Plain, Italy. *Hydrogeology journal* 16: 1541.
- APHA. 1998. *Standard Methods for the Examination of Water and Wastewater*. Washington, DC: American Public Health Association Water Environment Federation.
- Ardón M, Helton AM, Bernhardt ES. 2016. Drought and saltwater incursion synergistically reduce dissolved organic carbon export from coastal freshwater wetlands. *Biogeochemistry* 127: 411–426.
- Ardón M, Helton AM, Bernhardt ES. 2018. Salinity effects on greenhouse gas emissions from wetland soils are contingent upon hydrologic setting: a microcosm experiment. *Biogeochemistry* 140: 217–232.
- Ardón M., Montanari S, Morse J, Doyle M, Bernhardt ES. 2010. Phosphorus export from a restored wetland ecosystem in response to natural and experimental hydrologic fluctuations. *Journal of geophysical research* 115: 341.
- Ardón M, Morse JL, Colman BP, Bernhardt ES. 2013. Drought-induced saltwater incursion leads to increased wetland nitrogen export. *Global change biology* 19: 2976–2985.
- Ardón Marcelo, Morse JL, Doyle MW, Bernhardt ES. 2010. The water quality consequences of restoring wetland hydrology to a large agricultural watershed in the southeastern coastal plain. *Ecosystems* 13: 1060–1078.
- Asner GP. 1998. Biophysical and biochemical sources of variability in canopy reflectance. *Remote Sensing of the Environment* 64: 234–253.
- Bache BW. 2008. Base Saturation In: Chesworth W, ed. *Encyclopedia of Soil Science*. Dordrecht: Springer Netherlands, 52–54.
- Berdugo M, Delgado-Baquerizo M, Soliveres S, *et al.* 2020. Global ecosystem thresholds driven by aridity. *Science* 367: 787–790.

- Bhattachan A, Emanuel RE, Ardón M, *et al.* 2018. Evaluating the effects of land-use change and future climate change on vulnerability of coastal landscapes to saltwater intrusion. *Elem Sci Anth* 6.
- Bivand R, Keitt T, Rowlingson B, Pebesma E. 2016. *rgdal: Bindings for the geospatial data abstraction library*.
- Blankespoor B, Dasgupta S, Laplante B. 2014. Sea-Level Rise and Coastal Wetlands. *Ambio* 43: 996–1005.
- Bojanowski M, Edwards R. 2016. *alluvial: R package for creating alluvial diagrams*.
- Borchert SM, Osland MJ, Enwright NM, Griffith KT. 2018. Coastal wetland adaptation to sea level rise: Quantifying potential for landward migration and coastal squeeze. *The Journal of applied ecology* 55: 2876–2887.
- Breiman L. 2001. Random forests. *Machine learning* 45: 5–32.
- Brinson MM. 1991. Landscape properties of pocosins and associated wetlands. *Wetlands* 11: 441–465.
- Carmichael MJ, Smith WK. 2016. Growing season ecophysiology of *Taxodium distichum* (L.) Rich. (bald cypress) saplings in a restored wetland: a baseline for restoration practice. *Botany* 94: 1115–1125.
- Carter LJ. 1975. Agriculture: A New Frontier in Coastal North Carolina. *Science* 189: 271–275.
- Chambers LG, Davis SE, Troxler T, Boyer JN, Downey-Wall A, Scinto LJ. 2014. Biogeochemical effects of simulated sea level rise on carbon loss in an Everglades mangrove peat soil. *Hydrobiologia* 726: 195–211.
- Chambers LG, Osborne TZ, Reddy KR. 2013. Effect of salinity-altering pulsing events on soil organic carbon loss along an intertidal wetland gradient: a laboratory experiment. *Biogeochemistry* 115: 363–383.
- Chambers LG, Reddy KR, Osborne TZ. 2011. Short-Term Response of Carbon Cycling to Salinity Pulses in a Freshwater Wetland. *Soil Science Society of America Journal* 75: 2000–2007.
- Charles SP, Kominoski JS, Troxler TG, Gaiser EE. 2019. Experimental saltwater intrusion drives rapid soil elevation and carbon loss in freshwater and brackish Everglades marshes. *Estuaries*.
- Church JA, Clark PU, Cazenave A, *et al.* 2013. Sea Level Change In: Stocker TF, Qin D, Plattner GK, *et al.*, eds. *Climate Change 2013: The Physical Science Basis. Contribution of Working Group I to the Fifth Assessment Report of the Intergovernmental Panel on Climate Change*. Cambridge, United Kingdom and New York, NY, USA: Cambridge University Press, 895–900.

- Cloern JE, Abreu PC, Carstensen J, *et al.* 2016. Human activities and climate variability drive fast-paced change across the world's estuarine-coastal ecosystems. *Global Change Biology* 22: 513–529.
- Conner WH. 1995. Woody plant regeneration in three South Carolina Taxodium/Nyssa stands following Hurricane Hugo. *Ecological engineering* 4: 277–287.
- Conner WH, Askew GR. 1992. Response of baldcypress and loblolly pine seedlings to short-term saltwater flooding. *Wetlands* 12: 230–233.
- Creed IF, Bergström A-K, Trick CG, *et al.* 2018. Global change-driven effects on dissolved organic matter composition: Implications for food webs of northern lakes. *Global change biology* 24: 3692–3714.
- Crowley MA, Cardille JA. 2020. Remote Sensing's Recent and Future Contributions to Landscape Ecology. *Current Landscape Ecology Reports* 5: 45–57.
- Cui B, Yang Q, Yang Z, Zhang K. 2009. Evaluating the ecological performance of wetland restoration in the Yellow River Delta, China. *Ecological engineering* 35: 1090–1103.
- Dang C, Morrissey EM, Neubauer SC, Franklin RB. 2019. Novel microbial community composition and carbon biogeochemistry emerge over time following saltwater intrusion in wetlands. *Global change biology* 25: 549–561.
- Desantis LRG, Bhotika S, Williams K, Putz FE. 2007. Sea-level rise and drought interactions accelerate forest decline on the Gulf Coast of Florida, USA. *Global Change Biology* 13: 2349–2360.
- Doroski AA, Helton AM, Vadas TM. 2019. Greenhouse gas fluxes from coastal wetlands at the intersection of urban pollution and saltwater intrusion: A soil core experiment. *Soil biology & biochemistry* 131: 44–53.
- Douglas BC, Richard Peltier W. 2002. The puzzle of global sea-level rise. *Physics today* 55: 35–40.
- Doyle TW, Krauss KW, Conner WH, From AS. 2010. Predicting the retreat and migration of tidal forests along the northern Gulf of Mexico under sea-level rise. *Forest ecology and management* 259: 770–777.
- Doyle TW, O'Neil CP, Melder MPV, From AS, Palta MM. 2007. Tidal Freshwater Swamps of the Southeastern United States: Effects of Land Use, Hurricanes, Sea-level Rise, and Climate Change In: Conner WH, Doyle TW, Krauss KW, eds. *Ecology of Tidal Freshwater Forested Wetlands of the Southeastern United States*. Dordrecht: Springer Netherlands, 1–28.
- Duarte CM, Losada IJ, Hendriks IE, Mazarrasa I, Marbà N. 2013. The role of coastal plant communities for climate change mitigation and adaptation. *Nature climate change* 3: 961–968.

- Fagherazzi S, Anisfeld SC, Blum LK, *et al.* 2019. Sea level rise and the dynamics of the marsh-upland boundary. *Frontiers in Environmental Science* 7.
- Fierer N, Allen AS, Schimel JP. 2003. Controls on microbial CO₂ production: a comparison of surface and subsurface soil horizons. *Global change biology*.
- Haer T, Kalnay E, Kearney M, Moll H. 2013. Relative sea-level rise and the conterminous United States: Consequences of potential land inundation in terms of population at risk and GDP loss. *Global environmental change: human and policy dimensions* 23: 1627–1636.
- Hanley ME, Gove TL, Cawthray GR, Colmer TD. 2016. Differential responses of three coastal grassland species to seawater flooding. *Journal of Plant Ecology* 10: 322–330.
- Hart BT, Bailey P, Edwards R, *et al.* 1990. Effects of salinity on river, stream and wetland ecosystems in Victoria, Australia. *Water Research* 24: 1103–1117.
- Helton AM, Ardón M, Bernhardt ES. 2019. Hydrologic context alters greenhouse gas feedbacks of coastal wetland salinization. *Ecosystems* 22: 1108–1125.
- Herbert ER, Boon P, Burgin AJ, *et al.* 2015. A global perspective on wetland salinization: ecological consequences of a growing threat to freshwater wetlands. *Ecosphere* 6: 206.
- Herbert ER, Schubauer-Berigan J, Craft CB. 2018. Differential effects of chronic and acute simulated seawater intrusion on tidal freshwater marsh carbon cycling. *Biogeochemistry* 138: 137–154.
- Hijmans RJ. 2020. *Geographic Data Analysis and Modeling [R package raster version 3.4-5]*. Comprehensive R Archive Network (CRAN).
- Hillebrand H, Kunze C. 2020. Meta-analysis on pulse disturbances reveals differences in functional and compositional recovery across ecosystems (S Saavedra, Ed.). *Ecology letters*: ele.13457.
- Hoepfner SS, Shaffer GP, Perkins TE. 2008. Through droughts and hurricanes: Tree mortality, forest structure, and biomass production in a coastal swamp targeted for restoration in the Mississippi River Deltaic Plain. *Forest Ecology and Management* 256: 937–948.
- Holden J, Chapman PJ, Labadz JC. 2004. Artificial drainage of peatlands: hydrological and hydrochemical process and wetland restoration. *Progress in Physical Geography: Earth and Environment* 28: 95–123.
- Hosner JF, Others. 1960. Relative tolerance to complete inundation of fourteen bottomland tree species. *Forest Science* 6: 246–251.
- Huang J, Yu H, Guan X, Wang G, Guo R. 2016. Accelerated dryland expansion under climate change. *Nature climate change* 6: 166–171.

- Jackson MB, Colmer TD. 2005. Response and adaptation by plants to flooding stress. *Annals of botany* 96: 501–505.
- Jardine PM, McCarthy JF, Weber NL. 1989. Mechanisms of dissolved organic carbon adsorption on soil. *Soil Science Society of America journal. Soil Science Society of America* 53: 1378–1385.
- Kasischke ES, Amiro BD, Barger NN, *et al.* 2013. Impacts of disturbance on the terrestrial carbon budget of North America: DISTURBANCE AND CARBON CYCLING. *Journal of geophysical research. Biogeosciences* 118: 303–316.
- Kaushal SS, Groffman PM, Likens GE, *et al.* 2005. Increased salinization of fresh water in the northeastern United States. *Proceedings of the National Academy of Sciences of the United States of America* 102: 13517–13520.
- Kaushal SS, Likens GE, Pace ML, *et al.* 2018. Freshwater salinization syndrome on a continental scale. *Proceedings of the National Academy of Sciences of the United States of America* 115: E574–E583.
- Kennedy RE, Andréfouët S, Cohen WB, *et al.* 2014. Bringing an ecological view of change to Landsat-based remote sensing. *Frontiers in ecology and the environment* 12: 339–346.
- Kirwan ML, Gedan KB. 2019. Sea-level driven land conversion and the formation of ghost forests. *Nature climate change* 9: 450–457.
- Kirwan ML, Megonigal JP. 2013. Tidal wetland stability in the face of human impacts and sea-level rise. *Nature* 504: 53–60.
- Kirwan ML, Temmerman S, Skeeahan EE, Guntenspergen GR, Fagherazzi S. 2016. Overestimation of marsh vulnerability to sea level rise. *Nat. Clim. Chang.* 6: 253–260.
- Kissel DE, Sonon L, Vendrell PF, Isaac RA. 2009. Salt Concentration and Measurement of Soil pH. *Communications in soil science and plant analysis* 40: 179–187.
- Kombo MM, Vuai SA, Ishiki M, Tokuyama A. 2005. Influence of Salinity on pH and Aluminum Concentration on the Interaction of Acidic Red Soil with Seawater. *Journal of Oceanography* 61: 591–601.
- Krauss KW, Whitbeck J. 2012. Soil Greenhouse Gas Fluxes during Wetland Forest Retreat along the Lower Savannah River, Georgia (USA). *Wetlands* 32: 73–81.
- Laderman AD. 1989. *The Ecology of Atlantic White Cedar Wetlands: A Community Profile*. Washington, DC: U.S. Dept. of the Interior, Fish and Wildlife Service, Research and Development, National Wetlands Research Center.
- Lauber CL, Hamady M, Knight R, Fierer N. 2009. Pyrosequencing-based assessment of soil pH as a predictor of soil bacterial community structure at the continental scale. *Applied and environmental microbiology* 75: 5111–5120.

- Liaw A, Wiener M. 2002. Classification and Regression by RandomForest. *R News* 2/3.
- Liu X, Conner WH, Song B, Jayakaran AD. 2017. Forest composition and growth in a freshwater forested wetland community across a salinity gradient in South Carolina, USA. *Forest ecology and management* 389: 211–219.
- Liu X, Ruecker A, Song B, Xing J, Conner WH, Chow AT. 2017. Effects of salinity and wet-dry treatments on C and N dynamics in coastal-forested wetland soils: Implications of sea level rise. *Soil biology & biochemistry* 112: 56–67.
- Lozupone CA, Knight R. 2007. Global patterns in bacterial diversity. *Proceedings of the National Academy of Sciences of the United States of America* 104: 11436–11440.
- Luo M, Huang J-F, Zhu W-F, Tong C. 2019. Impacts of increasing salinity and inundation on rates and pathways of organic carbon mineralization in tidal wetlands: a review. *Hydrobiologia* 827: 31–49.
- Manda AK, Giuliano AS, Allen TR. 2014. Influence of artificial channels on the source and extent of saline water intrusion in the wind tide dominated wetlands of the southern Albemarle estuarine system (USA). *Environmental Earth Sciences* 71: 4409–4419.
- Manda AK, Reyes E, Pitt JM. 2018. In situ measurements of wind-driven salt fluxes through constructed channels in a coastal wetland ecosystem. *Hydrological processes* 32: 636–643.
- Marinos RE, Bernhardt ES. 2018. Soil carbon losses due to higher pH offset vegetation gains due to calcium enrichment in an acid mitigation experiment. *Ecology* 99: 2363–2373.
- Marton J, Herbert E, Craft CB. 2012. Effects of Salinity on Denitrification and Greenhouse Gas Production from Laboratory-incubated Tidal Forest Soils. *Wetlands* 32.
- Mavi MS, Sanderman J, Chittleborough DJ, Cox JW, Marschner P. 2012. Sorption of dissolved organic matter in salt-affected soils: effect of salinity, sodicity and texture. *The Science of the total environment* 435–436: 337–344.
- McCarron JK, McLeod KW, Conner WH. 1998. Flood and salinity stress of wetland woody species, buttonbush (*Cephalanthus occidentalis*) and swamp tupelo (*Nyssa sylvatica* var. *biflora*). *Wetlands* 18: 165–175.
- Meehl GA, Gregory JM, Kitoh A, *et al.* 2007. Global Climate Projections. *Climate Change 2007: The Physical Science Basis. Contribution of Working Group I to the Fourth Assessment Report of the Intergovernmental Panel on Climate Change*: 747–845.
- Mehlich A. 1984a. Photometric determination of humic matter in soils, a proposed method. *Communications in soil science and plant analysis* 15: 1417–1422.
- Mehlich A. 1984b. Mehlich 3 soil test extractant: A modification of Mehlich 2 extractant. *Communications in soil science and plant analysis* 15: 1409–1416.

- Mehlich A, Bowling SS, Hatfield AL. 1976. Buffer pH acidity in relation to nature of soil acidity and expression of lime requirement. *Communications in soil science and plant analysis* 7: 253–263.
- Miao S, Zou CB, Breshears DD. 2009. Vegetation responses to extreme hydrological events: sequence matters. *The American naturalist* 173: 113–118.
- Mitsch WJ, Gosselink JG. 2015. *Wetlands, 5th edition*. Hoboken, NJ: John Wiley & Sons, Inc.
- Moorhead KK, Brinson MM. 1995. Response of wetlands to rising sea level in the lower coastal plain of North Carolina. *Ecological applications: a publication of the Ecological Society of America* 5: 261–271.
- Morse JL, Ardón M, Bernhardt ES. 2012. Greenhouse gas fluxes in southeastern U.S. coastal plain wetlands under contrasting land uses. *Ecological applications: a publication of the Ecological Society of America* 22: 264–280.
- Mulholland PJ, Best GR, Coutant CC, *et al.* 1997. Effects of climate change on freshwater ecosystems of the south-eastern United States and the Gulf Coast of Mexico. *Hydrological processes* 11: 949–970.
- Munns R, Tester M. 2008. Mechanisms of salinity tolerance. *Annual review of plant biology* 59: 651–681.
- Myers N, Mittermeier RA, Mittermeier CG, da Fonseca GAB, Kent J. 2000. Biodiversity hotspots for conservation priorities. *Nature* 403: 853–858.
- Myers-Smith IH, Hik DS. 2018. Climate warming as a driver of tundra shrubline advance (R Aerts, Ed.). *The Journal of ecology* 106: 547–560.
- Needham R. 2006. *Implementation plan for agricultural restoration at Timberlake Farms*. Needham Environmental Incorporated, Wilmington, NC.
- Neubauer SC. 2013. Ecosystem Responses of a Tidal Freshwater Marsh Experiencing Saltwater Intrusion and Altered Hydrology. *Estuaries and Coasts* 36: 491–507.
- Neubauer SC, Franklin RB, Berrier DJ. 2013. Saltwater intrusion into tidal freshwater marshes alters the biogeochemical processing of organic carbon. *Biogeosciences* 10: 8171–8183.
- Neubauer SC, Givler K, Valentine S, Megonigal JP. 2005. Seasonal patterns and plant-mediated controls of subsurface wetland biogeochemistry. *Ecology* 86: 3334–3344.
- Nicholls RJ. 2004. Coastal flooding and wetland loss in the 21st century: changes under the SRES climate and socio-economic scenarios. *Global environmental change: human and policy dimensions* 14: 69–86.

- NOAA. 2016. *National Weather Service Advanced Hydrologic Prediction Service*. <https://water.weather.gov/ahps2/hydrograph.php?wfo=mhx&gage=orin7>. 7 Feb. 2020.
- Noss RF, Platt WJ, Sorrie BA, *et al.* 2015. How global biodiversity hotspots may go unrecognized: lessons from the North American Coastal Plain. *Diversity & distributions* 21: 236–244.
- NRCS. 2017. *National Resources Conservation Service*. websoilsurvey.nrcs.usda.gov/app/WebSoilSurvey.aspx. 5 Dec. 2018.
- Ohno T, First PR. 1998. Assessment of the folin and ciocalteu's method for determining soil phenolic carbon. *Journal of environmental quality* 27: 776–782.
- Oksanen J, Blanchet FG, Friendly M, *et al.* 2016. *vegan: Community Ecology Package*. R package version 2.4-3.
- Palmquist KA, Peet RK, Weakley AS. 2014. Changes in plant species richness following reduced fire frequency and drought in one of the most species-rich savannas in North America. *Journal of vegetation science* 25: 1426–1437.
- Pastick NJ, Jorgenson MT, Goetz SJ, *et al.* 2019. Spatiotemporal remote sensing of ecosystem change and causation across Alaska. *Global change biology* 25: 1171–1189.
- Peet RK, Lee MT, Boyle MF, *et al.* 2012. Vegetation-plot database of the Carolina Vegetation Survey. *Biodiversity and ecology* 4: 243–253.
- Peet RK, Palmquist KA, Wentworth TR, Schafale MP, Weakly AS, Lee MT. 2018. Carolina Vegetation Survey: An initiative to improve regional implementation of the U.S. National Vegetation Classification. *Phytocoenologia* 48: 171–179.
- Peet RK, Wentworth TR, White PS. 1998. A Flexible, Multipurpose Method for Recording Vegetation Composition and Structure. *Castanea* 63: 262–274.
- Pekel JF, Cottam A, Gorelick N, Belward AS. 2016. High-resolution mapping of global surface water and its long-term changes. *Nature* 540: 418–422.
- Pennings SC, Grant M-B, Bertness MD. 2005. Plant Zonation in Low-Latitude Salt Marshes: Disentangling the Roles of Flooding, Salinity and Competition. *The Journal of ecology* 93: 159–167.
- Poulter B. 2005. Interactions between landscape disturbance and gradual environmental change: plant community migration in response to fire and sea level rise (Doctoral dissertation, Duke University).
- Poulter B, Halpin PN. 2008. Raster modelling of coastal flooding from sea-level rise. *International journal of geographical information science: IJGIS* 22: 167–182.

- R Development Core Team. 2017. *R: A language and environment for statistical computing*. Vienna, Austria.
- R Development Core Team. 2020. *R: A language and environment for statistical computing*. Vienna, Austria.
- Rath KM, Maheshwari A, Rousk J. 2017. The impact of salinity on the microbial response to drying and rewetting in soil. *Soil biology & biochemistry* 108: 17–26.
- Rath KM, Rousk J. 2015. Salt effects on the soil microbial decomposer community and their role in organic carbon cycling: A review. *Soil biology & biochemistry* 81: 108–123.
- Reed DJ. 1995. The response of coastal marshes to sea-level rise: Survival or submergence? *Earth Surface Processes and Landforms* 20: 39–48.
- Reilly MJ, Wimberly MC, Newell CL. 2006. Wildfire effects on plant species richness at multiple spatial scales in forest communities of the southern Appalachians. *The Journal of ecology* 94: 118–130.
- Richardson CJ. 1983. Pocosins: Vanishing Wastelands or Valuable Wetlands? *Bioscience* 33: 626–633.
- Riegel JB, Bernhardt E, Swenson J. 2013. Estimating Above-Ground Carbon Biomass in a Newly Restored Coastal Plain Wetland Using Remote Sensing. *PLoS one* 8: e68251.
- Robichaud A, Bégin Y. 1997. The Effects of Storms and Sea-Level Rise on a Coastal Forest Margin in New Brunswick, Eastern Canada. *Journal of Coastal Research* 13: 429–439.
- Rocca JD, Simonin M, Bernhardt ES, Washburne AD, Wright JP. 2020. Rare microbial taxa emerge when communities collide: freshwater and marine microbiome responses to experimental mixing. *Ecology* 101: e02956.
- Schafale MP. 2012. Classification of the natural communities of North Carolina, 4th Approximation. *North Carolina Department of Environment, Health, and Natural Resources, Division of Parks and Recreation, Natural Heritage Program, Raleigh*.
- Schafale M P, Weakley A S. 1990. *Classification of the Natural Communities of North Carolina, Third Approximation*. North Carolina Heritage Program.
- Scheffer M. 2009. *Critical Transitions in Nature and Society*. Princeton, NJ: Princeton University Press.
- Schieder NW, Kirwan ML. 2019. Sea-level driven acceleration in coastal forest retreat. *Geology* 47: 1151–1155.
- Schoepfer VA, Bernhardt ES, Burgin A. 2014. Iron clad wetlands: Soil iron-sulfur buffering determines coastal wetland response to salt water incursion. *Journal of geophysical research* 119: 2209–2219.

- Schuerch M, Spencer T, Temmerman S, *et al.* 2018. Future response of global coastal wetlands to sea-level rise. *Nature* 561: 231–234.
- Setia R, Smith P, Marschner P, *et al.* 2012. Simulation of salinity effects on past, present, and future soil organic carbon stocks. *Environmental science & technology* 46: 1624–1631.
- Shainberg I, Letey J. 1984. Response of soils to sodic and saline conditions. *Hilgardia* 52: 1–57.
- Shirley LJ, Battaglia LL. 2006. Assessing vegetation change in coastal landscapes of the northern Gulf of Mexico. *Wetlands* 26: 1057–1070.
- Silvestri S, Defina A, Marani M. 2005. Tidal regime, salinity and salt marsh plant zonation. *Estuarine, coastal and shelf science* 62: 119–130.
- Singh K. 2016. Microbial and enzyme activities of saline and sodic soils: Microbial activities and salt-affected soil. *Land Degradation & Development* 27: 706–718.
- Slik JWF, Aiba S-I, Brearley FQ, *et al.* 2010. Environmental correlates of tree biomass, basal area, wood specific gravity and stem density gradients in Borneo's tropical forests: Forest carbon and structure gradients. *Global ecology and biogeography: a journal of macroecology* 19: 50–60.
- Smart LS, Taillie PJ, Poulter B, *et al.* 2020. Aboveground carbon loss associated with the spread of ghost forests as sea levels rise. *Environmental research letters* 15: 104028.
- Soil Survey Staff. 2008. *Natural Resources Conservation Service, United States Department of Agriculture*. https://soilseries.sc.egov.usda.gov/OSD_Docs/H/HYDE.html. 8 Feb. 2021.
- Soil Survey Staff. 2010. *Natural Resources Conservation Service, United States Department of Agriculture*. https://soilseries.sc.egov.usda.gov/OSD_Docs/P/PONZER.html#:~:text=The%20Ponzer%20series%20consists%20of,from%200%20to%202%20percent. 8 Feb. 2021.
- Soil Survey Staff. 2017. *Web Soil Survey*. <https://websoilsurvey.sc.egov.usda.gov/>. 6 Dec. 2018.
- Spencer T, Schuerch M, Nicholls RJ, *et al.* 2016. Global coastal wetland change under sea-level rise and related stresses: The DIVA Wetland Change Model. *Global and planetary change* 139: 15–30.
- Spivak AC, Sanderman J, Bowen JL, Canuel EA, Hopkinson CS. 2019. Global-change controls on soil-carbon accumulation and loss in coastal vegetated ecosystems. *Nature geoscience* 12: 685–692.
- Stroh CL, De Steven D, Guntenspergen GR. 2008. Effect of climate fluctuations on long-term vegetation dynamics in Carolina Bay wetlands. *Wetlands* 28: 17–27.

- Sulman BN, Moore JAM, Abramoff R, *et al.* 2018. Multiple models and experiments underscore large uncertainty in soil carbon dynamics. *Biogeochemistry* 141: 109–123.
- Taillie PJ, Moorman CE, Poulter B, Ardón M, Emanuel RE. 2019. Decadal-Scale Vegetation Change Driven by Salinity at Leading Edge of Rising Sea Level. *Ecosystems* 22: 1918–1930.
- Taillie PJ, Moorman CE, Smart LS, Pacifici K. 2019. Bird community shifts associated with saltwater exposure in coastal forests at the leading edge of rising sea level (AJ Kroll, Ed.). *PLoS one* 14: e0216540.
- Tolliver KS, Martin DW, Young DR. 1997. Freshwater and saltwater flooding response for woody species common to barrier island swales. *Wetlands* 17: 10–18.
- Tully K, Gedan K, Epanchin-Niell R, *et al.* 2019. The Invisible Flood: The Chemistry, Ecology, and Social Implications of Coastal Saltwater Intrusion. *Bioscience* 69: 368–378.
- Ury EA, Anderson SM, Peet RK, Bernhardt ES, Wright JP. 2020. Succession, regression and loss: does evidence of saltwater exposure explain recent changes in the tree communities of North Carolina’s Coastal Plain? *Annals of botany* 125: 255–264.
- US Fish and Wildlife Services Southeast Region Fire Management Organization. 2011. *FY2011 Fire Division Report*. <https://www.fws.gov/southeast/pdf/report/fire-report-2011.pdf>. 7 Feb. 2020.
- U.S. Geological Survey. 2017. 1 meter Digital Elevation Models (DEMs).
- USGS. *USGS EROS Archive - Aerial Photography - High Resolution Orthoimagery (HRO)*. <https://doi.org/10.5066/F73X84W6>. 1 Sep. 2019.
- Ustin SL. 2013. Remote sensing of canopy chemistry. *Proceedings of the National Academy of Sciences of the United States of America* 110: 804–805.
- Ustin SL, Gitelson AA, Jacquemoud S, *et al.* 2009. Remote Sensing of Environment Retrieval of foliar information about plant pigment systems from high resolution spectroscopy. *Remote sensing of environment* 113: S67–S77.
- Vermeer M, Rahmstorf S. 2009. Global sea level linked to global temperature. *Proceedings of the National Academy of Sciences of the United States of America* 106: 21527–21532.
- Vitousek S, Barnard PL, Fletcher CH, Frazer N, Erikson L, Storlazzi CD. 2017. Doubling of coastal flooding frequency within decades due to sea-level rise. *Scientific Reports* 7.
- Wassmann R, Hien NX, Hoanh CT, Tuong TP. 2004. Sea level rise affecting the Vietnamese Mekong delta: Water elevation in the flood season and implications for rice production. *Climatic change* 66: 89–107.

- Wasson K, Woolfolk A, Fresquez C. 2013. Ecotones as indicators of changing environmental conditions: Rapid migration of salt marsh–upland boundaries. *Estuaries and coasts: journal of the Estuarine Research Federation* 36: 654–664.
- Weishaar JL, Aiken GR, Bergamaschi BA, Fram MS, Fujii R, Mopper K. 2003. Evaluation of specific ultraviolet absorbance as an indicator of the chemical composition and reactivity of dissolved organic carbon. *Environmental science & technology* 37: 4702–4708.
- Weissman DS, Tully KL. 2020. Saltwater intrusion affects nutrient concentrations in soil porewater and surface waters of coastal habitats. *Ecosphere* 11: e03041.
- Wen Y, Bernhardt ES, Deng W, *et al.* 2019. Salt effects on carbon mineralization in southeastern coastal wetland soils of the United States. *Geoderma* 339: 31–39.
- Weston NB, Dixon RE, Joye SB. 2006. Ramifications of increased salinity in tidal freshwater sediments: Geochemistry and microbial pathways of organic matter mineralization. *Journal of Geophysical Research: Biogeosciences* 111: G01009.
- Weston NB, Vile MA, Neubauer SC, Velinsky DJ. 2011. Accelerated microbial organic matter mineralization following salt-water intrusion into tidal freshwater marsh soils. *Biogeochemistry* 102: 135–151.
- White AC, Colmer TD, Cawthray GR, Hanley ME. 2014. Variable response of three *Trifolium* repens ecotypes to soil flooding by seawater. *Annals of botany* 114: 347–355.
- White E, Kaplan D. 2017. Restore or retreat? saltwater intrusion and water management in coastal wetlands. *Ecosystem Health and Sustainability* 3: e01258.
- Wichern J, Wichern F, Joergensen RG. 2006. Impact of salinity on soil microbial communities and the decomposition of maize in acidic soils. *Geoderma* 137: 100–108.
- Wickham H. 2016. ggplot2: Elegant Graphics for Data Analysis.
- Wickham H, Averick M, Bryan J, *et al.* 2019. Welcome to the tidyverse. *Journal of Open Source Software* 4: 1686.
- Williams K, Ewel KC, Stumpf RP, Putz FE, Workman TW. 1999. Sea-level rise and coastal forest retreat on the west coast of Florida, USA. *Ecology* 80: 2045–2063.
- Williams K, Michelina MacDonald, Leonel da Silveira Lobo Sternberg. 2003. Interactions of Storm, Drought, and Sea-Level Rise on Coastal Forest: A Case Study. *Journal of Coastal Research* 19: 1116–1121.
- Windham-Myers L, Cai W-J, Alin S, *et al.* 2018. *Chapter 15: Tidal Wetlands and Estuaries. Second State of the Carbon Cycle Report.* U.S. Global Change Research Program.

- Xi W, Peet RK, Urban DL. 2008. Changes in forest structure, species diversity and spatial pattern following hurricane disturbance in a Piedmont North Carolina forest, USA. *Journal of Plant Ecology* 1: 43–57.
- Yang L, Jin S, Danielson P, *et al.* 2018. A new generation of the United States National Land Cover Database: Requirements, research priorities, design, and implementation strategies. *ISPRS journal of photogrammetry and remote sensing: official publication of the International Society for Photogrammetry and Remote Sensing* 146: 108–123.
- Zedler JB. 2003. Wetlands at your service: reducing impacts of agriculture at the watershed scale. *Frontiers in ecology and the environment* 1: 65–72.
- Zhang Y, Li W, Sun G, *et al.* 2018. Understanding coastal wetland hydrology with a new regional-scale, process-based hydrological model. *Hydrological processes* 32: 3158–3173.
- Zhang Y, Li W, Sun G, King JS. 2019. Coastal wetland resilience to climate variability: A hydrologic perspective. *Journal of Hydrology* 568: 275–284.